Appendix PA

Attachment SOTERM

This page intentionally left blank

Table of Contents

List of Figures

List of Tables

ACRONYMS AND ABBREVIATIONS

An	actinide(s)
atm	atmosphere (a unit of pressure)
aq	aqueous
ASTP	Actinide Source Term Program
BNL	Brookhaven National Laboratory
brucite	$Mg(OH)_2$
calcite	$CaCO_3$
CFR	Code of Federal Regulations
CPR	cellulosics, plastics, and rubber
DOE	(U.S.) Department of Energy
DRZ	disturbed rock zone
EDTA	ethylenediaminetetra acetate
EPA	(U.S.) Environmental Protection Agency
eq	equivalent(s)
ERDA	(U.S.) Energy Research and Development Administration
FA-Suw	fulvic acid isolated from the Suwannee River acquired from the International Humic Substances Society, Golden, Colorado
FMT	Fracture-Matrix Transport
f_{CO_2}	the fugacity of a gaseous species, f_i (similar to the partial pressures of that species, p_i)
g	gaseous or gram(s)
gal	gallon(s)
GWB	Generic Weep Brine
HAal-Ald	aliphatic humic acid purchased from Aldrich Chemical Co., purified by Florida State University
HAal-LBr	aliphatic humic acid isolated from sediments collected from Lake Bradford, Florida, prepared by Florida State University
HAar-Gor	aromatic humic acid isolated from groundwaters near Gorleben, Germany, obtained from Professor J.-I. Kim, Institut für Radiochemie, München
HAar-Suw	aromatic humic acid isolated from the Suwannee River acquired from the International Humic Substances Society, Golden, Colorado
HMW/FW	Harvie-Møller-Weare/Felmy and Weare
hydromagnesite	$Mg_4(CO_3)_3(OH)_2{\cdot}3H_2O$ or $Mg_5(CO_3)_4(OH)_2{\cdot}4H_2O$
L	Liter(s)
LANL	Los Alamos National Laboratory
LLNL	Lawrence Livermore National Laboratory
m	molal
M	molar
meq	milliequivalent(s)
mL	milliliter(s)
mol	mole(s)
PA	performance assessment
periclase	MgO
pH	the negative logarithm of the activity of hydrogen ion (H^+)

redox	oxidation-reduction
s	second
SIT	Specific-Ion Interaction Theory
SPC	Salado Primary Constituent
STTP	(WIPP) Actinide Source Term Waste Test Program
SWCF	Sandia National Laboratories WIPP Central File
TRU	transuranic
TWBIR	Transuranic Waste Baseline Inventory Report
UV	ultraviolet
WIPP	Waste Isolation Pilot Plant

SOTERM-1.0 INTRODUCTION

The actinide source term used in the performance assessment (PA) calculations for the Waste Isolation Pilot Plant (WIPP) represents the aqueous concentrations of thorium (Th), uranium (U), plutonium (Pu), and americium (Am) in the repository. The source term is the sum of the dissolved species (solubilities) and the mobile suspended (colloidal) species of these radioelements. The actinide source term establishes the mobile concentrations of Th, U, Pu, and Am that may be released from the repository in brine. Brine releases to the accessible environment may occur through the sealed shafts, up possible intrusion boreholes, and/or out laterally through Salado Formation interbeds. (For a discussion of release scenarios and pathways, see Chapter 6.0, Section 6.3). Quantification of the impact of these releases contributes directly to assessing compliance with Title 40 Code of Federal Regulations (CFR) Part 191. Direct releases of particulate actinides to the surface associated with solid waste resulting from drilling (cuttings, cavings, and spallings) are not included in the actinide source term.

The actinide source term is limited to those radionuclides that could significantly impact the long-term performance of the WIPP. These radionuclides are all isotopes of Th, U, Pu, and Am. From the standpoint of their potential effects on the long-term performance of the repository, the order of importance of these actinides is Pu ≈ Am >> U > Th (Helton et al. 1998). Other actinides, especially neptunium (Np), have been included in the laboratory and modeling studies used to develop the actinide source term because it was not known at the outset which actinides could significantly affect the long-term performance of the repository. Other radioelements, such as strontium (Sr), cesium (Cs), and radium (Ra), are not included in the actinide source term because of their relatively short half-lives or limited waste inventory.

Attachment SOTERM (SOurce TERM) focuses on the development of actinide-source-term parameter values and the implementation of these parameters in PA calculations. In Section 2.0, an overview of near-field chemical processes and conditions is presented. Sections 3.0 and 4.0 focus on the development of the dissolved-actinide solubility parameters and oxidation-state distribution, respectively. Section 5.0 focuses on the impact of organic ligands on dissolved actinide concentrations. The colloidal actinide source term is described in Section 6.0. In Section 7.0 the PA implementation of the dissolved and colloidal components of the source term is described.

This attachment is a supplement to information presented in Chapter 6, Sections 6.4.3.3, 6.4.3.4, 6.4.3.5, and 6.4.3.6 of this application.

SOTERM-2.0 OVERVIEW OF NEAR-FIELD PROCESSES AND CONDITIONS

This section presents an overview of near-field processes and conditions that will affect actinide solubilities in the WIPP. Ambient geochemical conditions are described first. The effects of human intrusion and waste are then described. Emphasis is placed on how various components and processes within the repository will affect the dissolution and colloidal suspension of actinides. Excess magnesium oxide (MgO) will be added to the repository for assurance

purposes, so the effect of MgO is included in this discussion. Simplifications and assumptions used to model the components and processes are discussed in each section.

SOTERM-2.1 Ambient Geochemical Conditions

The Salado is predominantly nearly pure halite (NaCl), with interbeds ("marker beds") consisting mainly of anhydrite ($CaSO_4$). The nearly pure halite contains accessory evaporite minerals such as anhydrite ($CaSo_4$), gypsum ($CaSO_4 \bullet 2H_2O$), polyhalite ($K_2MgCa_2(SO_4)_4 \bullet 2H_2O$), magnesite ($MgCO_3$), and clays. Small quantities of intergranular (grain-boundary) brines and intragranular brines (fluid inclusions) are associated with the salt at the repository horizon. These brines are highly concentrated solutions (up to 8 M) of predominantly sodium (Na^+), Mg^{2+}, potassium (K^+), chloride (Cl^-), and sulfate (SO_4^{2-}) with smaller amounts of Ca^{2+}, CO_3^{2-}, and B. These brines have been in contact with the Salado evaporite minerals for about 250 million years and are saturated with respect to these minerals.

Underlying the Salado is the Castile Formation, composed of alternating units of interlaminated carbonate and anhydrite, and nearly pure halite. The Castile in the vicinity of the WIPP site is known to contain localized brine reservoirs under sufficient pressure to force brine to the land surface if penetrated by a borehole. Castile brines are predominantly saturated NaCl solutions containing Ca^{2+} and SO_4^{2-}, and small concentrations of other elements, and are about eight times more concentrated than seawater. Overlying the Salado in the vicinity of the WIPP site is the Culebra Member of the Rustler Formation, a fractured dolomite ($CaMg(CO_3)_2$) layer. It is significant because it is expected to be the most transmissive geologic pathway to the accessible environment. Culebra brines are generally more dilute than the Salado and Castile brines, and are predominantly NaCl with K^+, Mg^{2+}, Ca^{2+}, SO_4^{2-}, and CO_3^{2-}. (See Chapter 2.0, Section 2.4.2.1 of this application for information on the distribution of Culebra brine salinity.)

SOTERM-2.2 Repository Chemical Conditions

Three aspects of the repository chemical environment can have a major impact on the dissolution and colloidal suspension of actinides. These are:

- brine composition;
- microbial consumption of cellulosic, plastic, and rubber (CPR) materials and concomitant production of carbon dioxide (CO_2); and
- anoxic corrosion of steels and other iron-base (Fe-base) alloys in the waste containers and the waste and concomitant production of hydrogen (H_2).

For each of these, the effect, the range of possible behavior, and the simplifications used in modeling are discussed below.

SOTERM-2.2.1 Brine

The compositions of brines required for mobilization of actinides will affect the quantities of actinidies that may be dissolved or suspended. For example, high-ionic-strength brines have

been shown to increase the solubilities of actinides and to increase the coagulation and settling rate of mineral-fragment colloids.

In human-intrusion scenarios, Salado and/or Castile brine will enter the repository, depending on whether the intrusion penetrates a brine reservoir in the Castile. However, in addition to Salado and Castile brines, brines from the Rustler and Dewey Lake Formation could flow down the borehole to the repository, mix with the waste, and then be forced back up a borehole. Rustler and Dewey-Lake brines are considerably less concentrated than Salado and Castile brines. If the Rustler and Dewey-Lake brines flow into the repository, they would dissolve Salado halite until they attain compositions between those of Salado and Castile brines (see Section 7.1.2). Under any intrusion scenario, therefore, the brine dissolving actinides would have the composition of Salado, Castile, or a mixture of Salado and Castile brines.

The Salado and Castile brine compositions bracket the range of possibilities within the repository, so experimental and modeling studies of repository and actinide chemistry have been performed using the end-member brines only. Inclusion of brine mixing in PA has been considered and rejected because it would not be sufficiently accurate to reduce the uncertainty associated with brine mixing and related brine chemistry compared to bracketing this uncertainty with end-member brines. Brine mixing is addressed in Section 7.1.2.

The two synthetic solutions that best represent the end-member brines that could be present in the repository are: (1) Generic Weep Brine (GWB), which simulates intergranular (grain-boundary) brines from the Salado at or near the stratigraphic horizon of the repository (Snider 2003a); and (2) Energy Research and Development Administration-6 (ERDA-6), typical of fluids in Castile brine reservoirs (Popielak et al. 1983). Through the time of the CCA, Brine A (Molecke 1983) and Salado Primary Constituents (SPC) Brine, a version of Brine A from which trace elements had been removed, were used to simulate Salado brines for laboratory and modeling studies. Since the CCA, however, GWB has been shown to be more representative of intergranular Salado brines than either Brine A or SPC Brine (Brush and Xiong 2003a; Snider 2003a). In particular, the Mg^{2+} concentration of GWB (1.0 M) simulates the average concentration of this element in Salado brines more closely than Brine A (1.44 M). Table SOTERM-1 provides the compositions of GWB and ERDA-6.

In addition to using the end-member brines, other simplifying assumptions have been made, including the following:

- Any brine present in the repository is well-mixed with waste.
- Equilibria with halite and anhydrite, the most abundant Salado minerals at or near the stratigraphic horizon of the repository, are established. Oxidation-reduction (redox) equilibria with waste materials have not been assumed.
- For modeling purposes, brine compositions attained after equilibration of GWB or ERDA-6 with the MgO engineered barrier are assumed for the entire 10,000-year regulatory period.

Table SOTERM-1. Compositions of GWB and ERDA-6 Prior to Equilibration with MgO

Element or Property	GWB[2]	ERDA-6[3]
$B(OH)_3$	155 mM	63 mM
Na^+	3.48 M	4.87 M
Mg^{2+}	1.00 M	19 mM
K^+	458 mM	97 mM
Ca^{2+}	14 mM	12 mM
SO_4^{2-}	175 mM	170 mM
Cl^-	5.51 M	4.8 M
Br^-	26 mM	11 mM
Total inorganic C (as HCO_3^-)	Not reported	16 mM
pH	Not reported	6.17
Specific gravity	1.2	1.216
TDS	Not reported	330,000 mg/l

[1] From Molecke (1983).
[2] From Snider (2003a).
[3] From Popielak et al. (1983).
[4] Reported by Molecke (1983) as BO_3^{3-}.

SOTERM-2.2.2 Microbial Consumption of Cellulosic, Plastic, and Rubber Materials

A large quantity of CPR materials will be emplaced in the WIPP, and could be consumed by microorganisms. There are large uncertainties as to whether significant microbial consumption of CPR materials will occur during the 10,000-year WIPP regulatory period. Therefore, it is assumed that significant microbial consumption of CPR materials is possible, but by no means certain. To incorporate these uncertainties in PA, Wang and Brush (1996a, 1996b) developed a conceptual model for microbial activity in the repository. According to this model, there is a probability of 0.50 for significant microbial activity. In the event of significant microbial activity, microbes would consume 100 percent of the cellulosic materials in the repository. Furthermore, there is a conditional probability of 0.50 that microbes would consume all of the plastic and rubber materials after consumption of all of the cellulosic materials. Thus, there is microbial consumption of all of the cellulosic materials, but no plastic or rubber materials, in about 25 percent of the PA realizations (vectors); microbial consumption of all of the CPR materials in 25 percent of the vectors; and no microbial activity in the remaining 50 percent of the vectors.

Microbial consumption of CPR materials could affect the actinide source term in four ways:

- production of significant quantities of CO_2, which could acidify any brine present and increase the solubilities of actinide elements;
- reduction of oxidized actinide species, which in most cases are more soluble;
- consumption of solubilizing organic ligands; and

- production of humic and microbial colloids, thereby increasing the amount of actinide sorbed on colloidal surfaces.

The effect of CO_2 production is discussed in this section. The remaining three effects are considered in the analyses that have studied the oxidation-state distributions (Section 4.0), the effects of organic ligands (Section 5.0), and the effects of colloids (Section 6.0). The simplifications used in PA calculations for all four of these effects are discussed at the end of this section.

Microbial activity, if it occurs to a significant extent in the WIPP, would consume CPR materials by the following sequential reactions (Brush 1990; Francis and Gillow 1994; Brush 1995; Wang and Brush1996a; Francis and Gillow 1997):

$$C_6H_{10}O_5 + 4.8H^+ + 4.8NO_3^- \rightarrow 7.4H_2O + 6CO_2 + 2.4N_2; \quad (1)$$

$$C_6H_{10}O_5 + 6H^+ + 3SO_4^{2-} \rightarrow 5H_2O + 6CO_2 + 3H_2S; \quad (2)$$

$$C_6H_{10}O_5 + H_2O \rightarrow 3CH_4 + 3CO_2. \quad (3)$$

An analysis by Snider (2003b) based on the estimated quantities of CPR materials, nitrate (NO_3^-), and SO_4^{2-} (see Appendix Data, Attachment F) implies that, in the event all of the CPR materials are consumed, denitrification (Reaction (1)) would account for 4.72 mol percent, sulfate reduction (Reaction (2)) would account for 0.82 mol percent, and methanogenesis (Reaction (3)) would account for 94.46 percent of the consumption of CPR materials. (Appendix BARRIERS, Section BARRIERS-2.5, describes these calculations in detail.) Therefore, methanogenesis would be the primary microbial respiratory pathway in the repository.

Microbial consumption of CPR materials could produce significant quantities of CO_2, which could in turn acidify any brine present in the repository and increase the solubilities of the actinides relative to those predicted for neutral and mildly basic conditions. Therefore, the DOE is emplacing MgO in the repository to decrease actinide solubilities by consuming essentially all of the CO_2 that could be produced by microbial consumption of CPR materials,

and by buffering (controlling) the f_{CO_2} and pH within ranges that are favorable from the standpoint of actinide speciation and solubility (see Appendix BARRIERS, Section BARRIERS-2.0).

Laboratory and modeling studies described in Appendix BARRIERS, Section BARRIERS-2.3 have shown that, in the event of significant microbial activity in the WIPP, the carbonation reaction

$$5Mg(OH)_2 + 4CO_2(aq \text{ or } g) \square Mg_5(CO_3)_4(OH)_2{\cdot}4H_2O \quad (4)$$

will buffer f_{CO_2} at a value of $10^{-5.50}$ atm in both GWB and ERDA-6. In this reaction, $Mg(OH)_2$ is the mineral brucite (the main hydration product of the mineral periclase (MgO) expected in the WIPP); $Mg_5(CO_3)_4(OH)_2{\cdot}4H_2O$ is the form of the mineral hydromagnesite expected in the

repository; and "aq" and "g" are the abbreviations for "aqueous" and "gaseous," respectively. Furthermore, the brucite-dissolution reaction

$$Mg(OH)_2 \quad Mg^{2+} + 2OH^- \tag{5}$$

will buffer pH in the WIPP at a value of 8.69 in GWB and 9.02 in ERDA-6. These values of f_{CO_2} and pH were used for the actinide speciation and solubility calculations for the CRA-2004 PA vectors with significant microbial activity (see Section 3.5 below).

In the absence of significant microbial activity in the WIPP, the carbonation reaction

$$Mg(OH)_2 + Ca^{2+} + CO_2(aq \text{ or } g) \square CaCO_3 + Mg^{2+} + H_2O(aq \text{ or } g) \tag{6}$$

will buffer f_{CO_2} at a value of $10^{-5.48}$ atm in GWB and $10^{-6.15}$ atm in ERDA-6, and the brucite-dissolution reaction (Reaction (5)) will buffer pH at a value of 8.69 in GWB and 8.99 in ERDA-6 (see Appendix BARRIERS, Section BARRIERS 2.3). In this reaction, $CaCO_3$ is the mineral calcite. These values of f_{CO_2} and pH were used for the actinide speciation and solubility calculations for the CRA-2004 PA vectors without microbial activity (see Section 3.0 below).

Four effects of microbial consumption of CPR materials are recognized in modeling system performance. A simplification has been made that the effects will be time independent after 100 years. The effects are

- CO_2 production. With the addition of excess MgO, the effects of CO_2 production are minimized, and it is assumed that the system may be modeled using the brucite-hydromagnesite ($Mg_5(CO_3)_4(OH)_2 \cdot 4H_2O$) buffer.

- Redox effects. After 100 years, the repository will have a reducing environment. Even though significant microbial action is only 50 percent likely, the corrosion of steel will also produce a reducing environment (Section 2.2.3).

- Possible consumption of organic ligands. While some microbes are known to consume some organic ligands, there is uncertainty as to the presence or viability of these particular microbes within the repository environment. Therefore, no credit has been taken for the microbial consumption of organic ligands. Other mechanisms for reducing the effect of organic ligands are discussed in Section 5.0.

- Production of humic and microbial colloids.

SOTERM-2.2.3 Anoxic Corrosion of Steels and Other Iron-Base Alloys

The corrosion of steels, other Fe-base alloys, and other metals in the repository will have several effects on the actinide source term. Corrosion is expected to:

- reduce the oxidation states of some actinides, especially Pu, from relatively mobile oxidation states, such as Pu(V) and Pu(VI), to relatively immobile oxidation states, such as Pu(III) and Pu(IV) (Section 4.0);

- produce colloidal corrosion products on which actinides may sorb (see Section 6.0).

It is expected that oxic corrosion of steels and aerobic microbial consumption of CPR materials will quickly consume the limited amount of oxygen (O_2) trapped within the repository at the time of closure. After O_2 is consumed, anoxic corrosion of metals will occur (Brush 1990; Brush 1995; Wang and Brush 1996a. In all of the vectors for the CRA-2004 PA, the EPA's 1997 Performance Assessment Verification Test (PAVT), and the CCA PA, there were significant amounts of uncorroded steels and other Fe-base alloys in the repository throughout the 10,000-year regulatory period. WIPP-specific experiments (Telander and Westerman, 1993; 1997) showed that steels and other Fe-base alloys will corrode by the following reactions:

$$Fe + (x + 2)H_2O \Leftrightarrow Fe(OH)_2 \cdot xH_2O + H_2; \quad (7)$$

$$3Fe + 4H_2O \Leftrightarrow Fe_3O_4 + 4H_2; \quad (8)$$

$$Fe + H_2O + CO_2 \Leftrightarrow FeCO_3 + H_2; \text{ and} \quad (9)$$

$$Fe + H_2S \Leftrightarrow FeS + H_2. \quad (10)$$

Metal hydroxides such as Fe(II) hydroxide ($Fe(OH)_2 \cdot xH_2O$) are more soluble in the WIPP high-ionic-strength brines than in dilute solutions, and significant amounts of Fe(II) may dissolve. Refait and Genin (1994) estimated Fe(II) solubilities between 10^{-4} and 10^{-6} M for pH between 8.5 and 10.5 under redox conditions expected for the repository. Sagoe-Crentsil and Glasser (1993) observed even higher solubilities at pH 13 with electrolytic dissolution of Fe.

Corrosion of metals will produce reducing conditions in the repository, but redox conditions have not been predicted quantitatively. The repository is not described using Eh, because in low-temperature geochemical systems, equilibria among the many redox couples are generally not attained, and Eh is generally poorly defined. For this reason, the oxidation states of the actinides have been determined experimentally, as described in Section 4.0.

SOTERM-2.2.4 Other Effects

High pressure in the repository after closure will have an insignificant effect on actinide solubilities and the association of actinides with colloids and, therefore, its effect is not included in PA. Temperature within the repository is not expected to change by more than a few degrees from ambient (28 ºC) (Munson et al. 1987; Sanchez and Trellue 1996; Wang and Brush 1996a). Because the effect on solubilities of a few degrees Celsius is insignificant compared to uncertainty of the measurements and modeling of solubilities, temperature effects were also discounted (Section 3.3).

Radiolysis of brine may affect redox conditions in the repository. When energy from radioactive decay is absorbed by H_2O, the H_2O molecule is broken into energetic fragments that reassemble

into oxidized and reduced species. Depending on the chemical reactivity of these species, the system may be effectively more oxidizing or more reducing as a result of the radiolysis. For example, radiolysis often occurs by the following reaction:

$$2H_2O + \text{radiation} = H_2(g) + H_2O_2 \quad (11)$$

Hydrogen peroxide (H_2O_2) is more reactive than hydrogen (H_2) (g) at low temperature, and peroxide redox reactions will affect the system more than the slow H_2 reactions. If the system is initially very oxidized, H_2O_2 will cause a reduction in the effective redox state, but if the system is initially very reduced, the peroxide will cause oxidation. In the WIPP, it is expected that the repository will be quite reducing due to the large amount of metallic Fe and dissolved Fe(II) species. Any oxidized species such as H_2O_2 generated from radiolysis are expected to quickly react with the metallic Fe and Fe(II), thus negating any oxidizing effect of radiolysis. Therefore, radiolysis is not expected to affect the redox state of the repository significantly.

Other components of the waste may influence the concentration of dissolved actinides within the repository. These include, for example, organic ligands (Section 5.0); other salts such as calcium chloride ($CaCl_2$), which may raise the ionic strength of the brine; vermiculite, which may sorb actinides; and phosphate (PO_4^{3-}), which may precipitate insoluble actinide phosphates. The effects of most of these components are assumed beneficial and would be difficult to quantify, so they were not included in PA.

SOTERM-2.2.5 Summary

Chemical conditions in the repository will be affected by whether brine is present (humid or inundated conditions) and the type of brine (Salado or Castile); microbial consumption of CPR materials, which will produce mainly methane (CH_4) and CO_2, and colloidal particles; MgO , which will control f_{CO_2} and pH; and corrosion of steels, other Fe-base alloys, and other metals in the repository, which will create reducing conditions.

SOTERM-3.0 PREDICTION OF DISSOLVED ACTINIDE SOLUBILITIES

This section describes the basic approach used to predictactinide solubilities for the CRA-2004 PA. Surveys of different possible conceptual and mathematical descriptions of the system are presented, followed by a more detailed discussion of the method selected.

The material in this section is intended to provide an overview of the modeling methods. More detailed descriptions can be found in the references.

SOTERM-3.1 Previous Approaches to Estimating Actinide Solubilities in the WIPP

Brine flow through the repository was not considered early in the WIPP Project because brine was not expected to enter the repository (see CCA Appendix MASS, Section MASS.2). When it was realized that brines from a variety of sources might enter the repository, scenarios involving brine flow were developed. These scenarios necessitated the investigation of potential

mobilization mechanisms, including dissolution of actinides in high-ionic-strength aqueous solutions applicable to WIPP brines.

The solubilities of actinides in WIPP brines were initially estimated by an expert panel that reviewed the existing literature on actinide solubilities (Trauth et al. 1992). The range of solubilities obtained was about 14 orders of magnitude because the chemical conditions surveyed included extremes of acidity and other conditions. With the addition of MgO and the demonstration of reducing conditions, it was realized that these extreme conditions would not occur in the WIPP. The expert panel also estimated the effect of high CO_3^{2-} concentrations, which are known to increase actinide solubilities significantly, despite the paucity of data for CO_3^{2-}-bearing solutions. Median solubilities developed by the panel were Th: 10^{-10} M; U: 10^{-3} M; Np: 10^{-7} M; Pu: 10^{-9} M; and Am and Cm: 10^{-9} M (Trauth et al. 1992, p. 4-5; Hobart et al. 1996). Published studies of actinides under environmental conditions have focused on actinides in surface waters and groundwaters that are considerably more dilute than WIPP brines, which contributed to the wide range of solubility estimates because more pertinent data were unavailable.

Experimental investigations for other radioactive waste projects (for example, Nitsche 1987) have measured the solubilities of actinides directly. Although this is possible for well-characterized and homogeneous waste and groundwaters, the waste intended for the WIPP is heterogeneous, and a relatively wide range of chemical conditions would be possible in the repository without MgO. Measuring solubilities directly in experiments using transuranic (TRU) waste and ensuring that the measurements reflect steady-state WIPP conditions would entail an extremely large number of measurements and considerable uncertainty. This approach was determined to be neither practical nor feasible. The DOE therefore decided to estimate actinide solubilities by using a thermodynamic model based on experimental parameterization.

SOTERM-3.2 Selection of the Pitzer Activity-Coefficient Model

The thermodynamic activity of a dissolved species is the product of its actual concentration and an activity coefficient. In dilute aqueous solutions, the activity coefficient is close to unity, but in high-ionic-strength solutions such as WIPP brines, the activity coefficient may deviate significantly from unity.

The calculation of activity coefficients is the central feature of thermodynamic models in concentrated electrolyte systems. Activity coefficients represent the deviation from the nearly ideal behavior observed or assumed in dilute solutions. Aqueous-electrolyte activity-coefficient models generally include the Debye-Hückel limiting law (see, for example, Pitzer 1991, 59 et seq.) to describe behavior in the dilute region (<0.1 m), and often include one or more adjustable parameters to reproduce measured behavior in more concentrated solutions.

Numerous activity-coefficient models for concentrated electrolytes have been proposed, including the Pitzer model (Pitzer 1991, Chapter 3), Harned's Rule (Wood 1975), and the Specific-Ion Interaction Theory (SIT) (Grenthe and Wanner 1992), given in order of approximately decreasing mathematical complexity. The Pitzer activity-coefficient model contains parameters that explicitly represent the contributions to the excess free energy from every two-moiety and three-moiety interaction, where a moiety is a cationic, anionic, or neutral

aqueous species. The Harned's-Rule model asserts that the "logarithm of the activity coefficient of one electrolyte in a mixture of constant total molality is directly proportional to the molality of the other component" (Robinson and Stokes 1959, 438), and thus by extension to multicomponent systems containing parameters for two-moiety interactions. The SIT model contains parameters for two-moiety cation-anion interactions.

A primary consideration for selecting an activity-coefficient model to predict actinide solubilities in the WIPP was the demonstrated applicability of existing models and databases to the brines and evaporite minerals at WIPP. The Pitzer model, especially as parameterized by Harvie et al. (1980a), Harvie et al. (1984), and Felmy and Weare (1986), includes an established database describing solubilities in the hydrogen-ion- (H^+)-B-Na^+-Mg^{2+}-K^+-Ca^{2+}-OH^--bicarbonate-(HCO_3^-) CO_3^{2-}-SO_4^{2-}-Cl^--H_2O-CO_2 system. This system includes the significant nonradioactive constituents of WIPP brines. The Harned's-Rule model has been parameterized for the Na^+-Mg^{2+}-K^+-Ca^{2+}-Cl^- and Na^+-Mg^{2+}-SO_4^{2-}-Cl^- systems (Wood 1975), but does not include CO_3^{2-}, one of the most important actinide complexants in aqueous systems. The SIT model (Grenthe and Wanner 1992) is most commonly used for extrapolating apparent stability constants to zero ionic strength. No demonstrations that the SIT model has been applied to multicomponent, concentrated electrolytes such as brine-evaporite-mineral systems have been identified in the literature.

The chemical behavior of the concentrated brines that occur in evaporites like those at WIPP has been extensively studied and documented. The applications of the Harvie et al. (1980a), Harvie et al. (1984), and Felmy and Weare (1986) parameterization of the Pitzer model include: prediction of the mineral-precipitation sequence accompanying seawater evaporation (Eugster et al. 1980; Harvie et al. 1980b); the formation of borate minerals in Searles Lake, CA (Felmy and Weare 1986); and an analysis of Permian seawater composition based in part on fluid-inclusion data from the Salado (Horita et al. 1991). Additional applications are given in Pitzer (1991, Chapters 6 and 7).

WIPP brines range from about 0.8 m to 8 m in ionic strength. The Pitzer model is developed for and has been shown to work for electrolytes as concentrated as those at WIPP, and has been applied successfully to brines with concentrations greater than 10 m (Felmy and Weare 1986). Rather than develop a new description of the chemical behavior of the nonradioactive constituents of WIPP brines, it was decided to use the Harvie et al. (1984)/Felmy and Weare (1986) (HMW/FW) parameterization of the Pitzer model as the reference activity-coefficient model and thermodynamic database for the WIPP actinide source term. Additional research for the WIPP focused on extending the database to include the actinides that could affect the long-term performance of the WIPP and the organic ligands that could affect the solubilities of these actinides (see Section 5.0).

SOTERM-3.3 The Fracture-Matrix Transport Computer Code

The solubility and speciation code Fracture-Matrix Transport (FMT) (Babb and Nowak 1997 and addenda) uses the Pitzer activity-coefficient model to calculate the solubilities of the actinide elements in equilibrium with the appropriate solubility-controlling solids in WIPP brines by minimizing the Gibbs free energy of the system. Where appropriate parameters already existed in the HMW/FW database, they have been used in FMT calculations for the WIPP. Additional

parameters, most notably those for dissolved actinide species, have been obtained from the literature or determined from experimental data (see Section 3.4) using the NONLIN code (Novak 1995; WIPP Performance Assessment Department 1996). NONLIN calculates the Pitzer parameters using a nonlinear least-squares fitting program.

The FMT calculations were done for three actinides: Am(III), Th(IV), and Np(V) that are oxidation-state analogs for actinides in the +III, +IV, and +V oxidation states, respectively. Because actinides in the same oxidation state exhibit similar chemical behavior, these FMT model calculations apply to all actinides in the same oxidation state; for example, the Am(III) speciation and solubility model applies to Pu(III); the Th(IV) model applies to U(IV), Np(IV), and Pu(IV); and the Np(V) model applies to Pu(V). However, Pu will not persist to a significant extent in the +V oxidation state (or the +VI oxidation state) in the WIPP (see Section 4.6.)

The dissolved concentrations of the actinides Th, U, Np, Pu, and Am will be limited by solubility-controlling solid for each of these actinides in WIPP brines. The important ions in WIPP brines are H^+, Na^+, Mg^{2+}, K^+, Ca^{2+}, OH^-, CO_3^{2-}, SO_4^{2-}, and Cl^-. Other ions, for example, fluoride (F^-), aluminum (Al^{3+}), PO_4^{3-}, Fe^{2+}, and Fe^{3+}, may affect actinide solubilities significantly. Pitzer parameters for these other ions are not included in the dissolved species and source term model, but enhance understanding of the chemical environment. For example, phosphates are known to precipitate actinides (Cotton and Wilkinson 1988), but this effect has conservatively been ignored due to the uncertainty of the phosphate inventory in the WIPP and the lack of a complete set of Pitzer parameters for its inclusion. The existence of Fe(II) from the anoxic corrosion of steels and other Fe-base alloys is accounted for in the oxidation state distribution (see Section 4.0), but is expected to have an insignificant effect on the solubilities of individual actinide oxidation state and distribution.

The expected temperature of the WIPP disposal rooms during the 10,000-year regulatory period is not expected to change by more than a few degrees from ambient (28 ºC) (Munson et al. 1987; Sanchez and Trellue 1996; Wang and Brush 1996). The small differences in thermodynamic properties caused by these changes are well within acceptable uncertainty for the WIPP system. For these reasons, the small differences in properties over this temperature range are not significant for the WIPP, and all information was developed for 25°C. Literature information taken at approximately 20°C was deemed acceptable for model parameterization as well.

The development of the +III, +IV, and +V actinide solubility models consisted largely of the development of a database that includes the standard chemical potentials of the aqueous and solid actinide-bearing species, and the ion-interaction parameters required to describe the interactions between these species and other constituents of WIPP brines. The following sections describe briefly how this database was built and how the needed parameters were obtained. The development of the oxidation-state distributions reflected in these sections is discussed in Section 4.0.

Section 3.4 provides a guide to the information that is needed to predict actinide solubilities. The FMT database currently used to predict the solubilities of the +III, +IV, and +V actinides is documented in Giambalvo (2002a, 2002b, 2002c, 2002d, 2002e, 2003).

SOTERM-3.4 Overview of the Experimental Data

Studies of the solubilities and speciation of actinides, especially Pu, are often conducted by employing the oxidation-state analogy, which states that lanthanides and actinides in the same oxidation state have similar chemical behavior. There are several important advantageous aspects of the use of oxidation-state analogs, such as Th(IV) for Pu(IV). Redox-inert analogs can considerably simplify experimental design and consequently improve reliability of experimental data, in contrast to Pu, which can be a very labile experimental component. Additionally, the lanthanide and actinide analogs possess physical and chemical characteristics that allow them to be used as probes in examination of the chemical behavior of Pu. For example, the luminescence lifetime of europium(III) (Eu(III)) can be directly correlated to the number of H_2O molecules in the inner coordination sphere, which allows interpretation of the nature of complexation of the trivalent lanthanides and actinides with ligands.

The 4f orbitals of the lanthanides and 5f orbitals of the actinides constitute the valence shells of the cations. The f orbitals are more diffuse than the p and d orbitals, and, upon ionization of the atom, become lower in energy than the 5d, 6s, and 6p orbitals in the case of the lanthanides, and comparable or slightly lower than the 6d, 7s, and 7p orbitals in the case of the actinides. The contraction of the radial component of the wave function of the f orbitals upon ionization of the element usually causes these orbitals to be unavailable for overlap with orbitals on other atoms, one of the conditions necessary for the formation of molecular orbitals. As a result, the lanthanide and actinide ions exhibit very little tendency to form covalent bonds.

Formation of complexes of most ligands with f elements is due to the electrostatic attraction between the metal cation and the electron-donating functionality of the ligand molecule. The effect of polarizability and Lewis acidity or basicity on formation of Lewis-acid or Lewis-base pairs has been described by Pearson (1963). Lanthanide and actinide cations, which have high charge density and low polarizability, are classified as hard cations. Similarly, ligands featuring O-donor atoms, such as citrate and oxalate, exhibit low polarizability and strong Lewis basicity, and are referred to as hard bases. Hard-acid metals interact with hard bases through electrostatic attraction. The stability of f-element complexes with many ligands is a function of the charge density on the donor atom. For example, progressively weaker Brönsted-Lowry acids (in order of increasing pKa: trichloroacetic < dichloroacetic < monochloroacetic < acetic acids) have progressively stronger conjugate bases due to increased electron density located on the carboxylic O's. As a result, the electrostatic attraction between the O and protons increases, resulting in weaker acidic behavior and corresponding increases in pKa values. Likewise, the force of electrostatic attraction between the carboxylate group and a metal ion increases with increasing basicity of the ligand.

The magnitude of electrostatic attraction between the f-element cations and ligands is dependent upon the local effective dielectric constant of the solution, the charge on the metal ion, and the distance of separation between the metal atom and the ligating atoms on the complexing agent. The magnitude of the local dielectric constant of the solution depends upon the ordering effect created by the electric-field gradient established by the cation. The charge densities of lanthanides and actinides with the same charge are similar enough that the responses of solvent molecules are similar, yielding local dielectric constants that are nearly constant for lanthanide

and actinide cations with the same charge. The local dielectric constant is primarily dependent upon the charge of the ion; the variation due to the effect of different-magnitude electric-field gradients that result from the differences in ionic radii are small enough to be overlooked to a first approximation in the oxidation-state-analogy approach.

The factors that exert a much more pronounced influence are the ionic radii, charge on the metal ion, and, to a lesser extent, degree of solvation of the metal ion. The Gibbs free energy of complex formation is inversely proportional to the distance between the metal and ligand, and directly proportional to the product of the numerical value of the electrostatic charges on the cation and anion. There are variations in the ionic radii of lanthanide and actinide ions that have the same charge, with decreasing ionic radii corresponding to increasing atomic number within the 4f and 5f series. However, the ionic radii of some of the metal ions are very similar. For example, neodymium ion (Nd^{3+}) and Am^{3+} have nearly identical ionic radii. As a result, the behavior of Nd(III) and Am(III) are very similar, with small differences attributable to the fact that the 5f orbitals of Am are closer in energy to the 6d, 7s, and 7p orbitals than the 4f orbitals of Nd are to the 5d, 6s, and 6p orbitals. Discussions of applications to the +III, +IV, +V, and +VI actinide oxidation states follow.

SOTERM-3.4.1 The +III Lanthanides and Actinides

The actinides most likely to occur in the +III oxidation state in the WIPP are Pu, Am, and Cu. Nd(III), Eu(III), Pu(III), Am(III), and Cu(III) have been widely used in studies of trivalent f-element chemical behavior in brines. The respective ionic radii for coordination number (CN) = 8 are 111, 17, 100, 109, and 97 pm (Shannon 1976). Due to the similarity of ionic radii, the magnitude of the electrostatic attraction between the metal ions and corresponding ligands is similar, yielding comparable thermodynamic stabilities. Each of the analog elements offers noteworthy advantages in probing various aspects of trivalent f-element solution behavior. For example, Nd(III) features hypersensitive absorption bands that respond to changes in the complexation environment, allowing examination of the nature of the metal-ligand interaction. The luminescence lifetime of Eu(III) can be used to measure the number of residual waters of hydration associated with the metal ion after formation of a complex. ^{241}Am, which has a 433-year half-life, undergoes α decay that is accompanied by 59.5-keV γ ray with a 35.9-percent yield. As a result, ^{241}Am may be used at tracer concentrations by well-developed radiochemical techniques, such as solvent extraction and ion exchange, as a means to study the thermodynamic behavior of trivalent actinides. Study of the solution behavior of Am(III) is uncomplicated by redox ability, unlike the situation for Pu(III), which requires Eh and pH controls of the solution to maintain a single oxidation state. Like Nd and Eu, Cu luminescence studies are useful to examine the coordination environment of the metal ion. Pu(III) does not have useful luminescence properties, making it impossible to study its complexation behavior by methods that are effective with the analogs.

The thermodynamic database for the +III actinides currently used in FMT was described by Giambalvo (2002a). Due to the redox ability of Pu, much of the experimental work carried out to develop an understanding of the chemical behavior of the +III actinides, particularly Pu, has been performed with Nd, Am, and Cm due to the stability of the trivalent oxidation states of these three elements. Speciation and solubility data for the +III actinides were parameterized for

use in the Pitzer activity-coefficient model by Felmy et al. (1989) for the Na^+- Pu^{3+}-Cl^--H_2O system; by Felmy et al. (1990) for the Na^+-Am^{3+}-OH^--HCO_3^--H_2O system; by Rai et al. (1995) for the Na^+-Am^{3+}-PO_4^{3-}-SO_4^{2-}-H_2O system; and by Rao et al. (1996) for the Na^+-Nd^{3+}-CO_3^{2-}-HCO_3^--H_2O system. The inorganic aqueous and solubility-limiting species featured in the model for Am(III) are:

$$Am^{3+} + CO_3^{2-} \rightleftharpoons AmCO_3^+; \quad (12)$$

$$Am^{3+} + 2CO_3^{2-} \rightleftharpoons Am(CO_3)_2^-; \quad (13)$$

$$Am^{3+} + 3CO_3^{2-} \rightleftharpoons Am(CO_3)_3^{3-}; \quad (14)$$

$$Am^{3+} + 4CO_3^{2-} \rightleftharpoons Am(CO_3)_4^{5-}; \quad (15)$$

$$Am^{3+} + OH^- \rightleftharpoons AmOH^{2+}; \quad (16)$$

$$Am^{3+} + 2OH^- \rightleftharpoons Am(OH)_2^+; \quad (17)$$

$$Am^{3+} + 3OH^- \rightleftharpoons Am(OH)_3(aq); \quad (18)$$

$$Am^{3+} + Cl^- \rightleftharpoons AmCl^{2+}; \quad (19)$$

$$Am^{3+} + 2Cl^- \rightleftharpoons AmCl_2^+; \quad (20)$$

$$Am^{3+} + SO_4^{2-} \rightleftharpoons Am(SO_4)^-; \quad (21)$$

$$Am^{3+} + 2SO_4^{2-} \rightleftharpoons Am(SO_4)_2^+; \quad (22)$$

$$Am^{3+} + OH^- + CO_3^{2-} \rightleftharpoons AmOHCO_3(s); \quad (23)$$

$$Na^+ + Am^{3+} + 2CO_3^{2-} + 6H_2O \rightleftharpoons NaAm(CO_3)_2 \cdot 6H_2O(s); \text{ and} \quad (24)$$

$$Am^{3+} + PO_4^{3-} \rightleftharpoons AmPO_4(cryst). \quad (25)$$

In these equations, "aq," "cryst," and "s" are the abbreviations for "aqueous," crystalline," and "solid," respectively. The actinide(III) database was extended to mixed Na^+-CO_3^{2-}-Cl^-- media, and was shown to reproduce the independently measured solubility of $NaAm(CO_3)_2(s)$ in 5.6 M NaCl (Runde and Kim 1994) and Nd(III) solubility in WIPP brines.

SOTERM-3.4.2 The +IV Actinides

The tetravalent actinides important to WIPP performance are Th(IV), U(IV), and Pu(IV). Np is not included in the WIPP actinide source term, but has been included in the WIPP Actinide Source Term Program (ASTP). The +IV oxidation state is the only stable one in aqueous solution for Th, whereas U(IV) and Np(IV) are both readily oxidized. As a result, Th is often used to represent the behavior of the +IV actinides. Th(IV) does not have spectroscopic characteristics that are valuable in its study, but does have both long-lived (^{232}Th, $t_{1/2}$ = 1.41×10^{10} year) and shorter-lived (^{228}Th and ^{230}Th $t_{1/2}$ = 1.913 and 7540 year, respectively)

isotopes that are useful in thermodynamic studies. The 105-pm ionic radius of the Th(IV) cation (C. N. = 8) is greater than the 96 pm Pu(IV) cation (Shannon 1976), resulting in complexation properties that vary in a systematic and predictable manner. The larger ionic radius of Th(IV) causes it to have complexes with stability constants lower than the corresponding complexes with Pu(IV). For example, the Pu(IV) complexes with OH^-, resulting from hydrolysis, have higher stability constants than Th(IV)-OH^- complexes. The actinide(IV) hydrolysis products are sufficiently stable that organic ligands present within the WIPP, (see Section 5.0) will be unable to effectively compete with OH^-. The net effect is that actinide(IV) complexation is dominated by OH^-, which forms very insoluble tetrahydroxide ($An(OH)_4$) precipitates. Pu has a pronounced tendency to form insoluble hydrolysis products that are less soluble than the corresponding Th(IV) oxides and hydroxides. The greater solubility of Th(IV) makes it a very good analog for Pu(IV) in the context of modeling the behavior of tetravalent actinides in the WIPP because the solubility of Th(IV) establishes an upper limit for the solubility of Pu(IV). Due to the experimental difficulty working with Pu(IV), it is more straightforward and defensible to establish upper limits rather than attempting to measure the solubility of Pu(IV) directly.

The thermodynamic database for the +IV actinides currently used in FMT was described by Giambalvo (2002c). Speciation and solubility data for Th(IV) were parameterized for the Pitzer activity-coefficient model for the Na^+-K^+-Mg^{2+}-Cl^--SO_4^{2-}-CO_3^{2-}-HCO_3^--OH^--H_2O system. The inorganic aqueous and solubility-limiting species featured in the model are:

$$ThO_2(am) + 2H_2O \rightleftharpoons Th(OH)_4(aq); \quad (26)$$

$$Th^{4+} + 4OH^- \rightleftharpoons Th(OH)_4(aq); \quad (27)$$

$$Th^{4+} + 3OH^- + CO_3^{2-} \rightleftharpoons Th(OH)_3CO_3^-; \quad (28)$$

$$Th^{4+} + 5CO_3^{2-} \rightleftharpoons Th(CO_3)_5^{6-}; \quad (29)$$

$$Th^{4+} + 2SO_4^{2-} \rightleftharpoons Th(SO_4)_2(aq); \quad (30)$$

$$Th^{4+} + 3SO_4^{2-} \rightleftharpoons Th(SO_4)_3^{2-}; \quad (31)$$

$$Th^{4+} + 2SO_4^{2-} + 9H_2O \rightleftharpoons Th(SO_4)_2 \bullet 9H_2O(s); \quad (32)$$

$$Th^{4+} + 2SO_4^{2-} + 8H_2O \rightleftharpoons Th(SO_4)_2 \bullet 8H_2O(s); \quad (33)$$

$$Th^{4+} + 2Na^+ + 3SO_4^{2-} + 6H_2O \rightleftharpoons Th(SO_4)_2 \bullet Na_2SO_4 \bullet 6H_2O(s); \quad (34)$$

$$Th^{4+} + 2K^+ + 3SO_4^{2-} + 4H_2O \rightleftharpoons Th(SO_4)_2 \bullet K_2SO_4 \bullet 4H_2O(s); \quad (35)$$

$$Th^{4+} + 4K^+ + 4SO_4^{2-} + 6H_2O \rightleftharpoons Th(SO_4)_2 \bullet 2K_2SO_4 \bullet 2H_2O\ (s); \text{ and} \quad (36)$$

$$Th^{4+} + 7K^+ + 5.5SO_4^{2-} \rightleftharpoons Th(SO_4)_2 \bullet 3.5K_2SO_4(s). \quad (37)$$

SOTERM-3.4.3 The +V Actinides

Both Np and Pu have accessible +V oxidation states; however, Pu(V) is not expected to persist in significant quantities in the WIPP. The model for Np(V) was developed for the German repository program (Fanghänel et al. 1995). The speciation and solubility of Np(V) were parameterized for the Na^+-Cl^--CO_3^{2-}-ClO_4^--H_2O system.

The thermodynamic database for the +V actinides currently used in FMT is described by Giambalvo (2002d). Np(V) speciation and solubility were parameterized in the Pitzer activity-coefficient model for the Na^+-K^+-Mg^{2+}-Cl^-- SO_4^{2-}-CO_3^{2-}-HCO_3^- -OH^--H_2O system. The inorganic aqueous and solubility limiting species used are:

$$NpO_2^+ + OH^- \rightarrow NpO_2OH(aq); \quad (38)$$

$$NpO_2^+ + OH^- \rightarrow NpO_2OH(s, am); \quad (39)$$

$$NpO_2^+ + OH^- \rightarrow NpO_2OH(s, aged); \quad (40)$$

$$NpO_2^+ + 2OH^- \rightarrow NpO_2(OH)_2^-; \quad (41)$$

$$NpO_2^+ + CO_3^{2-} \rightarrow NpO_2CO_3^-; \quad (42)$$

$$NpO_2^+ + 2CO_3^{2-} \rightarrow NpO_2(CO_3)_2^{3-}; \quad (43)$$

$$NpO_2^+ + 3CO_3^{2-} \rightarrow NpO_2(CO_3)_3^{5-}; \quad (44)$$

$$Na^+ + NpO_2^+ + CO_3^{2-} + 3.5H_2O \rightarrow NaNpO_2CO_3 \cdot 3.5H_2O(s); \quad (45)$$

$$3Na^+ + NpO_2^+ + 2CO_3^{2-} \rightarrow Na_3NpO_2(CO_3)_2(s); \quad (46)$$

$$K^+ + NpO_2^+ + CO_3^{2-} \rightarrow KNpO_2CO_3(s); \text{ and} \quad (47)$$

$$3K^+ + NpO_2^+ + 2CO_3^{2-} + 0.5H_2O \rightarrow K_3NpO_2(CO_3)_2 \cdot 0.5H_2O(s). \quad (48)$$

SOTERM-3.4.4 The +VI Actinides

The actinide(VI) speciation and solubility model for brines under basic conditions has not been developed sufficiently for use in FMT. The hydrolysis behavior of U(VI) is quite complicated and no satisfactory predictive models applicable to WIPP conditions are available. As documented in Hobart and Moore (1996), the solubility of U(VI) at pH 10, in the absence of CO_3^{2-}, was estimated to be 8.8×10^{-5} m.

SOTERM-3.5 Calculations of Actinide Solubilities Using the Fracture-Matrix Transport Computer Code

Details of the solubility calculations for the +III, +IV, and +V actinides and the estimation of the solubility of +VI actinides for the CRA-2004 PA are given in Brush and Xiong (2003a, 2003b, 2003c) and Downes (2003a, 2003b).

The FMT calculations of actinide solubilities for the CRA-2004 PA featured the establishment of equilibrium of Salado brine (GWB) or Castile brine (ERDA-6) with halite, and anhydrite, minerals present in large quantities in the Salado at the repository horizon. The effects of MgO included equilibration of Salado brine or Castile brine with brucite and hydromagnestie ($Mg_5(CO_3)_4(OH)_2 \cdot 4H_2O$) in the PA vectors with microbial activity, and with brucite and calcite in the vectors without microbial activity (see Reactions (4), (5), and (6) above; and Appendix BARRIERS, Section BARRIERS-2.3). For the CCA, it was assumed that Salado brine (Brine A) or Castile brine (ERDA-6) would be in equilibrium with brucite and magnesite ($MgCO_3$) in all of the PA vectors (both with and without microbial activity) (ERDA-6). For the 1997 PAVT, equilibria among Salado brine (Brine A) or Castile brine (CCA Appendix SOTERM; CCA Appendix BACK) and brucite and hydromagnesite ($Mg_5(CO_3)4(O4)_2 \bullet 4H_2O$) was assumed (EPA 1998a, 1998b).

The FMT calculations for the CRA-2004 PA also included the effects of acetate, citrate, EDTA, and oxalate on the speciation and solubilities of the +III, +IV, and +V actinides (see Section 5.0 below).

Table SOTERM-2 provides the solubilities calculated for the +III, +IV, and +V actinides and estimated for the +VI oxidation state for the CRA-2004 PA, and compares them to the solubilities calculated or estimated for the CCA PA and the 1997 PAVT.

SOTERM-3.6 Use of Fracture-Matrix Transport Results in Performance Assessment

Table SOTERM-2. Actinide Solubilities (M) Calculated (+III, +IV, and +V) or Estimated (+VI) for the CRA-2004 PA, the 1997 PAVT, and the CCA PA

Actinide Oxidation State and Brine	CRA Solubilities, Microbial Vectors[1]	CRA Solubilities, Nonmicrobial Vectors[1]	PAVT Solubilities[2]	CCA Solubilities[3]
+III, Salado brine	3.07×10^{-7}	3.07×10^{-7}	1.2×10^{-7}	5.82×10^{-7}
+III, Castile brine	1.69×10^{-7}	1.77×10^{-7}	1.3×10^{-8}	1.3×10^{-8}
+IV, Salado brine	1.19×10^{-8}	1.24×10^{-8}	1.3×10^{-8}	4.4×10^{-6}
+IV, Castile brine	2.47×10^{-8}	5.84×10^{-9}	4.1×10^{-8}	6.0×10^{-9}
+V, Salado brine	1.02×10^{-6}	9.72×10^{-7}	2.4×10^{-7}	2.3×10^{-6}
+V, Castile brine	5.08×10^{-6}	2.13×10^{-5}	4.8×10^{-7}	2.2×10^{-6}
+VI, Salado brine[4]	8.7×10^{-6}	8.7×10^{-6}	8.7×10^{-6}	8.7×10^{-6}
+VI, Castile brine[4]	8.8×10^{-6}	8.8×10^{-6}	8.8×10^{-6}	8.8×10^{-6}

[1] Brush and Xiong (2003a, 2003b) and Downes (2003a, 2003b).
[2] Trovato (1997, Attachment 2), EPA (1998a, Table 5), EPA (1998b, Subsection 4.10.4, Tables 4.10-1, 4.10-3 and 4.10-4; and Subsection 12.4, Table 12.4-1), and EPA (1998c, Subsections 5.26–5.32 and Section 6.0, Table 6.4).
[3] CCA Appendix SOTERM, Table SOTERM-2; based on Novak et al. (1996, Table 1, columns entitled "@Mg"), except that Novak et al. (1996) used molal instead of molar units.
[4] Hobart and Moore (1996).

Uncertainties in the solubility data and the NONLIN least squares refinement result in uncertainties in the model predictions. This is evident when the data of Runde and Kim (1994) are compared with FMT model results. A measure of these uncertainties was obtained by Bynum (1996) by examining the differences between the modeled solubilities for each oxidation-state analog and comparing these to the experimental data used to generate the respective Pitzer parameters. The results of Bynum's analysis are given in Figure SOTERM-1. These results were combined as shown in Figure SOTERM-2 for entry into the parameter database as a cumulative distribution. This distribution was sampled in PA, as discussed in Section 7.1.3. Note that the median of this distribution is -0.09 and not zero, indicating that slightly more experimental values were below the model predictions than above.

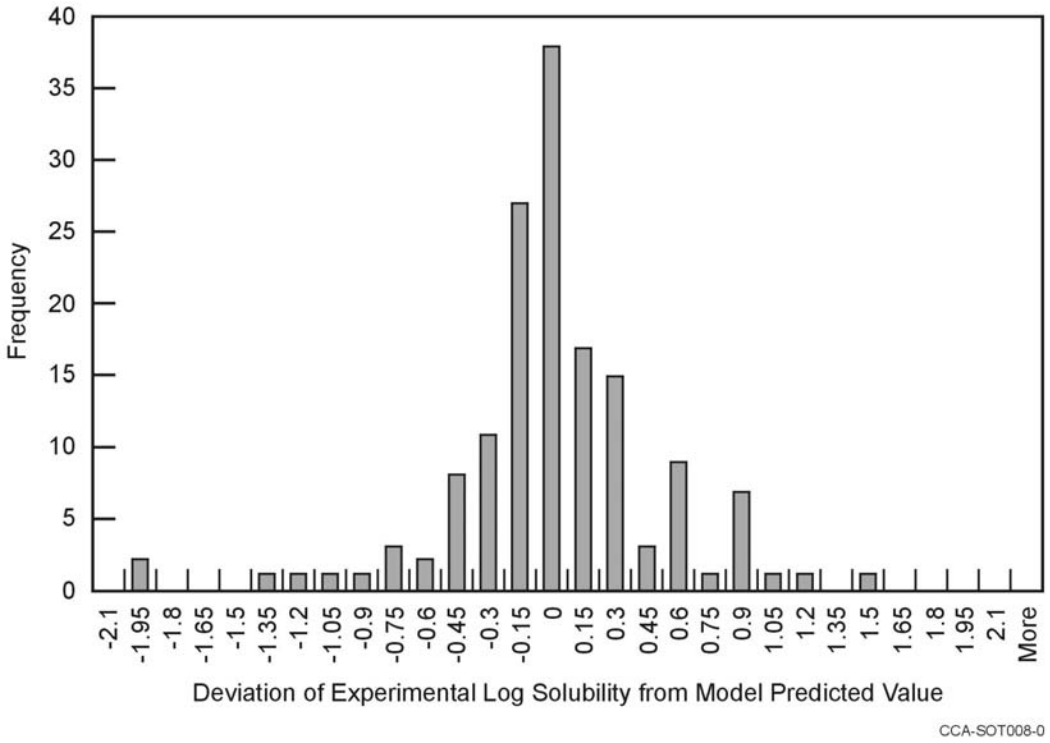

Figure SOTERM-1. Deviation of the log of 150 Experimental Solubilities from the Values Predicted by the Model.

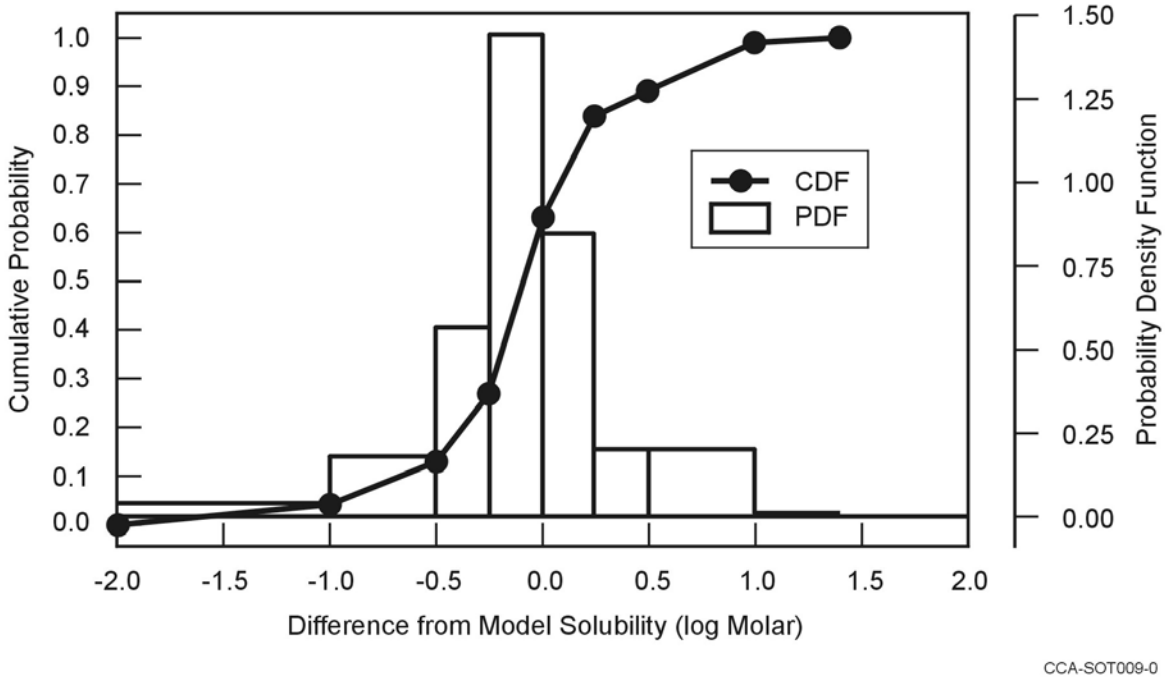

Figure SOTERM-2. Distribution of Actinide-Solubility Uncertainty Utilized in the CRA-2004 Performance Assessment.

SOTERM-4.0 OXIDATION-STATE DISTRIBUTION OF DISSOLVED ACTINIDES

This section describes the literature investigation and experimental program that identified the actinide oxidation states most likely to be stable under expected WIPP conditions.

SOTERM-4.1 Thorium

Th is a very electropositive metal, and Th(IV) is the only stable oxidation state in aqueous solutions and in the natural environment (Hobart 1990; Katz et al. 1986). Conditions in the WIPP cannot produce any other oxidation state of Th.

SOTERM-4.2 Uranium

U can exist in aqueous solution in the +III, +IV, +V, and +VI oxidation states (Hobart 1990; Keller 1971; Clark et al. 1995). The predominant oxidation states for U in the natural environment are +IV and +VI. U(III) may be prepared in aqueous solution but is easily oxidized to U(IV) (Katz et al. 1986, 1139 and following).

The standard reduction potential of U favors reduction of U(V) to U(IV) in aqueous solution, and the pentavalent oxidation state is the least stable oxidation state in solution. U(V) disproportionates in acidic aqueous solution by the reaction:

$$2UO_2^{+} + 4H^{+} \rightarrow UO_2^{2+} + U^{4+} + 2H_2. \quad (49)$$

However, the U(VI) species UO_2^{2+} is the most stable in low concentrations in the pH 2 to 4 range (Katz et al. 1986).

It is the disproportionation reaction of U(V) that limits it to trace level concentrations. U(VI) is a stable oxidation state, even under mildly reducing conditions, but may be reduced to U(IV) by a variety of reducing agents. In the chemically reducing environment expected in the WIPP, U(VI) will be reduced to U(IV). However, Reed et al. (1996) found that at pH 10 under anoxic conditions, U(VI) is stable as a CO_3^{2-} complex in simulated WIPP brines. U(IV) is the predominant oxidation state in half of the PA vectors, and U(VI) in the other half, due to uncertainty predicting the more stable oxidation state of U under WIPP conditions.

SOTERM-4.3 Neptunium

In the natural environment, Np may exist in the +IV, +V, and +VI oxidation states (Hobart 1990; Keller 1971; Clark et al. 1995). In the WIPP, Np(IV) is expected to be present (Rai and Strickert 1980; Rai et al. 1982; Kim et al. 1985; Pryke and Rees 1986). Np(V) appears to be the dominant oxidation state in natural groundwater (Hobart 1990). Nitsche and Edelstein (1985) observed that Np(V) is the most stable oxidation state in Yucca Mountain well water. Studies of the solubility of NpO_2OH in 1 M and 5 M NaCl at pH 6.5 suggest that Np(V) may be reduced to Np(IV) under these conditions (Kim et al. 1985; Neck et al. 1992). Np(VI) may be introduced into the WIPP or be produced by radiolysis, but it will not be stable in WIPP brines that contain or are in contact with reducing agents, such as metallic Fe or Fe(II) oxides and hydroxides. The reduction potential for the Np(VI)-Np(V) couple is +1.24 V in neutral solutions (Martinot and Fuger 1985, 651 et seq.) and +0.6 V in basic solutions (Katz et al. 1986, 470), suggesting that the potential for reduction of Np(VI) to Np(V) at a pH of about 9 will be about 1 V. Reed et al. (1996) found spectroscopic evidence for reduction of Np(VI) to Np(V) in ERDA-6 brine at pH 10, and observed total reduction of Np(VI) to Np(V) in G-Seep brine at pH 7. In the presence of organic ligands (see Section 5.0), Reed et al. (1996) observed rapid and complete reduction of Np(VI) to Np(V). Neck et al. (1995) showed Np(V)-CO_3^{2-} complexes to be stable in 5 M NaCl.

In order to capture the uncertainty in the redox speciation of Np, Np(IV) would be the dominant oxidation state in half of the PA vectors and Np(V) in the other half. However, Np is not transported in PA.

SOTERM-4.4 Plutonium

Pu can exist in the +III, +IV, +V, +VI, and +VII oxidation states (Katz et al. 1986, 781). Pu(III) is the favored oxidation state in acidic solutions, but oxidation of Pu(III) to Pu(IV) becomes progressively easier with increasing pH. This occurs because Pu(IV) features a very strong tendency to undergo hydrolysis, which has the effect of reducing the solution concentration of the free Pu(IV) ion Pu^{4+}. As the pH of a Pu solution is raised from acidic to neutral, Pu(IV) begins to precipitate, resulting in a shift of equilibrium concentrations of Pu(III) to Pu(IV). Consequently, Pu(III) is not a thermodynamically stable oxidation state in the basic environment that will be established by MgO in the WIPP (see Reaction (5) above). Although Pu(III) is unstable under expected WIPP conditions, Felmy et al. (1989) observed Pu(III) in PBB1 and PBB3 brines at neutral and slightly basic conditions.

Pu(V) and Pu(VI) can be produced from Pu(IV) under oxidizing conditions. It is not possible to produce Pu(V) by direct oxidation of Pu(IV) because the oxidation potential that must be applied exceeds the potential required for the oxidation of Pu(V) to Pu(VI). Therefore, in a solution with oxidizing conditions, any Pu(V) that arises from the oxidation of Pu(IV) will be immediately oxidized to Pu(VI). Pu(V) can be produced in solution only by first producing Pu(VI), followed by a carefully controlled reduction of Pu(VI) to Pu(V). Pu(V) may persist in neutral to basic solutions even when it is not the thermodynamically stable oxidation state, due to the reduction reaction's inverse fourth power dependence on the concentration of H^+, which can make the reduction of Pu(V) to Pu(IV) kinetically slow. Neither Pu(V) nor Pu(VI) will persist in significant quantities in the repository, since oxidizing conditions are required to produce them. Pu(VI) was shown to form complexes with Cl^- under oxic conditions in high-ionic-strength NaCl solutions (Clark and Tait 1996). Clark and Tait (1996) and Reed et al. (1996) showed the reduction of Pu(VI) to Pu(IV) by Fe and other reductants under expected WIPP repository conditions. Metallic Fe and Fe^{2+} reduce Pu(VI) in WIPP brines to either Pu(IV) or Pu(III). Clark and Tait (1996) and Felmy et al. (1996) experimentally observed the reduction of Pu(VI)-CO_3^{2-} complexes to Pu(IV) by either metallic Fe or Fe^{2+}. Reduction of Pu(VI) was also observed in the absence of CO_3^{2-}, but the oxidation state of the resulting species was not determined because the concentration was below the analytical detection limit, ca. 10^{-9} M. Neretnieks (1982) showed that dissolved actinides are reduced to a less soluble oxidation state and precipitated from moving groundwater upon coming in contact with Fe(II).

Pu(VII) can be produced in concentrated OH^- solutions that are also highly oxidizing. Pu(VII) will not be formed in the WIPP.

The DOE determined (Weiner 1996) that Pu(IV) will be the dominant oxidation state under WIPP conditions, but the possibility of the existence of Pu(III) cannot be excluded. As a result, Pu is modeled as Pu(III) in half of the PA vectors, and as Pu(IV) in half of the vectors.

SOTERM-4.5 Americium

Am(III) is the most stable aqueous oxidation state of Am (Katz et al. 1986, 912), and will be the only oxidation state of Am in the WIPP. Am(III) is not easily oxidized in aqueous solution (Hobart et al. 1982); however, Am(V) and Am(VI) are accessible at high pH under highly oxidizing conditions. Am(V) and Am(VI) are not stable in natural waters and are readily reduced. Am(V) and Am(VI) can oxidize H_2O, and as a result, they are thermodynamically unstable in aqueous solutions. Am(V) may be formed by oxidation of Am(III) by radiolysis products in NaCl solutions (Runde and Kim 1994), which may occur in microenvironments within WIPP disposal rooms, but Am(V) would not be stable in the homogeneous mixture of waste and brine. Solubility studies carried out by Pryke and Rees (1986) and Felmy et al. (1990) indicated that Am(V) is unstable in brine above pH 9 and reduces to Am(III). These studies also showed significant instability of Am(V) at pH 7. Due to the thermodynamic instability of Am(V) and Am(VI) in aqueous solution, and the lack of a credible mechanism for maintaining the highly oxidizing conditions necessary for persistence of these two oxidation states, Am(III) is the only oxidation state that is used in modeling the speciation and solubility of this element in the repository.

SOTERM-4.6 Curium

Cm is distinguished by the relatively great stability of the +III oxidation state with respect to oxidation or reduction (Katz et al. 1986, 970). The oxidation of Cm(III) is achieved only with the strongest oxidizing agents; one report claims evidence for an oxidation state higher than +IV (Korpusov et al. 1975). The Cm(III)-to-Cm(IV) transition has not been successfully induced by ozone or electrochemically, and the Cm(IV) phosphotungstate produced by oxidizing with peroxysulfate is considerably less stable than the Am(IV) analog (Katz et al. 1986, 971). Cm(III) is the only oxidation state expected to be stable in the WIPP. However, Cm is not transported in PA.

SOTERM-4.7 Summary of Oxidation-State Distributions

Table SOTERM-3 presents the oxidation-state distributions used in the CRA-2004 PA, the CCA PA, and the 1997 PAVT. Np would speciate entirely as Np(IV) in half of the PA vectors and as Np(V) in the other half, but Np is not transported in PA. Cm would speciate identically to Am, but Cm is not transported in PA.

Table SOTERM-3. Actinide Oxidation States Used for the CRA-2004 PA, the 1997 PAVT, and the CCA PA

Actinide Element	Oxidation States			
Th		+IV		
U		+IV		+VI
Pu	+III	+IV		
Am	+III			

SOTERM-4.8 Implications of the Source-Term Waste Test Program for Oxidation-State Distributions of Dissolved Actinides

The Actinide Source Term Waste Test Program (STTP) was an experimental program carried out at Los Alamos National Laboratory (LANL). The objective of the STTP was to examine the behavior of actinides in TRU wastes that will be present in the WIPP. The STTP was conducted by placing samples of various types of wastes from LANL in liter-scale (3-L) and drum-scale (65-gal) titanium (Ti) containers (Scherer and Villarreal 2000, 2001; Scherer et al. 2001a, 2001b, 2001c; Villarreal et al 2000; Villarreal et al. 2001a, 2001b, 2001c, 2001d; Villarreal et al. undated). This discussion focuses on the results from the liter-scale tests.

The samples were composed of process wastes solidified with Portland cement or Envirostone, and pyrochemical salts that resulted from Pu-refining processes. Metallic Fe and Nd, Th, U, Np, and Am were also added. Each waste sample was inundated with about 2 L of either Brine A or ERDA-6.

Pu(V) was identified in two of the liter-scale containers, and Pu(VI) was identified in three of these containers. The DOE's position is that the presence of Fe and other metals within the

WIPP will create and sustain a chemically reducing environment in the event of brine intrusion into the waste-disposal areas. The DOE further concludes that Pu will be maintained in the +III or +IV oxidation state due to the reducing conditions. The observance of Pu(V) and Pu(VI) in the STTP tests was noted by the EPA and the New Mexico Environmental Evaluation Group, which led to reexamination of the DOE position that Pu(V) and Pu(VI) are not expected to persist. The LANL reports on the STTP project consist primarily of process descriptions and extensive compilations of experimental data. The reports do not include extensive discussion of the meaning of the data, or explanations based on thermodynamic or kinetic principles.

Oxidized Pu was never observed in 34 of 39 liter-scale containers or in any of the 15 drum-scale containers, strongly supporting the DOE position that Pu will exist in the +III or the +IV oxidation state under the range of conditions that will exist within the repository. The data tables in the STTP final report are useful for plotting results on a container-by-container basis, to illustrate that in every case in which oxidized Pu was observed, the contents of the containers had not reached either a steady-state behavior or thermodynamic equilibrium. In many cases, first-order kinetic behavior was exhibited for both the solubilization and precipitation of solution components, including Pu. Solubilization of Pu due to oxidation as a consequence of build-up of radiolysis products is not supported by the data. A steady increase in radiolysis products, such as hypochlorite (OCl^-), would result in a steady-state condition of increased Pu(VI) concentrations. The presence of Pu(V) in two containers suggests that a reducing mechanism was available, which led to the reduction of Pu(VI) to Pu(V), followed by a kinetically slow reduction of Pu(V) to Pu(IV). LS-28 and LS-29 were the only two containers that exhibited Pu(VI) in large concentrations that did not decrease over time. However, LS-28 and LS-29 were pressurized with 60 bars of CO_2, and had pcH values about 5 (pH $\approx$ 4), conditions significantly different from those that will exist in the WIPP.

The STTP containers that were more nearly representative of WIPP conditions support the DOE position that oxidized Pu will not persist in the WIPP. The behavior of Nd, Th, U, Np, and Am in the STTP experiments also supports the DOE position that the solubilities of the actinides will be low in the event of brine influx into the repository.

SOTERM-5.0 THE ROLE OF ORGANIC LIGANDS

Organic ligands are present in the waste to be disposed of in the WIPP. Because organic ligands form dissolved complexes with the actinides, they could increase actinide solubilities. Therefore, the effects of these ligands have been included in the FMT calculations of actinide solubilities for the CRA-2004 PA. Organic ligands also form complexes with dissolved, cationic species of several metals that will be present in the repository, and thus metals compete with the actinides for the binding sites on these ligands. Therefore, the competitive effects of dissolved Mg^{2+} and Ca^{2+} have also been included in the solubility calculations for the CRA-2004 PA.

A number of organic ligands are capable of forming strong complexes with actinide ions, thereby increasing actinide solubilities . In general, the reactions that take place for one-to-one complexes are

$$An^{n+} + L^{m-} \rightleftharpoons AnL^{(n+m)}, \quad (50)$$

where An is a general symbol for an actinide, with charge n, and L is a general symbol for an organic ligand with charge m. The apparent stability constant for this reaction is

$$\beta = [AnL^{(n+m)}]/[An^{n+}][L^{m-}] . \quad (51)$$

The square brackets indicate concentrations. The constant β is referred to as astoichiometric stability constant. If activities are used instead of concentrations, β is referred to as the thermodynamic stability constant.

Four organic ligands are included in FMT calculations of actinide solubilities: acetate ($CH_3CO_2^-$), citrate ($(CH_2CO_2)_2C(OH)(CO_2))^{3-}$, ethylenediaminetetraacetate (EDTA, $(CH_2CO_2)_2N(CH_2)_2N(CH_2CO_2)_2^{4-}$), and oxalate ($C_2O_4^{2-}$). These ligands are included in the solubility calculations because: (1) approximately 60 organic compounds were identified among the nonradioactive constituents of the TRU waste to be emplaced in the WIPP (Brush 1990; Drez 1991; DOE 1996a, Appendix B); (2) 10 of these 60 organic compounds could, if present in the WIPP, increase actinide solubilities because they are soluble in aqueous solutions such as WIPP brines, and because they form complexes with dissolved actinides (Choppin 1988); and (3) of these 10 H_2O-soluble organic ligands that form complexes with actinides (acetate, citrate, EDTA, and oxalate) were identified in the WIPP inventory (DOE 1996a).

Brush and Xiong (2003d) calculated the current concentrations of acetate, citrate, EDTA, and oxalate in WIPP brines that could be present in the repository after filling and sealing. Brush and Xiong (2003d) obtained the total masses of acetic acid, Na-acetate, citric acid, Na-citrate, Na-EDTA, oxalic acid, and Na-oxalate in the WIPP inventory (see Appendix Data, Attachment F). Brush and Xiong (2003d) then converted the total masses of each of these organic ligands to total moles, assumed that all these ligands will dissolve in any brine present in the repository after filling and sealing, and divided the total moles of each ligand by 29,841 m^3, "the smallest quantity of brine required to be in the repository [for] transport away from the repository" (Larson 1996). These calculations were carried out identically to those by Brush and Xiong (2003b) for the FMT calculations of actinide solubilities for the CRA-2004 PA, except that Brush and Xiong (2003b) used the masses of ligands reported by Crawford (2003, Table 2, column labeled "Scaled mass (kg)"), not the masses in Appendix Data, Attachment F.

Actinide solubilities were not recalculated using the corrected concentrations of organic ligands from Brush and Xiong (2003d) because the corrections decreased the ligand concentrations slightly. Because the concentrations of these ligands decreased, the actinide solubilities calculated using the uncorrected ligand concentrations of Brush and Xiong (2003b) are slightly higher than they would be if recalculated using the corrected ligand concentrations of Brush and Xiong (2003d).

Table SOTERM-4 provides: (1) the current, corrected concentrations of organic ligands calculated by Brush and Xiong (2003d) based on the masses in Appendix Data, Attachment F; (2) the ligand concentrations calculated by Brush and Xiong (2003b) based on the masses provided by Crawford (2003) (these concentrations were used for the actinide-solubility calculations for the CRA-2004 PA); and (3) the ligand concentrations calculated for the CCA

(CCA Appendix SOTERM, Table SOTERM-4) based on the masses of organic ligands provided by DOE (1996a). Mistakes were apparently made in the calculation of the ligand concentrations for the CCA, the most significant of which was the likely transposition of citrate and oxalate in CCA Appendix SOTERM, Table SOTERM-4.

Table SOTERM-4. Concentrations of Organic Ligands in WIPP Brines That Could Be Present in the Repository after Closure

Organic Ligand	Concentrations Based on Corrected CRA Inventory[1]	Concentrations Used in FMT for the CRA-2004 PA[2]	CCA[3]
Acetate	3.56×10^{-3} M	5.05×10^{-3} M	1.1×10^{-3} m
Citrate	2.71×10^{-4} M	3.83×10^{-4} M	7.4×10^{-3} m
EDTA	2.73×10^{-6} M	3.87×10^{-6} M	4.2×10^{-6} m
Oxalate	1.53×10^{-2} M	2.16×10^{-2} M	4.7×10^{-4} m

[1] Concentrations calculated by Brush and Xiong (2003d) based on the masses of organic ligands in Appendix Data, Attachment F.
[2] Concentrations calculated by Brush and Xiong (2003b) based on the masses of organic ligands provided by Crawford (2003).
[3] Concentrations calculated for the CCA (CCA Appendix SOTERM, Table SOTERM-4) based on the masses of organic ligands provided by DOE (1996a).

Stability constants for complexes between acetate, citrate, EDTA, lactate, and oxalate and the +III, +IV, +V, and +VI actinides (or oxidation-state analogs of these actinides) were determined to incorporate these complexes in the actinide-speciation-and-solubility models described above (see Section 3.4). Stability constants for complexes between these ligands and Mg^{2+} were also determined to include competition between Mg^{2+} and the actinides for the binding sites on these ligands. Choppin et al. (2001) provided the results of all of these experiments. Giambalvo (2002b, 2002e) incorporated these results in the FMT database used for the calculation of actinide solubilities for the CRA-2004 PA. Giambalvo (2003) described this database in detail.

Brush and Xiong (2003a) used FMT, the thermodynamic database described by Giambalvo (2003), and the concentrations of acetate, citrate, EDTA, and oxalate calculated by Brush and Xiong (2003b) to calculate the solubilities of the +III, +IV, and +V actinides for the CRA-2004 PA. (No lactate has ever been identified in the TRU waste to be emplaced in the WIPP.) In the FMT calculations with ligands, all four ligands (acetate, citrate, EDTA, and oxalate) were present simultaneously in Salado or Castile brine at the concentrations calculated by Brush and Xiong (2003b). In these calculations, the stability constants for the complexes formed by these ligands and Ca^{2+} were assigned the same values as the stability complexes formed by these ligands and Mg^{2+} (Giambalvo 2003). However, these calculations did not include competition from dissolved metals such as vanadium (V), chromium (Cr), nickel (Ni), copper (Cu), and lead (Pb), all of which could be present at significant concentrations due to dissolution of steels and other metallic constituents of TRU waste (CCA Appendix SOTERM, SOTERM.5). The results of the FMT calculations for the CRA-2004 PA demonstrate that acetate, citrate, EDTA, and oxalate will not form complexes with the +III and +IV actinides to a significant extent under expected WIPP conditions, and thus will not affect the +III and +IV actinide solubilities significantly (Brush and Xiong 2003d; Downes 2003a, 2003b).

SOTERM-6.0 MOBILE COLLOIDAL ACTINIDE SOURCE TERM

Colloidal particles will be generated in the repository as a result of microbial consumption of cellulosics, and corrosion of steel waste containers and waste constituents, by the hydrodynamic entrainment of colloidal-sized mineral fragments and several other mechanisms. Those colloidal particles may sorb dissolved actinides or the dissolved actinides themselves may form colloidal particles. In an intrusion scenario, actinide-bearing colloidal particles, together with dissolved actinides, may be transported to the Culebra by Castile or Salado brines present in the repository. Additional colloidal particles may be present in natural Culebra groundwater and could form additional actinide-bearing colloidal particles. After introduction to the Culebra, the dissolved actinides and actinide-bearing colloidal particles are transported by Culebra groundwaters. Colloidal actinides may also be transported through the fractured anhydrite interbeds of the Salado.

The actinide source term at the WIPP is defined as the sum of contributions from dissolved actinide species and mobile colloidal actinide species. Colloidal actinides that are not suspended in the aqueous phase (that is, not mobile) are not included in the colloidal actinide source term. Sorption of colloidal actinides onto fixed substrates will also reduce the mobile colloidal actinide source term, but no credit is currently being taken for reduction by that means.

In this section, the quantification of the mobile actinide-bearing colloid component of the actinide source term is described. The quantification of colloid-facilitated transport of actinides in the overlying Culebra, in the event of an intrusion into the repository, is described in Chapter 6.0 (Section 6.4.6.2.2) and Appendix PA, Attachment MASS, Section MASS-15.3.

SOTERM-6.1 Introduction

Colloidal particles are generally defined as particles with at least one dimension between 1 nm and 1 μm, suspended in a liquid, and maintained in suspension for very long periods of time by Brownian (random thermal) motion (Hiemenz 1986; Buddemeier and Hunt 1988; Stumm 1992, 1993). Those size boundaries are approximately defined on the basis of physical phenomena. Particles larger than about 1 μm are too large for Brownian motion to overcome gravitational forces, and the particles will rather quickly settle by gravity. An exception is the case of microbes, which are considered to be colloidal, but may exceed 1 μm. The specific gravities of microbes are typically quite close to that of the dispersant, and so they may not settle by gravitational forces. Generally, particles smaller than approximately 1 nm behave in transport like dissolved ionic species.

SOTERM-6.1.1 Formation and Behavior of Colloidal Particles

Inorganic colloidal particles have been reported to form by a variety of processes. Colloidal particles may form by condensation or homogenous nucleation from dissolved species when a mineral phase is supersaturated or as hydrolyzed precipitates of mixed metal ions (Kim 1992). Colloidal particles may also form by release of particles from bulk material due to disruption of fragile aggregates by changes in ionic strength or hydrodynamic forces, dissolution of a more soluble surrounding matrix (Buddemeier and Hunt 1988; Kim 1994), mechanical grinding of

mineral surfaces, or mechanical disruption of secondary minerals present at mineral surfaces (McCarthy and Zachara 1989).

Organic colloidal particles may form from microbial consumption of CPR materials, condensation reactions of organic molecules to form humic substances, or microbial activity. A variety of naturally occurring organic materials, such as viruses, microbes, and pollen, are colloidal-sized particles (McCarthy and Zachara 1989; Stumm 1992, 243).

Colloidal particles may interact with actinides to form radiocolloids in two ways (see, for example, Lieser et al. 1986a, 1986b, 1990; Kim et al. 1984a, 1984b; Buddemeier and Hunt 1988; Kim 1992, 1994). First, radiocolloids may form as a result of chemical reactions involving dissolved polyvalent actinide ions. Hydrolysis and condensation reactions have been shown to form actinide macromolecules in which the actinide ions are bridged with hydroxyl ions to form polymers. Those radiocolloids are termed "actinide intrinsic colloids," "true colloids," "real colloids," "Eigenkolloide," or "type I colloids."

A second means to form radiocolloids is by sorption of actinides by ordinarily nonradioactive colloidal particles. In the actinide environmental geochemistry literature, the nonradioactive colloidal particle has been called a "groundwater colloid." Once actinide sorption has occurred, the resulting radiocolloids may be called "pseudo colloids," "carrier colloids," "Fremdkolloide," or "type II colloids." The colloidal substrate for sorption may be a mineral fragment, a microbial cell, or a humic substance. Bates et al. (1992) recently described radiocolloids, which they called "primary colloids," forming in situ at the surfaces of vitrified radioactive waste as it reacts chemically with H_2O. Considering that coprecipitation is a continuum with adsorption (see, for example, Comans and Middleburg 1987; Stumm 1992, 253 et seq.), the "primary colloid" can be included in the carrier-colloid category, and more specifically, a mineral-fragment-type colloidal particle. A similar sort of colloid would form by isomorphous lattice substitution of actinide ions during mineral precipitation (that is, coprecipitation) or precipitation of actinide minerals.

In the traditional colloid-chemistry literature, two types of colloidal particles are defined on the basis of how they interact with the dispersant (see, for example, Alexander and Johnson 1949, 114; Vold and Vold 1983; Hirtzel and Rajagopalan 1985; Hiemenz 1986; Ross and Morrison 1988; Hunter 1991-1992). Hydrophobic colloids are stabilized by electrostatic forces, whereas hydrophilic colloids are stabilized by solvation forces. In light of increased knowledge of aqueous surface chemistry gained over the past two decades, the terms hydrophilic and hydrophobic must be used cautiously, because even hydrophobic surfaces have hydrophilic surface functional groups. It is important, however, to make the distinction between how those two types of colloidal particles behave, because they exhibit different kinetic stability behaviors in electrolytes.

Kinetic stability differs from thermodynamic stability. Thermodynamic stability refers to the chemical equilibrium between the colloidal particles and the dispersant, whereas kinetic stability refers to the rate at which colloidal particles in a colloidal dispersion are removed from suspension due to agglomeration followed by gravitational settling. Thermodynamic stability may be most important for actinide intrinsic colloids, because that type of colloid forms directly from solution by chemical reactions. Kinetic stability is inversely related to the rate of particle aggregation, which is dependent on the frequency and efficiency (the fraction resulting in

permanent joining) of collisions between colloidal particles. The behavior of colloidal particle types as a function of ionic strength is probably the single most important phenomenon affecting the importance of colloid-facilitated actinide transport at the WIPP.

Hydrophobic colloidal particles are kinetically stabilized and destabilized by electrostatic forces. In an aqueous dispersant, hydrophobic colloidal particles are attracted to one another by van der Waals forces. That electrostatic attraction is countered by repulsive forces generated by a cloud of counterions surrounding each particle (Lyklema 1978; Hiemenz 1986). In a kinetically stable colloidal dispersion, colloidal particles are usually repelled from one another before they get close enough to become agglomerated. However, as the ionic strength of the dispersion is increased, the thickness of the cloud of counterions is compressed, allowing closer particle-particle interaction. The net effect is that as colloidal particles come into proximity with one another in the dispersion, a greater chance for sticking exists, and so the rate of agglomeration increases. That phenomenon is very effective at removing colloidal particles from suspension even at fairly low ionic strengths over periods of hours to days. Mineral fragments, which are a hydrophobic colloid type, are affected by ionic strength in this way.

Hydrophilic colloidal particles are stabilized by solvation forces, which are largely independent of the ionic strength of the dispersant (Alexander and Johnson 1949). This type of colloidal particle is essentially a dissolved macromolecule. Humic materials are an example of the traditional hydrophilic colloid type. Two major categories of hydrophilic colloidal particles are recognized. Micelles are aggregates of dissolved monomers, that are in thermodynamic equilibrium with those monomers. Polyelectrolytes are charged polymers that are not in thermodynamic equilibrium with a monomeric species (examples of polyelectrolytes include gum arabic, gelatin, pectin, and proteins). An important distinction, therefore, is that micelles require a minimum threshold concentration of monomers (the critical micellization concentration, or c.m.c.) to form. In contrast, the formation of polyelectrolytes is not dependent on monomer concentration. Polyelectrolytes may act as an association colloid by adsorbing on hydrophobic colloidal particles. The resulting dispersions may be extremely kinetically stable (Hiemenz 1986, 659).

The kinetic stability of hydrophobic colloidal particles may be modified by coatings of steric stabilizing compounds, which themselves are essentially hydrophilic materials (also referred to as protective or association colloids) which modify the surface behavior to inhibit close interaction of particles. Such colloidal systems are rendered kinetically stable. Particles stabilized by organic compounds in seawater are an example of a sterically stabilized colloidal system. Microbes can be considered as stabilized in a similar manner, except that the stability is imparted by molecules (for example, polysaccharides), attached to the surface of the microbe, which have hydrophilic parts extending into the dispersant.

Colloidal particles may have rigid or flexible structures, which may affect the way in which they interact with the host rock during transport. “Hard-sphere” colloidal particles, such as mineral fragments, have discrete well-defined boundaries at the particle-H_2O interface, and are rigid. “Soft-sphere” colloidal particles, such as humic substances, have less distinct boundaries at the particle-H_2O interface, are flexible and may undergo conformational changes in response to environmental variations. “Soft-sphere” colloids are essentially dissolved macromolecules and

are closest in form and behavior to particles referred to as hydrophilic colloids in the traditional colloid-chemistry literature (Lyklema 1978; Hiemenz 1986).

SOTERM-6.1.2 Definition of Colloidal Particle Types

On the basis of the phenomena described in the previous section, several classification schemes have been proposed by various workers, and a large number of descriptive terms have evolved and been propagated in the literature. For actinide environmental geochemistry, most of the classification schemes are based on how the colloidal particle interacts with radionuclides. Colloidal particles are classified into the following four types for evaluation of the impact of colloidal particles at the WIPP site:

1. Mineral fragments are hydrophobic, hard-sphere particles that are kinetically stabilized or destabilized by electrostatic forces, and may consist of crystalline or amorphous solids. Mineral fragments may be made kinetically stable by coatings with steric stabilizers that prevent close contact. Mineral fragments may act as substrates for sorption of actinides or they may consist of precipitated or coprecipitated actinide solids.

2. Actinide intrinsic colloids are macromolecules of actinides that, at least in some cases, may mature into a mineral-fragment-type of colloidal particle. When immature, they are hydrophilic; when mature, they become hydrophobic.

3. Humic substances are hydrophilic, soft-sphere particles that are stabilized by solvation forces. They are often powerful substrates for uptake of metal cations and are relatively small (less than 100,000 atomic mass units).

4. Microbes are relatively large colloidal particles that are stabilized by hydrophilic coatings on their surfaces, which behave as steric stabilizing compounds. They may act as substrates for extracellular actinide sorption or they may actively bioaccumulate actinides intracellularly.

SOTERM-6.2 Performance-Assessment Implementation

Results of the colloidal actinide investigation were used in the CRA-2004 PA, the CCA PA, and the 1997 PAVT in three types of parameter values: (1) constant concentration values; (2) concentration values proportional to the dissolved actinide concentration; and (3) maximum concentration values. The parameter types are summarized below and are described in parameter record packages (Papenguth 1996a, 1996b, 1996c, 1996d).

For actinide intrinsic colloids and mineral-fragment colloids, actinide concentrations associated with them were described as constant values. Table SOTERM-5 summarizes the material and parameter names and descriptions.

Experiments conducted to quantify actinide concentrations associated with humic substances and microbes provided the basis for a more sophisticated representation, in which colloidal actinide concentrations were related to the dissolved actinide concentration by proportionality constants. For microbes, the proportionality relationship was made by element. For humic actinides,

however, the relationship was made by oxidation state rather than by element. For microbes and humic substances, the experiments also provided a basis to define upper limits for the actinide concentration that could be associated with each of those colloid types. For both humic and microbial actinides, the upper-limit parameter was defined by element rather than oxidation state, and is in units of molarity. The use of the two upper-limit parameters is slightly different, and is described in the sections below discussing humic substances and microbes.

SOTERM-6.3 Development of Parameter Values

In this section, the experimental basis for the parameter values is described. For each of the four types of colloids, the characteristics of the colloidal particle type are described, the experimental program is outlined, methods of interpretation are described, and results are summarized.

Table SOTERM-5. Material and Property Names for Colloidal Parameters

Material	Property	Brief Description of Parameter
Th, U, Np, Pu, Am	CONCMIN	Concentration of actinide associated with mobile mineral fragment colloids
Th, U, Np, Pu, Am	CONCINT	Concentration of actinide associated with mobile actinide intrinsic colloids
Th, U, Np, Pu, Am	PROPMIC	Proportionality constant for concentration of actinides associated with mobile microbes.
PHUMOX3 [1] PHUMOX4 PHUMOX5 PHUMOX6	PHUMCIM	Proportionality constant for concentration of actinides associated with mobile humic colloids, in Castile brine, actinide solubilities are inorganic only (complexes with man-made organic ligands are not important), solubilities were calculated assuming equilibrium with Mg-bearing minerals (brucite and magnesite);
PHUMOX3 [1] PHUMOX4 PHUMOX5 PHUMOX6	PHUMSIM	Proportionality constant for concentration of actinides associated with mobile humic colloids, in Salado brine, actinide solubilities are inorganic only (complexes with man-made organic ligands are not important), solubilities were calculated assuming equilibrium with Mg-bearing minerals (brucite and magnesite).
Th, U, Np, Pu , Am	CAPMIC	Maximum (cap) concentration of actinide associated with mobile microbes;
Th, U, Np, Pu, Am	CAPHUM	Maximum (cap) concentration of actinide associated with mobile humic colloids.

[1] Proportionality constant for concentration of actinides associated with mobile humic substances, for PHUMOX3, for actinide elements with oxidation state ***+III*** (that is, Pu(III) and Am(III)); PHUMOX4, oxidation state ***+IV*** (Th(IV), U(IV), Np(IV), and Pu(IV)); PHUMOX5, oxidation state ***+V*** (Np(V)); and PHUMOX6, oxidation state ***+VI*** (U(VI)).

SOTERM-6.3.1 Mineral-Fragment Colloids

Mineral-fragment-type colloidal particles may be present in naturally occurring groundwaters, and they may be released from the host rock due to disruption of fragile aggregates by changes in ionic strength or hydrodynamic forces, dissolution of a more soluble surrounding matrix, mechanical grinding of mineral surfaces, or mechanical disruption of secondary minerals present at mineral surfaces. Under certain conditions, such as extreme changes in ionic strength of the groundwater or by physical disruption due to natural or human-induced events, mineral-

fragment-type colloidal particles could also be produced within the Culebra. In an intrusion scenario at the WIPP, mixing of repository brines with Culebra brines may result in mineral precipitation that may include coprecipitation of actinide-bearing mineral-fragment-type colloidal particles. Within the repository, mineral-fragment-type colloidal particles may form from corrosion of Fe-bearing waste and the steel packaging materials. In addition, Portland-cement-based matrixes will be attacked and will produce mineral-fragment-type colloidal particles. Bentonite, which may be a constituent of drilling mud is itself a potential source of mineral-fragment-type colloidal material that should be considered for actinide transport.

In terms of colloidal actinide transport, mineral-fragment-type colloids act as carriers, in that actinide ions sorb onto the surfaces of the colloids. Because each mineral substrate has a different affinity for actinides, quantification of actinide concentrations associated with the wide range of mineralogies likely to be present at the WIPP is insurmountable. Instead, a bounding approach was used based on residual concentrations of colloidal particles in WIPP-relevant brines coupled with estimates of reasonable maximum concentrations of actinides that could be sorbed onto the colloid surfaces. That approach requires three pieces of information: (1) the number of mineral-fragment-type colloidal particles in the aqueous phase; (2) the geometric surface area of individual colloidal particles; and (3) the site-binding capacity of the mineral surface. In the remainder of this section, descriptions of the determination of items (1) through (3), the interpretation of that information, and the development of parameter values are provided.

SOTERM-6.3.1.1 Description of Experiments

Hydrophobic colloidal particles, such as mineral fragments, are kinetically stabilized and destabilized by electrostatic forces (refer to detailed discussion in Papenguth and Behl 1996, Sections 2.5.1 and 2.6). In an aqueous dispersant, hydrophobic colloidal particles are attracted to one another by van der Waals forces. That electrostatic attraction is countered by repulsive forces generated by a cloud of counterions surrounding each particle. In a kinetically stable colloidal dispersion, colloidal particles are usually repelled from one another before they get close enough to become agglomerated. However, as the ionic strength of the dispersion is increased, the thickness of the cloud of counterions is compressed, allowing closer particle-particle interaction. The net effect is that as colloidal particles come into proximity with one another in the dispersion, a greater chance for sticking exists, and so the rate of agglomeration increases. That phenomenon is very effective at removing colloidal particles from suspension even at fairly low ionic strengths over periods of hours to days.

The kinetic stability of the mineral-fragment-type colloids in WIPP-relevant brines was evaluated in coagulation-series experiments. Colloidal dispersions of mineral fragments were prepared by mechanical disaggregation of representative mineral, rock samples, and other materials or by chemical precipitation from laboratory reagents. Brine simulants were prepared that covered the ranges of ionic strengths observed in WIPP brines. The brines were sequentially diluted with deionized H_2O by factors of 10 and adjusted to acidic, neutral, and basic pH conditions to evaluate the effects of ionic strength and pH on kinetic stability. At the ionic strength referred to as the critical coagulation concentration (c.c.c.), colloidal particles will rapidly coagulate, forming agglomerates large enough to settle by gravitational forces. The

number population of colloidal particles remaining in suspension in the various dispersions was measured over time to assess their stability as a function of solution ionic strength and time.

Colloidal dispersions were prepared for the following minerals or materials: bentonite, kaolinite, montmorillonite, vermiculite, illite, anhydrite, calcium carbonate, magnesite, hematite (mechanically disaggregated), hematite (chemical precipitate), limonite, goethite, magnetite, quartz, siderite, brucite, strontianite, diatomaceous earth, pyrite, and cellulosic materials (Masslinn paper towels and Scott paper towels). The brine solutions used included a Salado-like brine simulant (SPC brine) and a Culebra brine simulant (H-17). For c.c.c. experiments, sequential dilutions of those brines were made that spanned approximately five orders-of-magnitude. Brine simulants consisting of 0.5 M NaCl or $CaCl_2$ were also used. For the residual concentration measurements which were used as the basis for the CRA-2004 PA, the CCA PA, and the 1997 PAVT, the one order-of-magnitude dilution (that is, 10 percent of original strength) of the Salado-like brine and the Culebra brine simulants were used. That reduction in ionic strength provides a degree of conservatism in the results.

The c.c.c. experiments for the various concentrations of WIPP brine simulants were conducted under acidic (observed pH generally ranging from 3 to 4), neutral (pH 6 to 8), and basic (pH 9 to 12) conditions. Following the introduction of an aliquot of dispersed colloidal particles to a series of test tubes containing the sequentially diluted brine, colloidal particle concentrations remaining near the top of the fluid columns (residual concentration) were measured as a function of time. The degree of coagulation and settling was quantified using an inductively coupled argon-plasma atomic emission spectrophotometer, nephelometry, and direct particle counting.

Most of the experiments conducted relating to the kinetic stability of mineral-fragment colloidal particles were qualitative to semiquantitative, and were focused on evaluating whether a c.c.c. existed. For the final experiments, however, a state-of-the-art particle spectrometer was used with significantly greater sensitivity. That device was designed for semiconductor fabrication plants, which require extremely pure processing H_2O, and use a similar instrument to ascertain purity. The final experiments were conducted over an extended period of time using the more sensitive analytical technique to determine the number and size of colloids in the brine suspensions. Those experiments were conducted in a similar fashion to previous experiments for bentonite (supplied by the Aldrich Chemical Co.), goethite, and hematite (mechanically disaggregated), but in a relatively dilute (and therefore conservative) brine simulant consisting of 0.1 M NaCl. Residual particle concentrations made with the particle spectrometer compared favorably with measurements made with spectroscopic techniques made at similar experiment times. Generally after the first day of the c.c.c. experiments, the majority (greater than 99 percent) of the colloidal particles had already settled out of suspension. With the more sensitive particle spectrometer, however, residual concentrations of colloidal particles were observed to continue to decrease. For experiments analyzed by spectroscopic or light-scattering techniques, final residual colloid number populations remaining suspended in the test vessels were determined by multiplying the initial colloid number populations determined at the start of the experiments by the fraction of suspended colloids remaining at the final reading. Using the particle spectrometer, final number populations were measured directly.

SOTERM-6.3.1.2 Interpretation and Discussion

Parameter values (CONCMIN) describing the amount of actinide element bound by mineral-fragment-type colloidal particles were determined from the information described above, combined with estimates of adsorption-site densities.

Actinides sorbed to the surfaces of colloidal particles can be estimated using ranges of values for adsorption-site densities taken from published surface complexation modeling research. The actinide concentration contained by a single mineral-fragment-type colloidal particle is calculated by considering the geometrical surface area of a spherical particle:

$$[\mathrm{An}]_p = \frac{\pi D^2 N_s}{N_A} \quad , \tag{52}$$

where:

$[An]_p$ = concentration of an adsorbed actinide element (mol/particle)
D = spherical colloidal particle diameter (nm)
N_S = adsorption site density (sites/nm^2)
N_A = Avogadro's number.

An adsorption-site density of 1 site/nm^2 was used for N_S in the above equation, a value which is realistic, but probably conservative. With that site density, 1-nm- and 1-µ-diameter particles could have a maximum of about 10^{-24} and 10^{-18} mol actinide per particle, respectively. To obtain an estimate of the maximum actinide concentrations that could be associated with the colloids, the estimates of residual colloid number populations were multiplied by the estimated maximum actinide-transport capacity described by Equation (52). The use of a uniform adsorption-site density is a conservative approach, because the actual sorption on mineral surfaces should be described by some kind of isotherm that will result in less than 100 percent coverage. Further, if multivalent adsorbates are present (for example, U(VI)), multiple adsorption sites may be required for one adsorbate ion, reducing the net adsorption capacity of the surface.

Final residual colloid populations quantified by spectrophotometry or nephelometry showed that mineral-fragment-type colloidal particles are kinetically destabilized by brines similar in composition to those present at the WIPP site. Colloid number population values were, with a few exceptions, reduced to less than 5 percent of the initial values within one day. Conservative estimates of maximum actinide concentrations associated with those residual colloid populations are on the order of 10^{-7} to 10^{-9} moles actinide per liter of dispersion.

The final experiments, which utilized the particle spectrometer to measure the quantity of colloids remaining in suspension offered the most sensitive estimates. Moreover, those experiments were conducted for substantially longer periods of time than the semiquantitative c.c.c. experiments. Those experimental results are shown in Table SOTERM-6.

Table SOTERM-6. Experimental Results for Mineral-Fragment Colloids

Mineral	Time of Final Reading (days)	Estimated Actinide Concentration (moles/liter dispersion)

Hematite	12.8	1.6×10^{-8}
Goethite	12.9	9.5×10^{-10}
Bentonite	12.8	1.6×10^{-10}
Geometric mean		1.3×10^{-9}

The DOE believes that the experimental results using the particle spectrometer with the three distinct colloids (hematite, goethite, and bentonite), are representative of other mineral-fragment-type colloidal particles in terms of their behavior in brine solutions. The geometric mean was assumed to be a more representative average of the final colloid concentrations than the arithmetic mean because of the very small final colloid concentrations (which, for this particular case, is also conservative).

Mineral-fragment-type colloidal particles are unique among the four colloidal particle types addressed for the WIPP, because their concentrations are not generally linked to solubility, as are actinide intrinsic colloids and humic substances, or to a maximum supportable population in the case of microbes. Consequently, in an intrusion scenario at the WIPP, as dissolved actinide elements are introduced to the Culebra, it is possible that those dissolved actinides could sorb onto a separate population of indigenous mineral fragments, producing a supplemental source term. To account for that possibility, the geometric mean value listed above was multiplied by a factor of two, producing a final "most-likely value" of 2.6×10^{-9} moles actinide per liter of dispersion.

To capture uncertainty, mainly stemming from knowledge of the adsorption-site density value, a triangular distribution with "minimum values" and "maximum values" spanning one order of magnitude about the geometric mean was provided for the CRA-2004 PA, CCA PA, and 1997 PAVT calculations. Additional conservatism is incorporated into the mineral-fragment-parameter values in that the total concentration of actinides carried by mineral fragment colloidal particles have essentially been multiplied by a factor of five, because a separate population of colloidal particles has been assumed for each actinide element. No consideration of competition for sorption sites is incorporated into the calculations. The value used for adsorption-site density is conservative, but reasonable. For the PA calculations, however, the triangular distribution was not sampled. Instead, the maximum parameter values were used as constant values, which essentially results in a site density of 10 sites/nm^2. Parameter values for CONCMIN are summarized in Table SOTERM-11. Section 7.0 of this attachment discusses details on PA implementation.

SOTERM-6.3.2 Actinide Intrinsic Colloids

Actinide intrinsic colloids (also known as true colloids, real colloids, type I colloids, and Eigenkolloide) form by condensation reactions of hydrolyzed actinide ions and consist solely of actinide cations linked by anions. There are several stages in the development of actinide intrinsic colloids at which they have significantly different behaviors. When immature, actinide intrinsic colloids display physicochemical properties that are similar to ionized humic substances. With age, they become more similar to mineral fragment-type colloidal particles.

The experimental approach used was strongly influenced by reviews of published literature on actinide intrinsic colloids. Pertinent literature is discussed below (see also Papenguth and Behl 1996).

SOTERM-6.3.2.1 Intrinsic Colloids of Plutonium

The most well-known and well-studied actinide intrinsic colloid is the Pu(IV) intrinsic colloid, which has been used as a basis of comparison for investigating intrinsic colloids of other actinides. Most of the knowledge about the Pu(IV) intrinsic colloid comes from research at high Pu concentrations in highly acidic solutions, which was conducted to help improve the efficiency of processing techniques. The Pu(IV) intrinsic colloid is notorious in its propensity to polymerize to form a gel-like material, which can even plug process lines.

A conclusive demonstration of the mechanisms of formation of the Pu(IV) intrinsic colloid has not yet been made, but there is a preponderance of evidence that suggests that polymerization is strongly linked to hydrolysis, and that the initial polymerization, or condensation, produces a macromolecule that becomes progressively more crystalline with time. The final mature colloid has a composition between $Pu(OH)_4(am)$ and $PuO_2(c)$, although the latter compound may be only partly crystalline and both may include interstitial H_2O molecules.

The most convincing and consistent explanation for the chemistry of the Pu(IV) intrinsic colloid is presented by Johnson and Toth (1978). Those authors developed a conceptual model to explain the solution chemistry of a variety of metal cations and a variety of oxidation states. The conceptual model involves processes referred to as “olation” and “oxolation” in which metal cations become bridged with hydroxyl groups, which in turn undergo irreversible elimination of H_2O and concurrent formation of O bridges. Johnson and Toth demonstrate that the model is consistent with the observed behavior of the Pu(IV) intrinsic colloid.

Hydrolysis reactions for metal cations such as Pu may be written as follows:

first: $$Pu^{4+} + H_2O \rightarrow PuOH^{3+} + H^+ \quad (53)$$

second: $$PuOH^{3+} + H_2O \rightarrow Pu(OH)_2^{2+} + H^+ \quad (54)$$

third: $$Pu(OH)_2^{2+} + H_2O \rightarrow Pu(OH)_3^{+} + H^+ \quad (55)$$

fourth: $$Pu(OH)_3^{+} + H_2O \rightarrow Pu(OH)_4\,(aq) + H^+ \quad (56)$$

Johnson and Toth (1978) point out, however, that in interpreting the formation of the Pu(IV) intrinsic colloid, it makes better sense to include the implied waters of hydration that surround metal cations in solution. Hydrolysis Equations (53) through (56) can be rewritten as follows, where n equals 4:

first: $$[Pu(H_2O)_m]^{n+} \rightarrow [Pu(OH)(H_2O)_{m-1}]^{n-1} + H^+ \quad (57)$$

second: $$[Pu(H_2O)_{m-1}]^{n-1} \rightarrow [Pu(OH)(H_2O)_{m-2}]^{n-2} + H^+ \quad (58)$$

third: $[Pu(H_2O)_{m-2}]^{n-2} \rightarrow [Pu(OH)(H_2O)_{m-3}]^{n-3} + H^+$ (59)

fourth: $[Pu(H_2O)_{m-3}]^{n-3} \rightarrow [Pu(OH)(H_2O)_{m-4}]^{n-4} + H^+$ (60)

From the literature, it is clear that polymerization occurs nearly immediately after the first hydrolysis (Equation (57)) occurs. Johnson and Toth (1978) suggest the following reaction involving polymerization of two hydrolyzed species by loss of H_2O (oxolation):

$$2\{[(H_2O)_{d-2}Pu(OH)(H_2O)]^{+(y-1)}\} \rightarrow [(H_2O)_{d-2}Pu(OH)(OH)Pu(H_2O)_{d-2}]^{+2(y-1)} + 2H_2O \quad (61)$$

Aging or maturation of polymer then occurs by loss of H_2O (olation) as follows:

$$[Pu(OH)(OH)Pu(OH)(OH)Pu(OH)(OH)...] \rightarrow [Pu(O)Pu(O)Pu(O)...]_n + 3nH_2 \quad (62)$$

Maiti et al. (1989) and Laul et al. (1985) describe similar reactions, but it appears that they believe that the third hydrolysis reaction occurs, because they use the $Pu(OH)_3^+$ ion in their proposed polymerization reaction. Use of that ion does not appear to be consistent with observations by many workers that polymerization occurs immediately after the first hydrolysis reaction.

As the actinide polyelectrolytes mature through the olation process to become closer in composition to an actinide-oxide mineral, they will be kinetically destabilized by the high ionic strengths of the WIPP brines and will not be mobile. Further, the solubilities of the mature solid phase cannot be exceeded. In fairly long-term experiments, Nitsche et al. (1992, 1994) showed that the concentration of Pu(IV) intrinsic colloid stabilized at about 10^{-8} M. It is not known whether the form was Pu(IV) polyelectrolyte or Pu(IV) mineral-fragment-type colloid.

SOTERM-6.3.2.2 Intrinsic Colloids of other Actinides

Reference is made to a variety of intrinsic colloids of other actinides, but no systematic investigations of their formation and behaviors appear to have been made. Pu is apparently unique in its propensity to form an intrinsic colloid. No mention is made in the literature of maturation of polyelectrolytes of other actinides to form mineralfragment-type colloidal particles as Pu does.

In general, the tendency of actinides to hydrolyze and to polymerize to form intrinsic colloids follows the order:

$$An^{4+} >> An(VI)O_2^{2+} > An^{3+} > An(V)O_2^+ \quad (63)$$

(Cleveland 1979a, 1979b; Choppin 1983; Kim 1992; Lieser et al. 1991, 119). The order of oxidation states in the equation above results from the ionic-charge-to-ionic-radius ratios. The tendency for hydrolysis of $An(VI)O_2^{2+}$ is greater than for An^{3+} because the effective charge on the central cation on the linear $[O\text{-}An\text{-}O]^{2+}$ ion is 3.3 ± 0.1, slightly greater than 3. This trend generally holds true for the actinide elements, because of the very small changes in ionic radii among the actinide (this is the oxidation-state analogy; refer to Novak et al. 1996). There are

differences in the behaviors of the actinides from element to element that stem from very subtle changes in the charge-to-radius ratio and the nature of the configuration of the f molecular orbital.

Considering Pu as an example, hydrolysis becomes significant for Pu^{4+}, $Pu(VI)O_2^{2+}$, Pu^{3+}, and $Pu(V)O_2^{+}$ at pH values of <1, 4-5, 6-8, and 9-10, respectively (Choppin 1983). On the basis of the hydrolysis trend, it is not likely that An(III) and An(V) species will form actinide intrinsic colloids. There are suggestions in the literature, however, that Am^{3+} may form an intrinsic colloid, which is surprising because it does not undergo hydrolysis until relatively high pH. Th does not follow the trend described by Equation (63) because its large size makes it resistant to hydrolysis (Cotton and Wilkinson 1988). Nevertheless, thermodynamic data suggest that in almost all environments (near neutral or higher pH) Th exists as $Th(OH)_4(aq)$. Moreover, Th has been reported to form a polymer (Kraus 1956; Johnson and Toth 1978), although as discussed below, this species should be referred to as an oligomer.

Examples can be found in the literature of polymeric species of many of the actinides of importance to the WIPP (see, for example, Baes and Mesmer 1976; Kim 1992). It is important, however, to note the sizes of polymers described in the literature. It is well known that as polyvalent metals, the actinides can form polynuclear species, but they are largely lower polymers (that is, oligomers) such as dimers, trimers, tetramers, and hexamers (see, for example, Choppin 1983, 46). However, in terms of physical-transport behavior, lower polymers will behave no differently than dissolved monomeric species. In contrast, the higher polymers, such as the Pu(IV)-polymer, may reach colloidal sizes (1 nm to 1 μm) and will have different hydrodynamic properties than the subcolloidal-sized dissolved species. Johnson and Toth (1978) reported a molecular weight of 4000 for a Th polymer. Assuming that it consisted of $Th(OH)_4$, that polymer would consist of about 13 Th ions (that is, the degree of polymerization number, N). That observation is consistent with Kraus (1956), in which he quotes an N value of about 9 for Th polyelectrolyte.

Empirical evidence published in the literature does not always support the suggestion that Am, as a trivalent cation, will form an intrinsic colloidal particle. Avogadro and de Marsily (1984) suggested that, like Pu, Am is a likely candidate to form an insoluble hydroxide. Buckau et al. (1986) reported the formation of Am(III) intrinsic colloids at near neutral pH conditions, with a particle size greater than 1 nm. In their study of the hydrolysis of Am(III) over a pH range from 3 to 13.5, however, Kim et al. (1984a) found only monomers of Am. Regardless of whether Am(III) intrinsic colloids will form under highly idealized laboratory environments, it would be highly unlikely that they would form in a geologic system, because of the tremendously strong sorption properties of the Am(III) ion.

SOTERM-6.3.2.3 Experimental

The objective of experiments, conducted at Lawrence Livermore National Laboratory (LLNL), was to test phenomena described in the published literature, under WIPP-relevant conditions:

- critical coagulation concentration for mature Pu(IV) mineral-fragment-type colloid (refer to description of experiment AIC-1 in Papenguth and Behl (1996));

- formation of Pu(IV) colloid, from oversaturation and undersaturation in the absence of CO_2 (AIC-8 and AIC-9, respectively);
- inhibition of Pu(IV) polymerization due to organic complexants (AIC-2);
- depolymerization of Pu colloid due to organic complexants (AIC-2b);
- polyelectrolyte chain termination by nonactinide metal cations (AIC-4); and
- sorption effects of WIPP repository substrates on Pu(IV) colloid (AIC-5).

The last four experiments listed above provide evidence that, under some conditions at the WIPP, the Pu(IV) colloid is less likely to form or is sorbed. To parameterize the CRA-2004 PA, CCA PA, and 1997 PAVT, however, the first two experiments listed above were used. Both sets of experiments (AIC-1, AIC-8/9) can essentially be viewed as solubility experiments. The critical coagulation-experiments are solubility experiments conducted from undersaturation conditions, in which the in-growth of free Pu(IV) is observed (and are therefore equivalent to AIC-9). In both sets of experiments (AIC-1, AIC-8/9), the Pu solution concentration is measured as a function of time for as long as five weeks, as steady-state concentration is being reached. The two sets of experiments were anticipated to provide information to resolve the question of kinetic versus thermodynamic stability control on the formation and development of the Pu(IV) colloid. That question was not resolved, but the data still provide the necessary information for parameterizing the PA calculations. The values for the parameters submitted for calculations were derived from the experiments listed in Table SOTERM-7.

Table SOTERM-7. Pu Intrinsic-Colloid Experiments

Number	Experiment	Starting Material	pcH approx.	NaCl (m)	Duration
AIC-1	c.c.c. (equivalent to undersaturation experiment AIC-9)	Pu(IV) colloid: aged 1 month: about 2×10^{-4} M	4 7 10	0.001 0.01 0.1 0.8 3.0 5.0	3 to 5 weeks
AIC-8	Oversaturation	Pu(IV) aquo ion: about 1×10^{-4} M	3 7 10	0.05 0.5 1.0 5.0	4 weeks

The data from those experiments are plotted in Figure SOTERM-3 along with regression lines for data collected by Rai et al. (1980) for $Pu(OH)_4(am)$ and PuO_2 and Rai and Swanson (1981) for Pu(IV) polymer under acidic conditions. With MgO, the pH of the

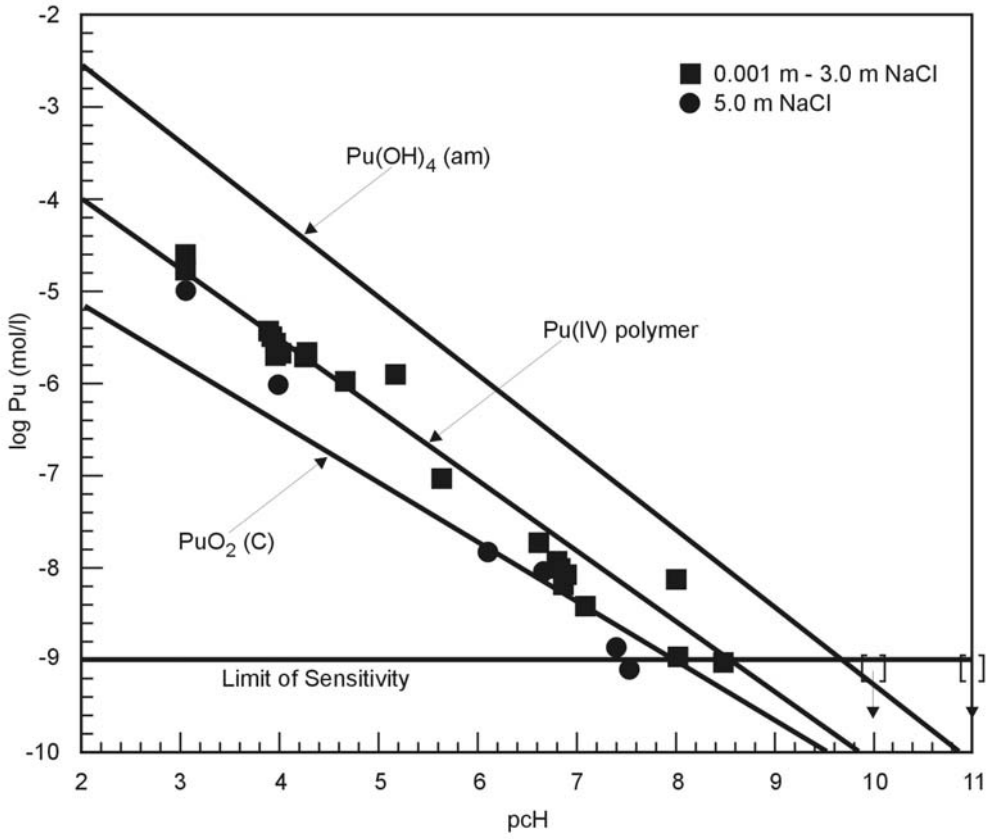

NOTE 1: Open brackets with arrows pointing down indicate Pu concentration is below the minimum analytical detection limit. Solubility lines for $Pu(OH)_{4amorphous}$ and $PuO_{2crystalline}$ are extrapolated from Rai et al. (1980). The solubility line for Pu(IV)-polymer is extrapolated from Rai and Swanson (1981). Plotted values were collected at LLNL as part of the WIPP colloid research program.

NOTE 2: Note that under basic pH conditions fixed by MgO, the solubility of the Pu(IV)-polymer is below the minimum analytical detection limit of 10^{-9} M.

CCA-SOT010-0

Figure SOTERM-3. Solubility of Pu(IV) Polymer in NaCl Media as a Function of pcH.

repository brine is expected to be between 8.69 and 9.02 (see Section 2.0), equivalent to a pcH of 9.40 to 9.72. As shown in Figure SOTERM-3, the regression line calculated from the LLNL data suggests that at a pcH of 9.40 to 9.72, the solubility of Pu(IV)-polymer is less than the minimum analytical detection limit of 1×10^{-9} M. Therefore, the detection limit was selected for use in PA. The LLNL results are consistent with the extrapolated relationships based on published results of Rai et al. (1980) and Rai and Swanson (1981).

SOTERM-6.3.2.4 Interpretation and Discussion

Parameter values (CONCINT) describing the amount of actinide element bound by actinide intrinsic colloidal particles was determined from the information described above. For the Pu(IV) polymer, the minimum analytical detection limit was selected. In the absence of conclusive evidence that intrinsic colloids of other actinides form, or form polymers rather than oligomers, the concentration of Th, U, Np, and Am intrinsic colloids was set to zero.

Geochemical conditions in the Culebra are not conducive to the formation of a new supplementary population of actinide intrinsic colloids. In particular, the concentration of actinide ions is reduced. Therefore, the source term for actinide intrinsic colloids reflects what would form in the WIPP repository, under most favorable conditions for the formation of the Pu(IV) polymer.

Parameter values for CONCINT are summarized in Appendix PA, Attachment SOTERM, Table SOTERM-11.

SOTERM-6.3.3 Humic Substances

Humic substances are defined as high-molecular-weight organic compounds generally present as anions in natural waters. Humic substances may consist of humic acids, which may be aliphatic or aromatic, or fulvic acids. The difference between humic acids and fulvic acids is largely an operational distinction; humic acids can be precipitated at pH values below about 2, whereas fulvic acids are soluble over the entire pH range. Fulvic acids generally have lower molecular weights than humic acids. The dominant functional group that may react with dissolved actinides are carboxyl groups, but phenolic hydroxyl and alcoholic hydroxyl groups also contribute to complexation. At the WIPP, humic substances may be introduced to the repository as a constituent of soil-bearing waste or may be a constituent of the organic-carbon (C) component of Castile, Salado, or Culebra groundwaters. Probably more importantly, humic substances may form from condensation reactions between microbial metabolites (for example, carboxylic acids), byproducts of the consumption of cellulosic materials, and the extracellular polymers associated with microbes. Because of the general lack of knowledge in the scientific community regarding the formation of humic substances, as well as very slow kinetics of formation, a direct attempt has not been made to quantify the amounts of humic substances that would form in situ. Instead, the contribution of humic-bound actinides was bounded through quantification of humic-actinide complexation behavior coupled with quantification of solubilities of humic substances in WIPP-relevant brines. Regardless of the source of humic substances, the total concentration of humic substance available to mobilize actinides is limited by the solubility of humic substances in WIPP brines. The chemical nature of humic substances generated in situ cannot be predicted either, but can be bounded by the three types of humic substances.

To determine the concentration of actinides associated with humic substances, four pieces of information are required: (1) the concentration of reactive humic substance in the aqueous phase (humic solubility); (2) the binding capacity of the humic substance; (3) actinide uptake (that is, actinide complexation constants); and (4) actinide solubilities. The quantification of actinide solubilities is described in Novak and Moore (1996) and results are summarized in Siegel (1996). In the remainder of this document, the focus is on the determination of items 1 through 3, the interpretation of that information, and the development of parameter values suitable for the CRA-2004 PA, CCA PA, and 1997 PAVT calculations.

SOTERM-6.3.3.1 Experimental

In general, humic substances encompass a broad variety of high-molecular-weight organic compounds. The range of their chemical behaviors, however, is covered by consideration of

three types: aliphatic humic acid (generally terrestrial); aromatic humic acid (generally marine); and fulvic acid. The following humic substances were used:

- FA-Suw: fulvic acid isolated from the Suwannee River acquired from the International Humic Substances Society, Golden, Colorado;
- HAal-LBr: aliphatic humic acid isolated from sediments collected from Lake Bradford, Florida, prepared by Florida State University;
- HAal-Ald: aliphatic humic acid purchased from Aldrich Chemical Co., purified by Florida State University;
- HAar-Gor: aromatic humic acid isolated from groundwaters near Gorleben, Germany, obtained from Professor J.-I. Kim, Institute for Radiochemistry, Munich; and
- HAar-Suw: aromatic humic acid isolated from the Suwannee River acquired from the International Humic Substances Society, Golden, Colorado.

Solubilities were measured in experiments conducted over periods of several weeks. The solubilities of humic substances remaining in the fluid column were determined using a scanning fluorometer, C coulometer, and UV/Visible light spectrophotometer, in WIPP-relevant brine simulants with FA-Suw, HAal-LBr, HAal-Ald, and HAar-Suw. In addition to spectroscopic data, visible inspection proved valuable. In oversaturation experiments, humic substances were dissolved in deionized H_2O under basic conditions to enhance dissolution and then added as a spike to a brine . In undersaturation experiments, humic substances were added directly to brines and allowed to dissolve until equilibrium was reached. In either case, equilibrium was reached between dissolved (that is, ionic) and precipitated humic substances. The precipitated humic substances coagulated and settled. The kinetics of precipitation were sufficiently slow that several weeks were required for equilibrium to be reached. Brines consisted of a NaCl matrix with various concentrations of Mg^{2+} and Ca^{2+}. The concentration of Na^{+} in the brine had little effect on solubility except at very high concentrations, but the concentration of the divalent cations had a significant impact on humic-substance solubilities. Consequently, experiments were conducted with a NaCl background electrolyte concentration with concentrations of Mg^{2+} and Ca^{2+} ranging from 10 mM each (representative of natural WIPP brines) to 500 mM each (representative of MgO). At Sandia National Laboratories (SNL), solubilities between approximately 1.5 mg/L and 2.0 mg/L were observed in systems containing 10 mM or greater Mg^{2+} and Ca^{2+}. For the calculations described below, the higher solubility value of 2.0 mg/L was used.

Site-binding-capacity values were determined by titration at Florida State University for two humic substances (HAal-LBr and HAal-Ald). Those values were supplemented with values for a variety of humic substances compiled from published literature. In general, site-binding capacities for humic substances are between 3 and 6 meq OH^{-}/g, but in isolated cases are as low as about 1.5 and as high as about 9.5 meq OH^{-}/g. For the calculations described below, values of 4.65, 5.38, and 5.56 meq OH^{-}/g were used for aliphatic humic acid, aromatic humic acid, and fulvic acid, respectively. The aliphatic humic acid value was determined from HAal-LBr at Florida State University. The aromatic humic acid value was from Gorleben (Gohy-573). The

fulvic acid value represents the mean of 11 published values for fulvic acids collected in Europe (Ephraim et al. 1995).

Actinide complexation factors for U(VI) and Am(III) binding on three humic substances (FA-Suw, HAal-LBr, and HAar-Gor) were measured at Florida State University. Complexation measurements were made at measured pH_{obs} values of approximately 4.8 and 6, conditions at which the humic substances are highly deprotonated, and U and Am have not undergone extensive hydrolysis. Those conditions were chosen to maximize complexation between the humic substances and those actinide elements. Measurements were made in NaCl media with ionic strengths of approximately 3 and 6 m. These experiments were completed prior to the DOE establishing the position that MgO would be emplaced to sequester CO_2 and fix pH at about 9. The experiments conducted at Florida State University represent conservative conditions designed to provide high-end estimates of actinide uptake by humic substances. Actinide complexation by humic substances generally decreases at basic pH values because of the reduction in actinide-complex charges due to hydrolysis. In addition, the high concentrations of Mg^{2+} in solution due to the presence of MgO will compete with actinides for binding sites on humic substances and reduce the actinide uptake. Florida State University reported the first and second stability constants defined as follows (square brackets represent concentration):

$$An + HS \square AnHS;\ \beta_{1;An} = [AnHS]/[An][HS] \tag{64}$$

$$An + 2(HS) \square An(HS)_2;\beta_{2;An} = [An(HS)_2]/[An][HS]^2 \tag{65}$$

where:

- HS = humic substance (eq OH-/L, that is, site-binding capacity incorporated)
- An = actinide element
- $\beta_{1;An}$ = first stability constant, for 1:1 An:humic binding
- $\beta_{2;An}$ = second stability constant, for 1:2 An:humic binding

For the calculations described below, complexation constants were selected from the most relevant experimental conditions, which were pH_{obs} 6 and 6 m NaCl. The following stability constants reported by Florida State University were used (reported as log values), as shown in Table SOTERM-8.

Table SOTERM-8. Humic Substances Experimental Results

Humic Substance	Am^{3+} : β_1	Am^{3+} : β_2	$U(VI)O_2^{2+}$: β_1	$U(VI)O_2^{2+}$: β_2
HAal-LBr	6.09 +/- 0.05	10.46 +/- 0.12	5.91 +/- 0.16	10.43 +/- 0.19
HAal-Gor	6.02 +/- 0.04	10.40 +/- 0.10	5.35+/- 0.15	8.98 +/- 0.26
FA-Suw	4.6 +/-0.3	8.95 +/- 0.45	Not measured	Not measured

The Florida State University results show that there is little difference in $U(VI)O_2^{2+}$ and Am(III) uptake by aliphatic and aromatic humic acids, but that uptake by fulvic acid is significantly less. The Florida State University results also show that an increase of NaCl ionic strength from 3 to 6 has little effect on actinide uptake. Those observations aid in justifying the use of published stability constants for other actinide elements experimentally determined at lower ionic strengths and for other humic substances. On the basis of the similarities in stability constants for $U(VI)O_2^{2+}$ and Am(III) for the humic acids, SNL has used the Am(III) stability constant for FA-Suw for $U(VI)O_2^{2+}$ on FA-Suw.

Stability constants for Th(IV) with several humic and fulvic acids were reported by Nash and Choppin (1980). In NaCl media at pH values between 3.95 and 5.03, those authors reported log stability constants between 9.7 and 13.2. Under the mildly basic conditions expected in the WIPP repository, it is likely that complexation of Th(IV) will be markedly less, because the dominant Th(IV)-bearing aqueous species will be $Th(OH)_4(aq)$ (Novak and Moore 1996). No reports of direct investigations of Th-complex binding on humic substances were found. For the calculations described herein, the published results from Baskaran et al. (1992) describing the distribution of Th(IV) in seawater were used. From that work, a ratio of dissolved versus colloidal Th(IV) of 6.349 was calculated, assuming that the solubility of colloidal organic material in seawater is equivalent to our measured value of humic substances in WIPP-relevant brines (that is, 2.0 mg/L). The nature of the humic substances is likely to be dominated by aromatic humic acid, but may also contain fulvic acid.

For the calculations described herein, a log stability constant for $Np(V)O_2^+$ of 3.67 measured at pH 9 for a Gorleben humic acid (Gohy-573; Kim and Sekine 1991) was used. Results presented in Rao and Choppin (1995) for Lake Bradford humic acid and a Gorleben humic acid (Gohy-573) show little effect of pH on Np(V) stability constants, presumably because of the absence of Np(V) hydrolosis over the pH range studied. The Gorleben humic acid is aromatic in nature.

No published stability constants were found for Pu. For the calculations described herein, an oxidation-state analogy was used for the Pu oxidation species, an approach that is conservative. Allard et al. (1980) have shown that at pH 9, Pu(IV) undergoes hydrolysis to a greater extent than Th(IV), which should result in reduced complexation of Pu(IV).

An oxidation-state analogy was used to develop parameter values for elements expected to have multiple oxidation states in the WIPP repository. Redox speciation of the actinide elements was evaluated as part of the dissolved ASTP. Weiner (1996) concluded that in the WIPP, the following species will be present: Th(IV); U(IV) and U(VI); Np(IV) and Np(V); Pu(III) and Pu(IV); and Am(III). The relative concentrations of the oxidation states of a particular element

are designated by their respective solubility values. The substitutions made following the oxidation-state analogy are summarized in Table SOTERM-9.

Table SOTERM-9. Oxidation State Analogy Substitutions

Required Binding Constant	Substitute	Source of Data
Th(IV)	None required	Baskaran et al. (1992)
U(IV)	Th(IV)	Baskaran et al. (1992)
U(VI)	None required	WIPP-specific data, Florida State University
Np(IV)	Th(IV)	Baskaran et al. (1992)
Np(V)	None required	Kim and Sekine (1991)
Pu(III)	Am(III)	WIPP-specific data, Florida State University
Pu(IV)	Th(IV)	Baskaran et al. (1992)
Am(III)	None required	WIPP-specific data, Florida State University

To compensate for the effects of competition for actinide complexation by the high concentrations of Mg^{2+} and Ca^{2+} in repository brines in the presence of MgO, stability constants for Mg^{2+} and Ca^{2+} were used in simultaneously solved equations (described below). Stability constants for Mg^{2+} and Ca^{2+} at basic pH values are not available, but several published reports provide values in the acidic range. Choppin and Shanbhag (1981) reported log stability constants of 2.25 to 3.32 for Ca^{+} in 0.1 M sodium perchlorate ($NaClO_4$) at pH 3.9 and 5.0 for an aliphatic humic acid (Aldrich humic acid). Schnitzer and Skinner (1967) reported log binding constants ranging from 2.2 to 3.72 for Ca^{2+} in low-ionic strength solutions over a pH range of 3.5 to 5.0 for fulvic acid. For Mg^{2+}, Schnitzer and Skinner (1967) reported log stability constants ranging from 1.23 to approximately 2.0 under the same experimental conditions. For the calculations, a log stability constant of 2.0 for the sum of Mg^{2+} and Ca^{2+} concentrations was used, which is a conservative value.

Binding of Mg^{2+} and Ca^{2+} to humic substances is described in the same way as Equation (64) above:

$$(Mg + Ca) + HS \rightleftharpoons (Mg,Ca)HS;\ \beta_{1;Mg,Ca} = \frac{[(Mg,Ca)HS]}{[Mg + Ca][HS]} \quad (66)$$

where:

$\beta_{1;Mg,Ca}$ = first stability constant, for 1:1 (Mg + Ca):humic binding (note that no second stability constants exist for divalent-cation binding).

SOTERM-6.3.3.2 Interpretation and Discussion

Proportionality constants (PHUMCIM and PHUMSIM) describing the amount of actinide element bound to humic substances were determined from the data listed above, coupled with dissolved actinide concentrations. In addition, maximum theoretical concentrations of actinides that could be associated with humic substances (CAPHUM) were calculated from the data above.

The concentration of an actinide element of a given oxidation state was calculated by simultaneous solution of Equations (64) and (66), combined with a mass-balance expression:

$$[HS_{tot}] = [AnHS] + [(Mg,Ca)HS] + [HS] \quad (67)$$

where:

$[HS_{tot}]$ = total concentration of humic substance
$[HS]$ = concentration of uncomplexed humic substance
$[AnHS]$ = concentration of humic complexed with an actinide element
$[(CaMg)HS]$ = concentration of humic complexed with divalent cations.

Equation (67) describes the effect of two humic substances binding with one actinide ion was disregarded for these calculations, because its contribution to the total humic-bound actinide concentrations was negligible.

Rearranging Equations (64) and (66) provides:

$$[AnHS] = \beta_{1;An}\,[An]\,[HS]\,, \quad (68)$$

$$[(Mg,Ca)HS] = \beta_{1;Mg,Ca}\,[Mg + Ca]\,[HS]\,. \quad (69)$$

Substituting Equations (68) and (69) into Equation (67) results in:

$$[HS_{tot}] = \beta_{1;An}\,[An]\,[HS] + \beta_{1;\,Mg,Ca}\,[Mg + Ca]\,[HS] + [HS]\,. \quad (70)$$

Rearranging Equation (70) provides:

$$[HS] = \frac{[HS_{tot}]}{\beta_{1;An}[An] + \beta_{1;CaMg}[Ca+Mg] + 1}\,. \quad (71)$$

Equations (68), (69), (70), and (71) were used to calculate humic-bound actinide concentrations ([AnHS]). The resulting AnHS concentration values were then summed for actinide elements with multiple oxidation states, and then divided by the dissolved concentration of the respective actinide element. The final forms of the parameter values PHUMCIM and PHUMSIM are proportionality constants in units of moles humic-bound colloidal actinide per mole of dissolved actinide. The proportionality values may be multiplied by the dissolved actinide concentration expressed in molarity or molality, depending on the desired final unit.

Depending on the intrusion scenario, the WIPP repository may be dominated by Castile brine or by intergranular Salado brine, resulting in different actinide solubilities, but also different solubilities of Mg^{2+} and Ca^{2+}. Under conditions characteristic of equilibrium with MgO, solubility parameters calculated for a system buffered by brucite and magnesite were used (Siegel 1996).

Equations (68), (69), and (71) were used to determine humic-bound actinide concentrations ([AnHS]) for one or more humic substance types for Th(IV), U(VI), Np(V), and Am(III). The oxidation-state analogy is most heavily utilized for Pu, because stability constants for Pu(III) or

Pu(IV) are not available. Concentrations of Mg^{2+} and Ca^{2+} in Salado and Castile brines in equilibrium with MgO were obtained from Novak and Moore (1996). In the PA calculations, the humic-bound actinide concentration in the +III oxidation state in Castile brine was sampled. All other humic-bound actinide concentrations were held constant.

The PHUMCIM and PHUMSIM parameters, used in conjunction with materials (idmtrls) PHUMOX3, PHUMOX4, PHUMOX5, or PHUMOX6, provide the means to calculate actinide-humic concentrations by actinide oxidation state and for intrusion scenarios involving different brines. For example, in an E1 scenario under strongly reducing conditions in the WIPP repository, PHUMCIM would be used with the following materials (idmtrls) to determine actinide-humic concentrations: Th = PHUMOX4; U = PHUMOX4; Np = PHUMOX4; Pu = PHUMOX3; and Am = PHUMOX3. For an E2 scenario under relatively less reducing conditions in the WIPP repository, PHUMSIM would be used with the following idmtrls to determine actinide-humic concentrations: Th = PHUMOX4; U = PHUMOX6; Np = PHUMOX5; Pu = PHUMOX4; and Am = PHUMOX3.

Uncertainties due to analytical precision are small compared to uncertainties in knowledge of the dominant humic substance type, site-binding densities, and actinide solubilities. The proportionality-factor approach coupled with the actinide-solubility-model uncertainty results in an adequate representation of the uncertainty in the concentration of actinides bound by mobile humic substances.

The CAPHUM parameter simply represents the theoretical maximum concentration of actinides that can be bound by a humic substance. Based on a solubility-limit concentration of humic substances of 2.0 mg/L, and the highest site-binding capacity (for fulvic acids) of 5.56 meq OH^-/g, the theoretical maximum is 1.1×10^{-5} eq/L. Assuming the conservative case in which actinide species are monovalent, the maximum theoretical concentration of actinides that can be bound by humic substances is 1.1×10^{-5} M. That number is conservative, because it assumes a pool of humic substances is available for each actinide element, when in reality, actinide elements will compete for the same pool of humic substances. CAPHUM is used in an expression such as the following:

$$[\text{AnHS}] = \text{MIN}(\text{AnHS value calculated with proportionality constant}, 1.1 \times 10^{-5}) \quad (72)$$

in which the calculated concentration of a particular actinide is compared to the upper-limit value. Parameter values for PHUMCIM, PHUMSIM, and CAPHUM are summarized in Table SOTERM-11.

SOTERM-6.3.4 Microbes

Potentially important colloidal-sized microorganisms include bacteria, fungi, yeast, and protozoa. For the WIPP site, the focus is on the halophilic and halotolerant microbes identified at the site (Brush 1990; Francis and Gillow 1994). Microbes are important to consider in PAbecause they may significantly affect the characteristics of the waste stored at the WIPP, and also participate in transport of actinides. Microbes are known to actively bioaccumulate actinides intracellularly as well as act as substrates for passive extracellular sorption.

At the WIPP site, concentrations of naturally occurring microbes are on the order of 10^4 to 10^7 cells per mL (Francis and Gillow 1994, Table 1). In the presence of nutrients provided by WIPP waste constituents, including nitrates, sulfates, and cellulosics such as protective clothing and wood, the population of microbes is likely to increase. Lysis, a natural phenomenon whereby cells die and release their constituents to the solution, also provides a source of nutrients to microbes.

When introduced to nutrients, microbes typically follow a predictable growth curve (defined by the population number of microbes plotted as a function of time), consisting of an initial period of inactivity (very early log phase) ranging up to several days, followed by a sharp increase in growth (early log phase). That level of growth is sustained for one or more days (log phase) during which time microbial metabolites, including carboxylic acids, enzymes, and exocellular polymers, are generated. The growth rate eventually begins to decline (late log phase) due to the effects of those metabolites, limitations in nutrients or substrates, or population dynamics, and reaches a steady-state population (stationary phase). Viable microbes may aggregate to form clusters.

SOTERM-6.3.4.1 Description of Experiments

Several types of experiments were conducted to evaluate the impact of microbes in support of the WIPP colloid research program (refer to descriptions in Papenguth and Behl 1996): (1) evaluation of indigenous concentrations of microbes; (2) quantification of mobile concentrations under nutrient- and substrate-rich conditions; (3) quantification and characterization of actinide bioaccumulation by microbes; and (4) evaluation of toxicity effects of actinide elements on microbe growth.

Experiments were conducted at Brookhaven National Laboratory (BNL) and as a collaborative effort between BNL and LANL. Evaluation of indigenous concentrations was a collaborative effort between BNL and LANL. Quantification of mobile concentrations was conducted at BNL. The bioaccumulation and toxicity work was conducted at BNL or LANL depending on the actinide element. Th and U were investigated at BNL. The other actinide elements of interest, Np, Pu, and Am, were investigated at LANL under the guidance of BNL personnel.

Experiments to determine the mobile concentrations of microbes remaining suspended in the fluid column were conducted similarly to experiments previously conducted in support of the WIPP Gas Generation Program (Brush 1990; Francis and Gillow 1994). Bacterial cultures were introduced to a solution containing nutrient and substrate, and sealed. The bacterial population was monitored over periods of several weeks or more using measurements of optical density or by direct counting of aliquots of fixed cells. An important change in protocol from previous experiments, however, is that instead of filtering the entire contents of the vessels, only the mobile cells remaining suspended in the fluid column were counted. Results of the experiments showed that the mobile concentration of microbes was a couple of orders-of-magnitude less than the total concentration of microbes. The existence of indigenous microbes in Salado groundwaters has been demonstrated in previous work (Francis and Gillow 1994). As part of the WIPP Colloid Research Program, samples of Culebra groundwater were carefully collected from the H-19 hydropad, processed, and characterized for indigenous microbes. Concentrations of

naturally occurring microbes were on the order of 10^5 cells per mL, determined using direct counting methods.

The evaluation of indigenous concentrations of microbes and quantification of mobile concentrations provided important supporting evidence for quantifying the microbial actinide source term and for evaluating microbe-facilitated transport of actinides in the Culebra. However, the basis for developing the actual parameter values used in the CRA-2004 PA, the CCA PA, and the 1997 PAVT calculations was established with bioaccumulation and toxicity experiments, referred to herein as filtration experiments. Those experiments were conducted by combining microbe cultures with various concentrations and complexes of ^{232}Th, ^{238}U, ^{237}Np, ^{239}Pu, or ^{243}Am. The actinide reagents used were Th(IV)-NO_3^-, Th(IV)-EDTA, U(VI)-NO_3^-, U(VI)-citrate, Np(V)-EDTA, Pu(V)-HClO4, Pu(V)-EDTA, and Am(III)-EDTA. For those experiments, a pure bacterial culture (WIPP-1A) and a mixed bacterial culture (BAB) were used. Most of the experiments were conducted with the WIPP-1A culture, because of the fast growth of that pure culture. The WIPP-1A mixed culture typically reaches steady-state concentration within several days, whereas the BAB mixed culture requires several weeks. Because of the rapid response of the WIPP-1A culture, most of the experiments were conducted with that culture to expedite the research program. A complementary set of experiments were repeated with the BAB mixed culture to evaluate the representativeness of the pure culture. Experiments were conducted over periods of 11 to 15 days for the WIPP-1A microbe culture, and up to 21 days for the BAB culture. Each experiment consisted of a subset of two or three replicate test vessels that were sampled during the overall test interval to provide time-sequence data. In addition, replicate test vessels that were not innoculated with microbes were included in each experiment to provide a control. Sequential filtration with 0.03-µm, 0.4-µm, and 10-µm filters was conducted on each vessel. The following size fractions were obtained as shown in Table SOTERM-10.

Table SOTERM-10. Microbe Experimental Results

Fluid Column Sample	Particle Size	Actinide Association with
Not filtered	all	All forms listed below
0.22-µm syringe filter, filtrate	< 0.22 µm	Dissolved; lysed microbes
10-µm filter, filter retentate	> 10 µm	Clumped microbes
10-µm filter, filtrate	< 10 µm	Dissolved; dispersed microbes; lysed microbes
0.4-µm filter, filter retentate	= 0.4 to 10 µm	Dispersed microbes
0.4-µm filter, filtrate	< 0.4 µm	Dissolved; lysed microbes
0.03-µm filter, filter retentate	= 0.03 to 0.4 µm	Lysed microbes
0.03-µm filter, filtrate	< 0.03 µm	Dissolved; lysed microbes

In addition to the potential actinide associations listed above, there was some evidence of the formation of inorganic precipitates in some of the experiments. The nutrient used in many experiments was phosphate PO_4^{3-}(1g/L), which is known to coprecipitate actinide cations. The inoculated control samples provided the means to evaluate the extent of that experimental artifact. The control samples also provided the means to assess the extent of sorption of actinides onto test vessels, sampling, and filtration equipment. All sequential filters were composed of the same material, which simplifies assessment of sorption on the filtration equipment.

The toxicity experiments were conducted as a component of the filtration experiments described above, by varying the actinide concentration, and comparing growth curves measured by optical density and/or by direct cell counting. To increase the total concentration of actinides in solution, EDTA was added in some experiments in a one-to-one molar ratio with the actinide element. That approach was taken for all of the experiments with Th, Np, and Am, and for some of the experiments with Pu.

SOTERM-6.3.4.2 Interpretation and Discussion

Proportionality constants (PROPMIC) describing the amount of actinide element bound to mobile microbes were determined from the data listed above. In addition, maximum concentrations of actinides that could be associated with microbes (CAPMIC) were determined from the experimental data. Those two parameters are suitable for use in the CRA-2004 PA, CCA PA, and 1997 PAVT calculations, when coupled with dissolved actinide solubilities (refer to Section 7.2 for details).

The 0.4-µm-filter retentate and 0.03-µm filtrate (acquired from the inoculated vessels, not the uninoculated control vessels) were selected to represent the microbial actinide and dissolved actinide concentrations, respectively. The ratio between the microbial actinide and dissolved actinide, both expressed in molarity, represents the proportionality constant value used for the PROPMIC parameter. The 0.4-µm-filter retentate was selected to represent the microbial fraction because nearly all of the bacterial biomass was associated with that filter. A small

concentration of actinides was associated with suspected biomass trapped on the 10-µm filter, as clumped microbes, and on the 0.03-µm filter, as lysed microbes. The contribution of actinide-associated biomass consisting of clumped and lysed microbes was typically at least one order-of-magnitude less than the actinide concentration associated with the dispersed microbes collected on the 0.4-µm filter. The concentration of dissolved actinides measured from the 0.03-µm-filter filtrate was used in the ratio because it provides the best indication of final dissolved actinide concentration. Representative values for PROPMIC were developed on an element-by-element basis. Results of experiments using the BAB culture were disregarded, because of their lower uptake of actinides (especially Pu), and because of the limited number of experiments conducted with that culture. For the WIPP-1A culture, the first sampling period (2 to 4 days, but generally 3 days) was disregarded in determining proportionality constants because steady state population had not yet been reached. The remaining values were averaged arithmetically.

The filtration experiments discussed above also provided the basis for determining CAPMIC values. Final cell population numbers in the test vessels were estimated using measurements of optical density at a wavelength of 600 nm or by direct counting with epifluorescent microscopy. The magnitude of the toxicity effects was estimated by comparing final cell numbers obtained from a series of test vessels with varying actinide concentration. The direct-counting technique provided the most dependable measure of cell number and was used where available. The CAPMIC value is defined as the actinide concentration in molarity at which no growth was observed. For cases where growth clearly diminished as actinide concentration increased, but the actinide concentration was not great enough to stop growth, CAPMIC values were determined by linear extrapolation of population numbers, and then adding an order-of-magnitude to account for uncertainty. On the basis of WIPP experimental results (Papenguth 1996b), it appears that the toxicity effects are due to chemical toxicity rather than radiotoxicity. Because of the high radiation levels of Am and safety considerations in the laboratory facility used, the molar concentration could not be increased to the point at which toxicity effects could be observed. Consequently no CAPMIC value is currently available for Am. CAPMIC values are used similarly to the CAPHUM values (see Equation (72)), except that the upper limit for microbe concentration is due to toxicity rather than geometric limitations imposed by the colloid itself. Consequently, for microbes, the total concentration of mobile actinides in a PA realization is used in the comparison, rather than the amount of actinides associated with the microbes.

The experiments conducted do not provide sufficient information to formulate a distribution of values for PROPMIC and CAPMIC. Therefore, single values for PROPMIC and CAPMIC were used in the CRA-2004 PA, the CCA PA, and the 1997 PAVT. Uncertainties due to analytical precision are small compared to uncertainties in knowledge of the microbe culture that might predominate in the WIPP repository or in the Culebra in an intrusion scenario. The proportionality-factor approach coupled with the actinide-solubility-model uncertainty results in an adequate description of the uncertainty in the concentration of actinides bound by mobile microbes.

Parameter values for PROPMIC and CAPMIC are summarized in Table SOTERM-11.

SOTERM-6.3.5 Summary of Parameter Values

Parameter values for CONCMIN, CONCINT, PROPMIC, CAPMIC, PHUMSIM, PHUMCIM, and CAPHUM are summarized in Table SOTERM-11.

SOTERM-6.4 Summary

Results of the colloidal actinide investigation were used in the 1996 PA, the CRA-2004 PA, and the 1997 PAVT in three types of parameter values: (1) constant-concentration values for actinides associated with mineral fragment and actinide intrinsic colloids; (2) concentration values proportional to the dissolved actinide concentration for actinides associated with microbes and humic substances; and (3) maximum concentration values providing an upper limit for actinide concentrations associated with microbes and humic substances. The parameter values are summarized in Table SOTERM-11. Given the actinide solubilities calculated for Salado and Castile brines in equilibrium with MgO, the largest contributors to the mobile colloidal actinide source term are actinides associated with humic substances and microbes. The contribution from mineral fragment and actinide intrinsic colloids is comparatively small. More details can be found in the SNL WIPP Records Center (formerly referred to as the SNL WIPP Central File, SWCF) parameter record packages describing the determination of the mobile colloidal actinide source term (Papenguth 1996a, 1996b, 1996c, 1996d).

Table SOTERM-11. Colloid Concentration Factors

	CONCMIN Concentration on Mineral Fragments [1]	CONCINT Concentration as Intrinsic Colloid [1]	PROPMIC Proportion Sorbed on Microbes [2,3]	CAPMIC Maximum Sorbed on Microbes [4]	Proportion Sorbed on Humics [2]		CAPHUM Maximum Sorbed on Humics [1]
					PHUMSIM Salado	PHUMCIM Castile	
Th(IV)	2.6×10^{-8}	0.0	3.1	0.0019	6.3	6.3	1.1×10^{-5}
U(IV)	2.6×10^{-8}	0.0	0.0021	0.0021	6.3	6.3	1.1×10^{-5}
U(VI)	2.6×10^{-8}	0.0	0.0021	0.0023	0.12	0.51	1.1×10^{-5}
Np(IV)	2.6×10^{-8}	0.0	12.0	0.0027	6.3	6.3	1.1×10^{-5}
Np(V)	2.6×10^{-8}	0.0	12.0	0.0027	9.1×10^{-4}	7.4×10^{-3}	1.1×10^{-5}
Pu(III)	2.6×10^{-8}	0.0	0.3	6.8×10^{-5}	0.19	1.37[e]	1.1×10^{-5}
Pu(IV)	2.6×10^{-8}	1.0×10^{-9}	0.3	6.8×10^{-5}	6.3	6.3	1.1×10^{-5}
Am(III)	2.6×10^{-8}	0.0	3.6	NA	0.19	1.37[d]	1.1×10^{-5}

[1] In units of moles colloidal actinide per liter

[2] In units of moles colloidal actinide per mole dissolved actinide

[3] For the CRA-2004 PA, there were no microbial colloids in nonmicrobial vectors

[4] In units of moles total mobile actinide per liter

[5] A cumulative distribution from 0.065 to 1.60 with a mean value of 1.1 was used

NOTE: The colloidal source term is added to the dissolved source term to arrive at a total source term. Mineral fragments were provided with distributions, but the maximum was used as described in SOTERM-7.1.3. Humic proportionality constants for III, IV, and V were provided with distributions, but only the Castile Am(III) and Pu(III) were sampled.

SOTERM-7.0 USE OF THE ACTINIDE SOURCE TERM IN PERFORMANCE ASSESSMENT

As described in the preceding sections, the s ASTP provided the parameters that were needed to construct maximum dissolved and suspended colloidal actinide concentrations for use in modeling the mobilization and transport of actinides in the disposal system, as modeled by NUTS and PANEL. Prior to these transport calculations, however, some simplifications and manipulations (using PANEL) were required as discussed in the following sections.

SOTERM-7.1 Simplifications

The DOE has concentrated on those processes most likely to have a significant impact on system performance. Therefore, several simplifications were used in the modeling of radionuclide mobilization in the CRA-2004 PA, the CCA PA, and the 1997 PAVT calculations. These include

- using constant solubility and colloid parameters throughout the repository and regulatory period for a given realization,
- limiting the number of isotopes modeled to the ones most important to compliance,
- using the chemistries of Castile and Salado brines — the end member brines — to bracket the behavior of mixtures of these brines within the repository,
- sampling only the uncertain parameters having the most significant effect on repository performance,
- combining dissolved and colloidal species for transport within the disposal system, as modeled by NUTS and PANEL.

SOTERM-7.1.1 Elements and Isotopes Modeled

Selection of isotopes for modeling transport in the disposal system with NUTS and PANEL is described in Appendix TRU WASTE, Section TRU WASTE-2.0. PANEL runs included nearly all isotopes of the six actinides studied in the ASTP: Th, U, Np, Pu, Am, and Cm. NUTS runs included five isotopes: Th, ^{234}U, ^{238}Pu, ^{239}Pu, and ^{241}Am.

SOTERM-7.1.2 Use of Brine End Members

Brine from three sources may enter the repository, depending on the nature of future human intrusion. The general scenarios described in Chapter 6.0 (Section 6.3), and considered in the source-term calculations may be categorized into three groups: (1) undisturbed performance (UP), (2) intrusion through the repository and into the Castile intersecting a pressurized brine reservoir (E1 and E1E2); and (3) intrusion through the repository but not into a pressurized brine reservoir (E2).

Under all scenarios, brine may flow from the surrounding Salado through the disturbed rock zone (DRZ) and into the repository in response to the difference between the hydraulic head in the repository and the surrounding formation. For scenarios in which a borehole is drilled into the repository, brine may flow down the borehole from the Rustler and/or the Dewey Lake. For scenarios in which a pressurized Castile brine reservoir is intercepted, brine from the Castile may flow up the borehole into the repository. As mentioned in Section 2.2.1, the brines in these three formations have different compositions and the solubilities of actinides are somewhat different in each of these end-member compositions. The composition of the more dilute groundwaters from the Rustler and Dewey Lake, however, are expected to change rapidly upon entering the repository due to fast dissolution of host Salado minerals, about 90-95 percent halite and about 1-2 percent each of polyhalite, gypsum, anhydrite, and magnesite (Brush 1990) from the walls and floor of the repository. Calculations titrating Salado rock into dilute brines with the geochemical software package EQ3/6 (Wolery 1992; Wolery and Daveler 1992) show that gypsum, anhydrite and magnesite saturate before halite. When halite saturates, the brine composition is very similar to that of Castile brine. One hundred times as much polyhalite must be added to the system before the resulting brine has a composition similar to Salado brines. These calculations indicate that if dilute brines dissolve away only the surfaces of the repository, they will obtain Castile-like compositions, but if they circulate through the Salado after saturating with halite, they may obtain compositions similar to Salado brine. Similarly, if Castile brine circulates through enough host rock, it may also approach Salado brine composition. In either case, the actual brine within the repository may be described as a mixture of the two concentrated-brine end members — Salado and Castile. This mixture, however, is very hard to quantify, because it is both temporally and spatially variable. Only in the undisturbed scenario is the mixture well defined as 100 percent Salado brine over the 10,000-year regulatory period.

For a panel intersected by a borehole, the BRAGFLO calculations show that in the 10 percent of the repository represented by the BRAGFLO panel computational cells, the ratio of brine inflow that enters by the borehole versus inflow from the repository walls varies through time and depends on the sampled parameter values and scenario being considered. This ratio was the only measure of brine mixing available to the source-term runs in the CRA-2004 PA, CCA PA, and 1997 PAVT calculations. This ratio was quite crude because it (1) did not account for compositional changes that occur when H_2O was consumed by corrosion reactions, (2) did not resolve the details of flow, diffusion and brine interaction with internal pillars and the DRZ, and (3) was an average over one tenth of the repository. It is expected that the fraction of Salado brine will be quite high in areas of the repository distant from the borehole and the fraction will be much lower near the borehole. Because radionuclide travel up the borehole is required for significant release, it is the solubility of radionuclides near the borehole that is most important. Given these uncertainties, the DOE decided to calculate radionuclide solubilities using the Castile end-member composition for scenarios in which a borehole penetrates a brine reservoir and Salado end-member composition for scenarios where it does not.

SOTERM-7.1.3 Sampling of Uncertain Parameters

Distributions of parameter values for up to 30 source-term parameters are available, but many of these are expected to have very limited impact on disposal-system performance. The most

important parameters are expected to be the oxidation-state parameter and the solubilities of Pu(III), Pu(IV), and Am(III) in the two brine end members.

A single distribution (Figures SOTERM-1 and SOTERM-2) was provided for modeling the solubilities of all oxidation states of all actinides in both brines. However, the amount of correlation between the solubilities of the actinides was uncertain. Some factors that cause uncertainty in the solubilities affect all oxidation states of all actinides similarly and some factors will affect only some actinides or some oxidation states. For example, uncertainties in the SO_4^{2-} concentrations will have more effect in the uncertainty of the solubility of the actinides in the +IV oxidation state, while uncertainties in the ionic strength have a more generalized effect of increasing the uncertainty in the stability of any highly charged species. In nature, solubilities show correlation due to redox effects as well as compositional effects. It is therefore expected that solubilities within the WIPP should show some correlation, but not 100 percent correlation.

The use of the end-member brines in the calculations results in a correlation of solubilities due to ionic strength and major-ion effects, and the use of the oxidation-state parameter results in a correlation due to redox effects. The DOE assumes these effects (that is, ionic strength, major ions, and redox state) encompass the major correlations and therefore imposes no further correlations. A better estimate of this correlation would be necessary for more detailed chemical modeling, but for use in PA, this is unnecessary.

The parameters to be sampled were selected based on expectations of their significance of effect on disposal-system performance.

- A 100 percent correlation was made between Am and Cm solubilities. Only the parameters for Am were sampled, and these were copied for Cm.

- Np solubilities were not sampled because Np does not have a very large EPA unit during the 10,000-year regulatory period (see Appendix TRU WASTE, Section TRU WASTE-2.0 for a discussion of EPA unit**s** and the relative importance of Np).

- The parameter for actinide concentration on mineral fragments was not sampled because the concentrations of actinides that may be mobilized on mineral fragments were in most cases much lower that the possible concentrations of dissolved actinides.

- Of the humic-acid proportionality constants, only the one for the +III oxidation state in Castile brine was sampled because it was high and it applied to significant elements (Pu and Am).

Parameters not sampled were fixed at a maximum reasonable value during the calculations.

Fourteen parameters were sampled in the CRA-2004 PA for the source term (see Appendix PAR):

Material Name	Parameter Name
SOLAM3	SOLSIM, SOLCIM

SOLPU3	SOLSIM, SOLCIM
SOLPU4	SOLSIM, SOLCIM
SOLU4	SOLSIM, SOLCIM
SOLU6	SOLSIM, SOLCIM
SOLTH4	SOLSIM, SOLCIM
GLOBAL	OXSTAT
PHUMOX3	PHUMCIM

where

SOLAM3 = distribution parameter for SOLubility of AM(III),
SOLSIM = solubility variability in Salado brine,
SOLCIM = solubility variability in Castile brine,
OXSTAT = OXidation-STATe parameter,
PHUMOX3 = the Proportionality constant for HUMic colloids and actinides in the +3 OXidation state,
PHUMCIM = the Proportionality constant for HUMic colloids in Castile brine.

In the CCA PA and the 1997 PAVT, 12 parameters were sampled (all of the 14 parameters listed above except SOLU4, SOLCIM; and SOLTH4, SOLCIM).

SOTERM-7.1.4 Combining the Transport of Dissolved and Colloidal Species in the Salado

Dissolved and colloidal species may transport differently because of different diffusion rates, sorption onto stationary materials, and size exclusion effects (filtration and hydrodynamic chromatography). With maximum molecular diffusion coefficients of about 4×10^{-10} m^2 per s, actinides are estimated to diffuse about 10 m in 10,000 years, a negligible distance. Sorption and filtration have beneficial but unquantifiable effects on performance. Hydrodynamic chromatography may increase colloid transport over dissolved transport by at most a factor of two for theoretically perfect colloidal transport conditions. In real situations, the increase is much less. Given the small or beneficial nature of these effects, they were not included in the CRA-2004 PA, the CCA PA and the 1997 PAVT calculations of radionuclide transport in the repository.

Because there was no modeled mechanism to differentiate dissolved from colloidal species, the DOE combined them for transport within the Salado. In the modeling of transport within the Culebra, however, these simplifications were inappropriate. While transport within the repository is through at most hundreds of meters of poorly defined waste that is undergoing decomposition, transport through the Culebra is over kilometers in a relatively homogeneous (as compared to waste) fractured dolomite. Dissolved and colloidal species could be transported differently through the Culebra. Therefore, the mobilized actinides delivered to the Culebra by Salado transport codes are separated into five components (dissolved, humic, microbial, mineral-fragment, and intrinsic colloids).

SOTERM-7.2 Construction of Source Term

The parameters required for constructing the source term were (1) solubilities for four oxidation states in each brine end member, (2) an uncertainty distribution to be applied to the solubilities, (3) a scheme for assigning sampled oxidation states, (4) colloidal concentrations or proportionality constants for the five actinides or the four oxidation states for each of four types of colloids, and (5) caps on the actinide concentrations that may be applied to two types of colloids. Use of these parameters in the CRA-2004 PA, the CCA PA, and the 1997 PAVT calculations required combining them into a single maximum concentration for each modeled actinide. The term "total mobilized concentration" is used for the combined concentrations due to dissolved and colloidal species. The combined concentrations are not necessarily the actual concentrations, because the concentration may be lower due to inventory limits. Both NUTS and PANEL assume that the concentrations of actinides specified by the total mobilized concentration are attained instantaneously as long as sufficient inventory is available. When the inventory is insufficient, the actual mobilized concentration will be lower and is said to be inventory limited. The calculation of the total mobilized concentration is performed by PANEL, for each of 100 sampled vectors in a replicate,.

All of the source-term parameters and their distributions were entered into the PA parameter database. For each sampled parameter, the LHS code uses the distribution from the PA parameter database to create 100 sampled values. These values are combined with the parameters with constant values and stored in computational databases for each of the 100 vectors, which constitute one replicate. For each realization, PANEL uses both the constant and sampled values for all of the source-term parameters, and constructs the source term for NUTS and PANEL, as shown below. This process is repeated for scenarios using the Salado end-member total mobilized concentration and for scenarios using the Castile end-member total mobilized concentration. (Parameters that are sampled and values derived from them are indicated by italics. Parameters used by PANEL are in bold.)

Dissolved = **Model Solubility** * 10 ***Sampled from Solubility Distribution*** (73)

Humic = *Dissolved* * ***Proportionality Constant*** (74)
if *Dissolved* * ***Prop. Const***. < **Humic Cap**, otherwise

Humic = **Humic Cap** (75)

Microbe (microbial vectors only) = *Dissolved* * **Proportionality Constant** (76)

if the *Total Mobile* < **Microbe Cap**, otherwise

Microbe = **Microbe Cap** (77)

Mineral = **Database Concentration** (78)

Intrinsic = **Database Concentration** (79)

Total Mobile = *Dissolved* + *Humic* + *Microbe* + Mineral + Intrinsic (80)

For actinides with more than one oxidation state, the oxidation state is specified by the oxidation-state parameter:

Lower Oxidation State if OXSTAT ≤ 0.5
Higher Oxidation State if OXSTAT > 0.5,

where OXSTAT is the oxidation-state parameter that is sampled uniformly from 0 to 1.

For example, for one realization, in Salado brine, the sampled value for OXSTAT was 0.9 so Pu would be present in the +IV state. The sample of the solubility distribution was 0.8 for the modeled solubility for the +IV state, which has a model solubility of 1.19×10^{-8} M. The humic proportionality constant for the +IV oxidation state in Salado brine is 6.3, the microbe proportionality constant for Pu is 0.3, the humic cap is 1.1×10^{-5} M, the microbe cap for Pu is 2.1×10^{-3} M, the concentration of the actinide on mineral fragments is 2.6×10^{-8} M, and the Pu intrinsic-colloid concentration is 1×10^{-9} M.

For this realization, the maximum mobilized concentration of Pu used by PA would be:

Maximum concentration of dissolved Pu:

$$C_{Pu} = (1.19 \times 10^{-8}) \times (10^{0.8}) = 2.8 \times 10^{-5} \text{ M} \quad (81)$$

(This example has been rounded to two significant figures, although PA would not round at this intermediate point.) C_{Pu} is the maximum concentration of all combined isotopes of Pu.

The maximum humic complexed Pu would be:

$$(2.8 \times 10^{-5} \text{ M})(6.3 \text{ mol adsorbed per mol}) = 1.8 \times 10^{-4} \text{ M} \quad (82)$$

This value, however, exceeds the cap for humic-mobilized Pu, 1.1×10^{-5} M. Therefore, in this case, the cap would be used for the maximum humic mobilized actinide concentration.

The maximum microbial mobilized Pu would be:

$$(2.8 \times 10^{-5} \text{ M})(0.3 \text{ mol bioaccumulated per mol}) = 8.3 \times 10^{-6} \text{ M} \quad (83)$$

which is less than the cap.

The total maximum Pu concentration or total mobilized concentration for this realization would then be the sum of the dissolved and colloidal actinides:

Dissolved + Humic + Microbe + Mineral + Intrinsic

$$2.8 \times 10^{-5} + 1.1 \times 10^{-5} + 8.3 \times 10^{-6} + 2.6 \times 10^{-8} + 1.0 \times 10^{-9} = 4.7 \times 10^{-5} \text{ M} \quad (84)$$

PANEL also calculates the fraction of each actinide mobilized by five different mechanisms, as follows:

$$\text{Fraction dissolved} = \text{Dissolved/Total Mobilized Conc.} \quad (85)$$

$$\text{Fraction on humics} = \text{Humic/Total Mobile} \quad (86)$$

$$\text{Fraction in/on microbes} = \text{Microbe/Total Mobile} \quad (87)$$

$$\text{Fraction on mineral fragments} = \text{Mineral/Total Mobile} \quad (88)$$

$$\text{Fraction as intrinsic colloid} = \text{Intrinsic/Total Mobile} \quad (89)$$

The total mobilized concentration and mobile fractions are then copied from Am to Cm. In addition, PA also combines isotopes (Appendix TRU WASTE, Section TRU WASTE-2.0) for the NUTS and SECOTP2D transport codes. For example, the U solubility is decreased to account for the shared solubility with the low-activity ^{238}U, which is not modeled, enabling NUTS to properly model the effect of the U isotopes on compliance using the single "lumped" isotope ^{234}U.

The output of the PANEL calculations is computational databases that contain the source term and effective inventories. NUTS and PANEL both assume instantaneous dissolution and colloidal mobilization up to the solubility limit when sufficient inventory is present, as discussed in Chapter 6.0 (Section 6.4.13.5). Table SOTERM-12 shows the dissolved and colloidal components of the source term and the total mobile actinide concentrations obtained when median parameter values are used.

Table SOTERM-12. Concentrations (M) of Dissolved, Colloidal, and Total Mobile Actinides Obtained Using Median Parameter Values

Actinide Oxidation State, and Brine	CRA, Microbial Vectors[1]	CRA, Nonmicrobial Vectors	PAVT	CCA
Pu(III), dissolved, Salado brine	2.50×10^{-7}	2.50×10^{-7}	9.75×10^{-8}	4.73×10^{-7}
Pu(III), colloidal, Salado brine	1.49×10^{-7}	7.44×10^{-8}	7.48×10^{-8}	2.59×10^{-7}
Pu(III), total mobile, Salado brine	3.99×10^{-7}	3.24×10^{-7}	1.72×10^{-7}	7.32×10^{-7}
Pu(III), dissolved, Castile brine	1.37×10^{-7}	1.44×10^{-7}	1.06×10^{-8}	1.06×10^{-8}
Pu(III), colloidal, Castile brine	2.56×10^{-7}	2.24×10^{-7}	4.46×10^{-8}	4.46×10^{-8}
Pu(III), total mobile, Castile brine	3.94×10^{-7}	3.68×10^{-7}	5.52×10^{-8}	5.52×10^{-8}
Am(III), dissolved, Salado brine	2.50×10^{-7}	2.50×10^{-7}	9.75×10^{-8}	4.73×10^{-7}
Am(III), colloidal, Salado brine	9.72×10^{-7}	7.34×10^{-8}	3.96×10^{-7}	1.82×10^{-6}
Am(III), total mobile, Salado brine	1.22×10^{-6}	3.23×10^{-7}	4.93×10^{-7}	2.29×10^{-6}
Am(III), dissolved, Castile brine	1.37×10^{-7}	1.44×10^{-7}	1.06×10^{-8}	1.06×10^{-8}
Am(III), colloidal, Castile brine	6.99×10^{-7}	2.13×10^{-7}	7.78×10^{-8}	7.78×10^{-8}
Am(III), total mobile, Castile brine	8.36×10^{-7}	3.57×10^{-7}	8.83×10^{-8}	8.83×10^{-8}
Th(IV), dissolved, Salado brine	9.67×10^{-9}	1.01×10^{-8}	1.06×10^{-8}	3.58×10^{-6}
Th(IV), colloidal, Salado brine	1.17×10^{-7}	8.95×10^{-8}	1.25×10^{-7}	2.21×10^{-5}
Th(IV), total mobile, Salado brine	1.27×10^{-7}	9.96×10^{-8}	1.36×10^{-7}	2.57×10^{-5}
Th(IV), dissolved, Castile brine	2.01×10^{-8}	4.75×10^{-9}	3.33×10^{-8}	4.88×10^{-9}
Th(IV), colloidal, Castile brine	2.15×10^{-7}	5.59×10^{-8}	3.39×10^{-7}	7.18×10^{-8}
Th(IV), total mobile, Castile brine	2.35×10^{-7}	6.07×10^{-8}	3.73×10^{-7}	7.67×10^{-8}
U(IV), dissolved, Salado brine	9.67×10^{-9}	1.01×10^{-8}	1.06×10^{-8}	3.58×10^{-6}

1

Table SOTERM-12. Concentrations (M) of Dissolved, Colloidal, and Total Mobile Actinides Obtained Using Median Parameter Values — Continued

Actinide Oxidation State, and Brine	CRA, Microbial Vectors[1]	CRA, Nonmicrobial Vectors	PAVT	CCA
U(IV), colloidal, Salado brine	8.70×10^{-8}	8.95×10^{-8}	9.26×10^{-8}	1.10×10^{-5}
U(IV), total mobile, Salado brine	9.66×10^{-8}	9.96×10^{-8}	1.03×10^{-7}	1.46×10^{-5}
U(IV), dissolved, Castile brine	2.01×10^{-8}	4.75×10^{-9}	3.33×10^{-8}	4.88×10^{-9}
U(IV), colloidal, Castile brine	1.53×10^{-7}	5.59×10^{-8}	2.36×10^{-7}	5.67×10^{-8}
U(IV), total mobile, Castile brine	1.73×10^{-7}	6.07×10^{-8}	2.69×10^{-7}	6.16×10^{-8}
Pu(IV), dissolved, Salado brine	9.67×10^{-9}	1.01×10^{-8}	1.06×10^{-8}	3.58×10^{-6}
Pu(IV), colloidal, Salado brine	9.08×10^{-8}	9.05×10^{-8}	9.67×10^{-8}	1.21×10^{-5}
Pu(IV), total mobile, Salado brine	1.01×10^{-7}	1.01×10^{-7}	1.07×10^{-7}	1.57×10^{-5}
Pu(IV), dissolved, Castile brine	2.01×10^{-8}	4.75×10^{-9}	3.33×10^{-8}	4.88×10^{-9}
Pu(IV), colloidal, Castile brine	1.60×10^{-7}	5.69×10^{-8}	2.47×10^{-7}	5.92×10^{-8}
Pu(IV), total mobile, Castile brine	1.80×10^{-7}	6.17×10^{-8}	2.80×10^{-7}	6.41×10^{-8}
U(VI), dissolved, Salado brine	7.07×10^{-6}	7.07×10^{-6}	7.07×10^{-6}	7.07×10^{-6}
U(VI), colloidal, Salado brine	8.89×10^{-7}	8.75×10^{-7}	8.89×10^{-7}	8.89×10^{-7}
U(VI), total mobile, Salado brine	7.96×10^{-6}	7.95×10^{-6}	7.96×10^{-6}	7.96×10^{-6}
U(VI), dissolved, Castile brine	7.15×10^{-6}	7.15×10^{-6}	7.15×10^{-6}	7.15×10^{-6}
U(VI), colloidal, Castile brine	3.69×10^{-6}	3.67×10^{-6}	3.69×10^{-6}	3.69×10^{-6}
U(VI), total mobile, Castile brine	1.08×10^{-5}	1.08×10^{-5}	1.08×10^{-5}	1.08×10^{-5}

1

REFERENCES

Alexander, A.E., and P. Johnson. 1949. *Colloid Science*. New York, NY: Oxford University Press. Vol. 1.

Allard, B., H. Kipatsi, and J. O. Liljenzin. 1980. "Expected Species of Uranium, Neptunium and Plutonium in Neutral Aqueous Solutions," *Journal of Inorganic Nuclear Chemistry*. Vol. 42, no. 7, 1015-1027.

Avogadro, A., and G. de Marsily. 1984. "The Role of Colloids in Nuclear Waste Disposal," *Scientific Basis for Nuclear Waste Management VII, Materials Research Society Symposia Proceedings, Boston, MA, November 14-17, 1983.* Ed. G.L. McVay. New York, NY: North-Holland. Vol. 26, 495-505.

Baes, C.F., Jr., and R.E. Mesmer. 1976. *The Hydrolysis of Cations.* New York, NY: Wiley Interscience.

Baskaran, M., P. H. Santschi, G. Benoit, and B. D. Honeyman. 1992. "Scavenging of Thorium Isotopes by Colloids in Seawater of the Gulf of Mexico," *Geochimica et Cosmochimica Acta*. Vol. 56, no. 9, 3375-3388.

Bates, J.K., J.P. Bradley, A. Teetsov, C.R. Bradley, and M. Buchholtz. 1992. "Colloid Formation During Waste Form Reaction: Implications for Nuclear Waste Disposal," *Science.* Vol. 256, no. 5057, 649-561.

Brush, L.H. 1990. *Test Plan for Laboratory and Modeling Studies of Repository and Radionuclide Chemistry for the Waste Isolation Pilot Plant.* SAND90-0266. Albuquerque, NM: Sandia National Laboratories. WPO 26015.

Brush, L.H. 1995. Systems Prioritization Method - Iteration 2 Baseline Position Paper: Gas Generation in the Waste Isolation Pilot Plant. Unpublished report, March 17, 1995. Albuquerque, NM: Sandia National Laboratories. ERMS 228740.

Brush, L.H., and Y. Xiong. 2003a. Calculation of Actinide Solubilities for the WIPP Compliance Recertification Application, Analysis Plan AP-098, Rev 1. Unpublished analysis plan. Carlsbad, NM: Sandia National Laboratories. ERMS 527714.

Brush, L.H., and Y. Xiong. 2003b. Calculation of Organic Ligand Concentrations for the WIPP Compliance Recertification Application. Unpublished analysis report. Carlsbad, NM: Sandia National Laboratories. ERMS 527567.

Brush, L.H., and Y. Xiong. 2003c. Calculation of Actinide Solubilities for the WIPP Compliance Recertification Application. Unpublished analysis report, May 8, 2003. Carlsbad, NM: Sandia National Laboratories. ERMS 529131.

Brush, L.H., and Y. Xiong. 2003d. Calculation of Organic Ligand Concentrations for the WIPP Compliance Recertification Application and for Evaluating Assumptions of Homogeneity in

WIPP PA. Unpublished analysis report. Carlsbad, NM: Sandia National Laboratories. ERMS 531488.

Buckau, G., R. Stumpe, and J.I. Kim. 1986. "Americium Colloid Generation in Groundwaters and Its Speciation by Laser-Induced Photoacoustic Spectroscopy," *Journal of the Less-Common Metals*. Vol. 122, 555-562.

Buddemeier, R.W., and J.R. Hunt. 1988. "Transport of Colloidal Contaminants in Groundwater: Radionuclide Migration at the Nevada Test Site," *Applied Geochemistry*. Vol. 3, no. 5, 535-548.

Bynum, R. V. May 23, 1996. Memo to M. S. Tierney and C. Stockman. "Update of Uncertainty Range and Distribution for Actinide Solubilities to be Used in CCA NUTS Calculation." WPO 35835.

Choppin, G.R. 1983. "Solution Chemistry of the Actinides," *Radiochimica Acta*. Vol. 32, no. 1-3, 43-53.

Choppin, G. R. 1988. Unpublished Letter to L. H. Brush, December 29, 1988, Tallahassee, FL. (Copy on file at Sandia WIPP Central Files.)

Choppin, G.R., A.H. Bond, M. Borkowski, M.G. Bronikowski, J.F. Chen, S. Lis, J. Mizera, O. Pokrovsky, N.A. Wall, Y.X. Xia, and R.C. Moore. 2001. Waste Isolation Pilot Plant Actinide Source Term Test Program: Solubility Studies and Development of Modeling Parameters. SAND99-0943. Albuquerque, NM: Sandia National Laboratories.

Choppin, G. R., and P. M. Shanbhag. 1981. "Binding of Calcium by Humic Acid," *Journal of Inorganic and Nuclear Chemistry*. Vol. 43, no. 5, 921–922.

Clark, D. L. and Tait, C. D. 1996. Monthly Reports Under SNL Contract AP2274, Sandia WIPP Central File A:WBS 1.1.10.1.1. These data are qualified under LANL QAPjP CST-OSD-QAP1-001/0. WPO 31106.

Clark, D.L., D.E. Hobart, and M.P. Neu. 1995. "Actinide Carbonate Complexes and Their Importance in Actinide Environmental Chemistry," *Chemical Reviews.* Vol. 95, no. 1, 25-48.

Cleveland, J.M. 1979a. *The Chemistry of Plutonium.* La Grange Park, IL: American Nuclear Society.

Cleveland, J.M. 1979b. "Critical Review of Plutonium Equilibria of Environmental Concern," *Chemical Modeling in Aqueous Systems: Speciation, Sorption, Solubility, and Kinetics, 176th Meeting of the American Chemical Society, Miami Beach, FL, September 11-13, 1978.* Ed. E.A. Jenne. Washington, DC: American Chemical Society. 321-338.

Comans, R.N.J., and J.J. Middelburg. 1987. "Sorption of Trace Metals on Calcite: Applicability of the Surface Precipitation Model," *Geochimica et Cosmochimica Acta.* Vol. 51, no. 9, 2587-2591.

Cotton, F.A., and G. Wilkinson. 1988. *Advanced Inorganic Chemistry*. 5th ed. New York, NY: John Wiley & Sons.

Crawford, B.A. 2003. "Updated Estimate of Complexing Agents in Transuranic Solidified Waste Forms Scheduled for Disposal and Emplaced at WIPP." Unpublished letter to C.D. Leigh, April 8, 2003. Carlsbad, NM: Los Alamos National Laboratory. ERMS 527409.

Downes, P.S. 2003a. "Spreadsheet Calculations of Actinide Solubilities for the WIPP Compliance Recertification Application." Unpublished memorandum to L.H. Brush, April 21, 2003. Carlsbad, NM: Sandia National Laboratories. ERMS 528395.

Downes, P.S. 2003b. "Spreadsheet Calculations of Actinide Solubilities for the WIPP Compliance Recertification Application in Support of AP-098, 'Calculation of Actinide Solubilities for the WIPP Compliance Recertification Application, Analysis Plan AP-098, Rev. 1.'" Unpublished analysis report. Carlsbad, NM: Sandia National Laboratories. ERMS 530441.

Drez, P.E. 1991. "Preliminary Nonradionuclide Inventory of CH-TRU Waste,"*Preliminary Comparison with 40 CFR Part 191, Subpart B for the Waste Isolation Pilot Plant, December 1991. Volume 3: Reference Data.* WIPP Performance Assessment Division Eds. R.P. Rechard, A.C. Peterson, J.D. Schreiber, H.J. Iuzzolino, M.S. Tierney, and J.S. Sandha. SAND91-0893/3. Albuquerque, NM: Sandia National Laboratories, A-43 through A-53.

Ephraim, J. H., C. Petersson, M. Norden, and B. Allard. 1995. "Potentiometric Titrations of Humic Substances: Do Ionic Strength Effects Depend on the Molecular Weight?" *Environmental Science and Technology*. Vol. 29, no. 3, 622-628.

Eugster, H.P., C.E. Harvie, and J.H. Weare. 1980. "Mineral Equilibria in the Six-component Seawater System, Na-K-Mg-Ca-SO_4-Cl-H_2O, at 25□C," *Geochimica et Cosmochimica Acta.* Vol. 44, no. 9, 1335-1347. WPO 30424.

Fanghänel, Th., V. Neck, and J.I. Kim. 1995. "Thermodynamics of Neptunium(V) in Concentrated Salt Solutions: II. Ion Interaction (Pitzer) Parameters for Np(V) Hydrolysis Species and Carbonate Complexes," *Radiochimica Acta.* Vol. 69, no. 3, 169-176. WPO 40233.

Felmy, A.R., and J.H. Weare. 1986. "The Prediction of Borate Mineral Equilibria in Natural Waters, Application to Searles Lake, California," *Geochimica et Cosmochimica Acta.* Vol. 50, no. 12, 2771-2783. WPO 30421.

Felmy, A. R., D. Rai, J. A. Schramke, and J. L. Ryan. 1989. "The Solubility of Plutonium Hydroxide in Dilute Solution and in High-Ionic-Strength Chloride Brines," *Radiochimica Acta.* Vol. 48, no. 112, 29-35.

Felmy, A. R., D. Rai, and R. W. Fulton. 1990. "The Solubility of $AmOHCO_3$(c) and the Aqueous Thermodynamics of the System Na^+-H CO_3--$(CO_3)^{2-}$-OH-H_2O," *Radiochimica Acta.* Vol. 50, no. 4, 193-204.

Felmy, A.R., D. Rai, S.M. Sterner, M.J. Mason, N.J. Hess, and S.D. Conradson. 1996. "Thermodynamic Models for Highly Charged Aqueous Species: The Solubility of Th(IV) Hydrous Oxide in Concentrated $NaHCO_3$ and Na_2CO_3 Solutions." In preparation. (Copy on file in the Sandia WIPP Central Files. A:1.1.10.1.1: TO: QA: Inorganic (IV) Actinide Thermodynamic Data, WPO 40226, 8/14/96).

Francis, A.J., and J.B. Gillow. 1994. *Effects of Microbial Processes on Gas Generation Under Expected Waste Isolation Pilot Plant Repository Conditions. Progress Report through 1992*. SAND93-7036. Albuquerque, NM: Sandia National Laboratories. WPO 26555.

Francis A.J., J.B. Gillow, and M.R. Giles. 1997. Microbial Gas Generation under Expected Waste Isolation Pilot Plant Repository Conditions. SAND96-2582. Albuquerque, NM: Sandia National Laboratories.

Garner, J. March 15, 1996. "Radioisotopes to Be Used in the 1996 CCA Calculations." Memorandum to Christine Stockman. WPO 35202.

Giambalvo, E.R. 2002a. "Recommended Parameter Values for Modeling An(III) Solubility in WIPP Brines." Unpublished memorandum to L.H. Brush, July 25, 2002. Carlsbad, NM: Sandia National Laboratories. ERMS 522982.

Giambalvo, E.R. 2002b. "Recommended Parameter Values for Modeling Organic Ligands in WIPP Brines." Unpublished memorandum to L.H. Brush, July 25, 2002. Carlsbad, NM: Sandia National Laboratories. ERMS 522981.

Giambalvo, E.R. 2002c. "Recommended Parameter Values for Modeling An(IV) Solubility in WIPP Brines." Unpublished memorandum to L.H. Brush, July 26, 2002. Carlsbad, NM: Sandia National Laboratories. ERMS 522986.

Giambalvo, E.R. 2002d. "Recommended Parameter Values for Modeling An(V) Solubility in WIPP Brines." Unpublished memorandum to L.H. Brush, July 26, 2002. Carlsbad, NM: Sandia National Laboratories. ERMS 522990.

Giambalvo, E.R. 2002e. "Recommended μ^0/RT Values for Modeling the Solubility of Oxalate Solids in WIPP Brines." Unpublished memorandum to L.H. Brush, July 31, 2002. Carlsbad, NM: Sandia National Laboratories. ERMS 523057.

Giambalvo, E.R. 2003. "Release of FMT Database FMT_021120.CHEMDAT." Unpublished memorandum to L.H. Brush, March 10, 2003. Carlsbad, NM: Sandia National Laboratories. ERMS 526372.

Grenthe, I., and H. Wanner. 1992. *Guidelines for the Extrapolation to Zero Ionic Strength.* NEA-TBD-2, Revision 2, Gif-sur-Yvette, France: OECD Nuclear Energy Agency, Data Bank. WPO 21109.

Harvie, C.E., N. Møller, and J.H. Weare. 1980a. "The Prediction of Mineral Solubilities in Natural Waters, The Na-K-Mg-Ca-Cl-SO_4-H_2O System from Zero to High Concentration at 25°C," *Geochimica et Cosmochimica Acta.* Vol. 44, no. 7, 981-997. WPO 30423.

Harvie, C.E., J.H. Weare, L.A. Hardie, and H.P. Eugster. 1980b. "Evaporation of Seawater: Calculated Mineral Sequences," *Science.* Vol. 208, no. 4443, 498-500.

Harvie, C.E., N. Møller, and J.H. Weare. 1984. "The Prediction of Mineral Solubilities in Natural Waters, The Na-K-Mg-Ca-H-Cl-SO_4-OH-HCO_3-CO_2-H_2O System to High Ionic Strengths at 25°C," *Geochimica et Cosmochimica Acta.* Vol. 48, no. 4, 723-751. WPO 30422.

Helton, J.S., J.E. Bean, J.W. Berglund, F.J. Davis, K. Economy, J.W. Garner, J.D. Johnson, R.J. MacKinnon, J. Miller, D.G. O'Brien, J.L. Ramsey, J.D. Schreiber, A. Shinta, L.N. Smith, D.M. Stoelzel, C.W. Stockman, and P. Vaughn. 1998. Uncertainty and Sensitivity Analysis Results Obtained in the 1996 Performance Assessment for the Waste Isolation Pilot Plant. SAND98-0365. Albuquerque, NM: Sandia National Laboratories.

Hiemenz, P.C. 1986. *Principles of Colloid and Surface Chemistry*. 2nd ed. New York, NY: Marcel Dekker, Inc.

Hirtzel, C.S., and R. Rajagopalan. 1985. *Colloidal Phenomena. Advanced Topics*. Park Ridge, NJ: Noyes Publications.

Hobart, D.E. 1990. "Actinides in the Environment," *Proceedings of the Robert A. Welch Foundation Conference on Chemical Research, No., XXXIV: 50 Years With Transuranium Elements, Houston, TX, October 22-23, 1990*. Vol. 34, 378-436.

Hobart, D.E., and R. Moore. 1996. "Analysis of Uranium (VI) Solubility Data for WIPP Performance Assessment: Implementation of Analysis Plan AP-028." Copy on file in Sandia WIPP Central File. WPO 39856 (5/28/96).

Hobart, D. E., K. Samhoun, and J. R. Peterson. 1982. "Spectroelectrochemical Studies of the Actinides: Stabilization of Americium (IV) in Aqueous Carbonate Solution," *Radiochimica Acta.* Vol. 31, no. 3/4, 139-145.

Hobart, D.E., C.J. Bruton, F.J. Millero, I-Ming Chou, K.M. Trauth, and D.R. Anderson. 1996. *Estimates of the Solubilities of Waste Element Radionuclides in Waste Isolation Pilot Plant Brines: A Report by the Expert Panel on the Source Term.* SAND96-0098. Albuquerque, NM: Sandia National Laboratories.

Horita, J., T. J. Friedman, B. Lazar, and H.D. Holland. 1991. "The Composition of Permian Seawater," *Geochimica et Cosmochimica Acta.* Vol. 55, no. 2, 417-432.

Hunter, R.J. 1991-1992. *Foundations of Colloid Science.* Reprinted. New York, NY: Oxford University Press. Vols. I-II.

Johnson, G.L., and L.M. Toth. 1978. *Plutonium(IV) and Thorium(IV) Hydrous Polymer Chemistry.* ORNL/TM-6365. Oak Ridge, TN: Oak Ridge National Laboratory, Chemistry Division.

Katz, J.J., G.T. Seaborg, and L.R. Morss, eds. 1986. *The Chemistry of the Actinide Elements.* 2nd ed. New York, NY: Chapman and Hall. Vols. 1-2.

Keller, C. 1971. *The Chemistry of the Transuranium Elements.* Weinheim, Germany: Verlag Chemie, GmbH.

Kim, J.I. 1992. "Actinide Colloid Generation in Groundwater," *Radiochimica Acta*. Vol. 52/53, pt. 1, 71-81.

Kim, J.I. 1994. "Actinide Colloids in Natural Aquifer Systems," *MRS Bulletin, A Publication of the Materials Research Society.* Vol. 19, no. 12, 47-53.

Kim, J.-I., and T. Sekine. 1991. "Complexation of Neptunium(V) with Humic Acid," *Radiochimica Acta.* Vol. 55, no. 4, 187-192.

Kim, J.I., M. Bernkopf, Ch. Lierse, and F. Koppold. 1984a. "Hydrolysis Reactions of Am(III) and Pu(VI) Ions in Near-Neutral Solutions," *Geochemical Behavior of Disposed Radioactive Waste*. Eds. G.S. Barney, J.D. Navratil, and W.W. Schulz. ACS Symposium Series 246. Washington, DC: American Chemical Society. 115-134.

Kim, J.I., G. Buckau, F. Baumgärtner, H.C. Moon, and D. Lux. 1984b. "Colloid Generation and the Actinide Migration in Gorleben Groundwaters," Scientific Basis for Nuclear Waste Management VII, Materials Research Society Symposia Proceedings, Boston, MA, November 14-17, 1983. Ed. G.L. McVay. New York, NY: North-Holland. Vol. 26, 31-40.

Kim, J.I., Ch. Apostolidis, G. Buckau, K. Bueppelmann, B. Kanellakopulos, Ch. Lierse, S. Magirius, R. Stumpe, I. Hedler, Ch. Rahner, and W. Stoewer. 1985. *Chemisches Verhalten von Np, Pu und Am in verschiedenen knozentrierten Salzloesunger = Chemical Behaviour of Np, Pu, and Am in Various Brine Solutions.* RCM 01085. Munich, Germany: Institut für Radiochemie der Technische Universitaet Muenchen. (Available from National Technical Information Service, 555 Port Royal Road, Springfield, VA 22161, 703/487-4650 as DE857 2334.)

Korpusov, G.V., E.N. Patrusheva, and M.S. Dolidze. 1975. "The Study of Extraction Systems and the Method of Separation of Trivalent Transuranium Elements Cm, Bk, and Cf," *Soviet Radiochemistry.* Vol 17, no. 1-6, 230-236.

Kraus, K.A. 1956. "Hydrolytic Behavior of the Heavy Elements," *Proceedings of the International Conference on the Peaceful Uses of Atomic Energy, Geneva, August 8-20, 1955.* New York, NY: United Nations. Vol. 7, 245-257.

Larson, K.L., March 13, 1996. "Brine Waste Contact Volumes for Scoping Analysis of Organic Ligand Concentration." Memorandum to R. V. Bynum. ERMS 236044.

Laul, J.C., M.R. Smith, and N. Hubbard. 1985. "Behavior of Natural Uranium, Thorium and Radium Isotopes in the Wolfcamp Brine Aquifers, Palo Duro Basin, Texas," *Scientific Basis for Nuclear Waste Management, Materials Research Society Symposia Proceedings, Boston, MA, November 26-29, 1984.* Eds. C.M. Jantzen, J.A. Stone, and R.C. Ewing. Pittsburgh, PA: Materials Research Society. Vol. 44, 475-482.

Lieser, K., B. Gleitsmann, S. Peschke, and T. Steinkopff. 1986a. "Colloid Formation and Sorption of Radionuclides in Natural Systems," *Radiochimica Acta*. Vol. 40, no. 1, 39-47.

Lieser, K., B. Gleitsmann, and T. Steinkopff. 1986b. "Sorption of Trace Elements or Radionculides in Natural Systems Containing Groundwater and Sediments," *Radiochimica Acta*. Vol. 40, no. 1, 33-37.

Lieser, K.H., A. Ament, R. Hill, R.N. Singh, U. Stingl, and B. Thybusch. 1990. "Colloids in Groundwater and Their Influence on Migration of Trace Elements and Radionuclides," *Radiochimica Acta*. Vol. 49, no. 2, 83-100.

Lieser, K.H., R. Hill, U. Mühlenweg, R.N. Singh, T. Shu-De, and Th. Steinkopff. 1991. "Actinides in the Environment," *Journal of Radioanalytical and Nuclear Chemistry, Articles.* Vol. 147, no. 1, 117-131.

Lyklema, J. 1978. "Surface Chemistry of Colloids in Connection with Stability," T*he Scientific Basis of Flocculation.* Ed. K.J. Ives. NATO Advanced Study Institute Series, Series E, Volume E27. Alphen aan den Rijn: Sijthoff & Noordhoff. 3-36.

Maiti, T.C., M.R. Smith, and J.C. Laul. 1989. "Colloid Formation Study of U, Th, Ra, Pb, Po, Sr, Rb, and Cs in Briny (High Ionic Strength) Groundwaters: Analog Study for Waste Disposal," *Nuclear Technology*. Vol. 84, no. 1, 82-87.

Martinot, L. and J. Fuger. 1985. "The Actinides," *Standard Potentials in Aqueous Solution.* Eds. A.J. Bard, R. Parsons, and J. Jordan. New York, NY: Marcel Dekker. 631-674.

McCarthy, J.F., and J.M. Zachara. 1989. "Subsurface Transport of Contaminants," *Environmental Science & Technology*. Vol. 23, no. 5, 496-502.

Molecke, M.A. 1983. A Comparison of Brines Relevant to Nuclear Waste Experimentation. SAND83-0516. Albuquerque, NM: Sandia National Laboratories.

Munson, D.E., R.L. Jones, D.L. Hoag, and J.R. Ball. 1987. Heated Axisymmetric Pillar Test (Room H): In Situ Data Report (February, 1985 - April, 1987), Waste Isolation Pilot Plant (WIPP) Thermal/Structural Interactions Program. SAND87-2488. Albuquerque, NM: Sandia National Laboratories.

Nash, K.L., and G.R. Choppin. 1980. "Interaction of Humic and Fulvic Acids with Th(IV)," *Journal of Inorganic and Nuclear Chemistry.* Vol. 42, no. 7, 1045–1050.

Neck, V., J.I. Kim, and B. Kanellakopulos. 1992. "Solubility and Hydrolysis Behavior of Neptunium (V)," *Radiochimica Acta.* Vol. 56, no. 1, 25-30.

Neck, V., W. Runde, and J.I. Kim. 1995. "Solid-Liquid Equilibria of Np(V) in Carbonate Solutions at Different Ionic Strengths: II," *Journal of Alloys and Compounds.* Vol. 225, 295-302.

Neretnieks, I. 1982. *The Movement of a Redox Front Downstream From a Repository for Nuclear Waste.* KBS Report TR 82-16. Stockholm: Svensk Kärnbränsleforsorjning AB.

Nitsche, H. 1987. "Effects of Temperature on the Solubility and Speciation of Selected Actinides in Near-Neutral Solution," *Inorganica Chimica Acta.* Vol. 127, no. 1, 121-128.

Nitsche, H., and N.M. Edelstein. 1985. "Solubilities and Speciation of Selected Transuranium Ions. A Comparison of a Non-complexing Solution with a Groundwater from the Nevada Tuff Site," *Radiochimica Acta.* Vol. 39, no. 1, 23-33.

Nitsche, H., K. Roberts, R.C. Gatti, T. Prussin, K. Becraft, S.C. Leung, S.A. Carpenter, and C.F. Novak. 1992. *Plutonium Solubility and Speciation Studies in a Simulant of Air Intake Shaft Water from the Culebra Dolomite at the Waste Isolation Pilot Plant.* SAND92-0659. Albuquerque, NM: Sandia National Laboratories. WPO 23480.

Nitsche, H., K. Roberts, R. Xi, T. Prussin, K. Becraft, I. Al Mahamid, H.B. Silber, S.A. Carpenter, R.C. Gatti, and C.F. Novak. 1994. "Long Term Plutonium Solubility and Speciation Studies in a Synthetic Brine," *Radiochimica Acta, Special Issue: Chemistry and Migration Behaviour of Actinides and Fission Products in the Geosphere, Proceedings of the Fourth International Conference, Charleston, SC, December 12-17, 1993.* Munich: R. Oldenbourg Verlag. Vol. 66/67, 3-8. WPO 21107.

Novak, C.F. 1995. *The WIPP Actinide Source Term: Test Plan for the Conceptual Model and the Dissolved Concentration Submodel.* SAND95-1985. Albuquerque, NM: Sandia National Laboratories. WPO 27860.

Novak, C.F., and R.C. Moore, March 28, 1996. "Estimates of Dissolved Concentrations for III, IV, V, and VI Actinides in Salado and Castile Brine Under Anticipated Repository Conditions." SNL Tech Memo. (Copy on file in the Sandia WIPP Central File A: WBS 1.2.0.7.1; WBS 1.1.10.1.1: WPO 36207.)

Novak, C.F., R.C. Moore, and R.V. Bynum. 1996. "Prediction of Dissolved Actinide Concentrations in Concentrated Electrolyte Solutions: A Conceptual Model and Model Results for the Waste Isolation Pilot Plant (WIPP)," *Proceedings of the International Conference on Deep Geological Disposal of Radioactive Waste, Winnipeg, Manitoba, Canada, September 16-19, 1996.*

Papenguth, H.W. 1996a: H.W. Papenguth to Christine T. Stockman: "Parameter Record Package for Colloidal Actinide Source Term Parameters" May 7, 1996: Attachment A: Rationale for Definition of Parameter Values for Actinide Intrinsic Colloids." WPO 35852.

Papenguth, H.W. 1996b: H.W. Papenguth to Christine T. Stockman: "Parameter Record Package for Colloidal Actinide Source Term Parameters" May 7, 1996: Attachment A: Rationale for Definition of Parameter Values for Microbes." WPO 35856.

Papenguth, H.W. 1996c: H.W. Papenguth to Christine T. Stockman: "Parameter Record Package for Colloidal Actinide Source Term Parameters" May 7, 1996: Attachment A: Rationale for Definition of Parameter Values for Humic Substances." WPO 35855.

Papenguth, H.W. 1996d: H.W. Papenguth to Christine T. Stockman: "Parameter Record Package for Colloidal Actinide Source Term Parameters" May 7, 1996: Attachment A: Rationale for Definition of Parameter Values for Mineral Fragment Type Colloids." WPO 35850.

Papenguth, H.W., and Y.K. Behl. 1996. "Test Plan for Evaluation of Colloid-Facilitated Actinide Transport at the Waste Isolation Pilot Plant." SNL Test Plan TP 96-01. (Copy on file in the Sandia WIPP Central File A:1.1.10.2.1. PUB:QA; WPO 31337.)

Pearson, R.G. 1963. "Hard and Soft Acids and Bases," Journal of the American Chemical Society, Vol. 85, no. 22, 3533-3539.

Pitzer, K.S., ed. 1991. *Activity Coefficients in Electrolyte Solutions.* 2nd ed. Boca Raton, FL: CRC Press.

Popielak, R.S., R.L. Beauheim, S.R. Black, W.E. Coons, C.T. Ellingson and R.L. Olsen. 1983. Brine Reservoirs in the Castile Formation, Waste Isolation Pilot Plant Project, Southeastern New Mexico. TME 3153. Carlsbad, NM: U.S. Department of Energy WIPP Project Office.

Pryke, D.C., and J.H. Rees. 1986. "Understanding the Behaviour of the Actinides Under Disposal Conditions: A Comparison between Calculated and Experimental Solubilities," *Radiochimica Acta.* Vol. 40, no. 1, 27-32.

Rai, D., and R.G. Strickert. 1980. "Chemical Aspects of Medium- and Long-Term Radioactive Waste Disposal," *Transactions of the American Nuclear Society and the European Nuclear Society.* Vol. 35, 185-186.

Rai, D., and J.L. Swanson. 1981. "Properties of Plutonium(IV) Polymer of Environmental Importance," *Nuclear Technology*. Vol. 54, no. 1, 107-111. WPO 30420.

Rai, D., R.J. Serne, and D.A. Moore. 1980. "Solubility of Plutonium Compounds and Their Behavior in Soils," *Soil Science Society of America Journal.* Vol. 44, no. 3, 490-495.

Rai, D., R.G. Strickert, and G.L. McVay. 1982. "Neptunium Concentrations in Solutions Contacting Actinide-Doped Glass," *Nuclear Technology.* Vol. 58, no. 1, 69-76.

Rai, D., A.R. Felmy, and R.W. Fulton. 1995. "Nd^{3+} and Am^{3+} Ion Interactions with Sulfate Ion," *Journal of Solution Chemistry.* Vol 24, no. 9, 879-895.

Rao, L., and G.R. Choppin. 1995. "Thermodynamic Study of the Complexation of Neptunium(V) with Humic Acids," *Radiochimica Acta*. Vol. 69, no. 2, 87-95.

Rao, L., D. Rai, A.R. Felmy, R.W. Fulton, and C.F. Novak. 1996. "Solubility of $NaNd(CO_3)_2 \cdot 6H_2O$ in Concentrated Sodium Carbonate and Sodium Bicarbonate Solutions." *Radiochimica Acta.* In press. WPO 36484.

Reed, D.T., D.G. Wygmans, and M.K. Richman. 1996. "Actinide Stability/Solubility in Simulated WIPP Brines." Interim Report under SNL WIPP Contract AP-2267. (Copy on file in the Sandia WIPP Central files.)

Refait, Ph. and J.-M.R. Génin. 1994. "The Transformation of Chloride-Containing Green Rust One Into Sulphated Green Rust Two by Oxidation in Mixed Cl^- and SO_4^{2-} Aqueous Media," *Corrosion Science.* Vol. 36, no. 1, 55-65.

Robinson, R.A., and R.H. Stokes. 1959. *Electrolyte Solutions, The Measurement and Interpretation of Conductance, Chemical Potential, and Diffusion in Solutions of Simple Electrolytes.* 2nd ed. (revised). London, England: Butterworths.

Ross, S., and I.D. Morrison. 1988. *Colloidal Systems and Interfaces.* New York, NY: John Wiley & Sons.

Runde, W. and J.I. Kim. 1994. Untersuchungen der Übertragbarkeit von Labordaten natürliche Verhältnisse. Chemisches Verhalten von drei- und fünfwertigem Americium in salinen NaCl-Lösungen. Report RCM-01094, Munich: Institut für Radiochemie, Technische Universität München. (Available from National Technical Information Service, 555 Port Royal Road, Springfield, VA, 22161, 703/487-4650 as DE 95752244.)

Sagoe-Crentsil, K.K., and F.P. Glasser. 1993. " 'Green Rust,' Iron Solubility and the Role of Chloride in the Corrosion of Steel at High pH," *Cement and Concrete Research.* Vol. 23, no. 4, 785-791.

Sanchez, L.C., and H.R. Trellue. January 17, 1996. "Estimation of Maximum RH-TRU Thermal Heat Load for WIPP." WPO 31165.

Scherer, C.P., I. Archuleta, and R. Villarreal. 2001a. Los Alamos National Laboratory STTP Data Historical Compilation, September 2000 (Revised July 2001), Volume I. LA-UR-01-5278. Los Alamos, NM: Los Alamos National Laboratory.

Scherer, C.P., I. Archuleta, and R. Villarreal. 2001b. Los Alamos National Laboratory STTP Data Historical Compilation, November 2000 (Revised July 2001), Volume II. LA-UR-01-6911. Los Alamos, NM: Los Alamos National Laboratory.

Scherer, C.P., I. Archuleta, and R. Villarreal. 2001c. Los Alamos National Laboratory STTP Data Historical Compilation (July 2001), Volume III. LA-UR-01-4245. Los Alamos, NM: Los Alamos National Laboratory.

Scherer, C.P., and R. Villarreal. 2000. A Study of Actinide and pcH Trends from Brine Analyses of the Liter-Scale Containers in the STTP Program. LA-UR-01-376. Los Alamos, NM: Los Alamos National Laboratory.

Scherer, C.P., and R. Villarreal. 2001. Phosphate Addition to Drums 7. 8, and 9 and Its Effect on Soluble Actinide Species. LA-UR-01-3081. Los Alamos, NM: Los Alamos National Laboratory.

Schnitzer, M., and S. I. M. Skinner. 1967. "Organo-Metallic Interactions in Soils: 7 Stability Constants of Pb^{++}, Ni^{++}, Mn^{++}, Co^{++}, Ca^{++}, and Mg^{++} - Fulvic Acid Complexes," *Soil Science*. Vol. 103, no. 4, 247-252.

Siegel, M.D. 1996. "Solubility Parameters for Use in the CCA NUTS and GRIDFLOW Calculations." SNL Technical memorandum dated 29 March 1996 to Martin S. Tierney. (Copy on file in the Sandia WIPP Central File A:WBS 1.2.0.7.1; WBS 1.1.10.61: WPO 35835.) Also WPO 37314.

Snider, A.C. 2003a. Verification of the Definition of Generic Weep Brine and the Development of a Recipe for This Brine. Unpublished report. Carlsbad, NM: Sandia National Laboratories. ERMS 527505.

Snider, A.C. 2003b. Calculation of MgO Safety Factors for the WIPP Compliance Recertification Application and for Evaluating Assumptions of Homogeneity in WIPP PA. Unpublished analysis report. Carlsbad, NM: Sandia National Laboratories. ERMS 531508.

Stumm, W. 1992. *Chemistry of the Solid-Water Interface.* New York, NY: John Wiley & Sons, Inc.

Stumm, W. 1993. "Aquatic Colloids as Chemical Reactants: Surface Structure and Reactivity," *Colloids in the Aquatic Environment.* Ed. T.F. Tadros and J. Gregory. New York, NY: Elsevier Applied Science. (Reprinted from Colloids and Surfaces. Vol. 73, 1-18.)

Trauth, K.M., S.C. Hora, R.P. Rechard, and D.R. Anderson. 1992. *The Use of Expert Judgment to Quantify Uncertainty in Solubility and Sorption Parameters for Waste Isolation Pilot Plant Performance Assessment.* SAND92-0479. Albuquerque, NM: Sandia National Laboratories. WPO 23526

Trovato, E.R. 1997. Untitled letter from E.R. Trovato to G. Dials, April 25, 1997. Washington, DC: U.S. Environmental Protection Agency Office of Radiation and Indoor Air.

U.S. Department of Energy (DOE). 1996a. Transuranic Waste Baseline Inventory Report, Rev. 3. DOE/CAO-95-1121. Carlsbad, NM: U.S. Department of Energy Carlsbad Area Office.

U.S. Department of Energy (DOE). 1996b. Title 40 CFR Part 191 Compliance Certification Application for the Waste Isolation Pilot Plant, Vol. 1-21. Carlsbad, NM: U.S. Department of Energy Carlsbad Area Office.

U.S. Environmental Protection Agency (EPA). 1998a. Compliance Application Review Documents for the Criteria for the Certification and Recertification of the Waste Isolation Pilot Plant's Compliance with the 40 CFR Part 191 Disposal Regulations: Final Certification Decision. CARD 23: Models and Computer Codes. EPA Air Docket A93-02-V-B-2. Washington, DC: U.S. Environmental Protection Agency Office of Radiation and Indoor Air.

U.S. Environmental Protection Agency (EPA). 1998b. Technical Support Document for Section 194.23 – Models and Computer Codes. EPA Air Docket A93-02-V-B-6. Washington, DC: U.S. Environmental Protection Agency Office of Radiation and Indoor Air.

Villareal, R., J.M. Bergquist, and S.L. Leonard. 2001a. The Actinide Source-Term Waste Test Program (STTP) Final Report, Volume I. LA-UR-01-6822. Los Alamos, NM: Los Alamos National Laboratory.

Villareal, R., J.M. Bergquist, and S.L. Leonard. 2001b. The Actinide Source-Term Waste Test Program (STTP) Final Report, Volume II. LA-UR-01-6912. Los Alamos, NM: Los Alamos National Laboratory.

Villareal, R., M. King, and S.L. Leonard. 2001. The Actinide Source-Term Waste Test Program (STTP) Final Report, Volume IV. LA-UR-01-6914. Los Alamos, NM: Los Alamos National Laboratory.

Villareal, R., A.C. Morzinski, J.M. Bergquist, and S.L. Leonard. 2001. The Actinide Source-Term Waste Test Program (STTP) Final Report, Volume III. LA-UR-01-6913. Los Alamos, NM: Los Alamos National Laboratory.

Villarreal, R., M. Neu, L. Field, S. Reilly, E. Medina, and M. King. Undated. The Actinide Source-Term Waste Test Program (STTP) Final Report, Volume III. LA-UR-02162. Los Alamos, NM: Los Alamos National Laboratory.

Villarreal, R., A. Trujillo, C. Scherer, M. Neu, S. Reilly, and A.C Morzinski. 2000. A Study of STTP Pyrochemical Salt Tests and Results Featuring Pu(VI). LA-UR-00-1606. Los Alamos, NM: Los Alamos National Laboratory.

Vold, R.D., and M.J. Vold. 1983. *Colloid and Interface Chemistry.* Reading, MA: Addison-Wesley.

Wang, Y. and L. Brush. January 26, 1996a. "Estimates of Gas-Generation Parameters for the Long-Term WIPP Performance Assessment." WPO 31943.

Wang, Y. and L.H. Brush. 1996b. "Modify the Stoichiometric Factor y in the BRAGFLO to Include the Effect of MgO Added to WIPP Repository as a Backfill." Unpublished memorandum to M.S. Tierney, February 23, 1996. Albuquerque, NM: Sandia National Laboratories. ERMS 232286.

Weiner, R. 1996. "Documentation Package For: Oxidation State Distribution of Actinides in the Repository." SNL Technical memorandum dated 27 March 1996 to SWCF-A: Records Center, SWCF-A: WBS 12.1.10.1.1:PDD: QA: Dissolved Species: Oxidation State Distribution: Actinides: OX3: OX4: OX5: OX6 (WPO 35194).

WIPP Performance Assessment Department. 1996. *User's Manual for NONLIN, Version 2.0*, ERMS 230740.

Wolery, T.J. 1992. EQ3/6, *A Software Package for Geochemical Modeling of Aqueous Systems: Package Overview and Installation Guide (Version 7.0)*. UCRL-MA-110662 PT 1. Livermore, CA: Lawrence, CA: Lawrence Livermore National Laboratory.

Wolery, T.J., and S.A. Daveler. 1992. *EQ6, A Computer Program for Reaction Path Modeling of Aqueous Geochemical Systems: Theoretical Manual, User's Guide, and Related Documentation (Version 7.0).* UCRL-MA-110662-Pt. 4. Livermore, CA: Lawrence Livermore National Laboratory.

Wood, J.R. 1975. "Thermodynamics of Brine-Salt Equilibria. I. The Systems NaCl-KCl-$MgCl_2$-$CaCl_2$-H_2O and NaCl-$MgSO_4$-H_2O at 25°C," *Geochimica et Cosmochimica Acta.* Vol. 39, no. 8, 1147-1163.